



NTNU – Trondheim
Norwegian University of
Science and Technology

Interaction of different crude oils with model shoreline surfaces

Adsorption and wettability studies

Jostein Kjemperud

Chemical Engineering and Biotechnology

Submission date: June 2013

Supervisor: Gisle Øye, IKP

Co-supervisor: Umer Farooq, SINTEF Marine Environmental Technology

Norwegian University of Science and Technology
Department of Chemical Engineering

Abstract

To improve shoreline cleanup operations in the current oil spill response systems, a better understanding of the interactions between the spilled crude oil and the shoreline surfaces is required. The objective of this study was to investigate how the interactions between model shorelines and different crude oils are affected by the difference in chemical composition between the oils. How long the oil has been at sea before the interaction, the weathering of the oil, was also studied. The effects of dispersants (Corexit 9500) and oil-in-seawater emulsification will also be studied.

The four crude oils investigated originated from different oil fields, and had different chemical compositions. The different oil types were an asphaltic oil (from the Grane field), a waxy oil (from Norne), a naphthenic oil (from Gullfaks A) and a paraffinic oil (from Oseberg). Fresh and weathered fractions from each field were studied. The shoreline was modeled by quartz crystals with different types of coatings; silica, calcium carbonate and aluminosilicate. The parameters investigated in the study were mass adsorption of oil on the crystals, and the wettability of sea water on the oil covered crystals. The mass adsorption was measured using Quartz Crystal Microbalance with Dissipation (QCM-D), and the wettability was measured by the contact angle of seawater on the oil coated crystals using CAM 200.

The results show that the asphaltic Grane oil adsorbed the most on the silica coated crystal, whilst the aluminosilicate coating tended to adsorb more of the other oil types as well. The calcium carbonate coated crystal also adsorbed a great deal of the Grane oil, but also adsorbed the paraffinic Oseberg oil to a great extent. The dissipation measured simultaneously with the mass adsorption showed that most of the oils adsorbed as a compact and rigid layer. For the wettability of the oil types, this seemed to follow adsorption; high mass adsorption gave a low wettability of seawater on the oil covered crystals, especially for the silica and calcium carbonate coated crystals.

With regards to weathering, some trends were observed. For the silica coating, the adsorption of the Norne, Oseberg and Grane oil tended to increase with increased weathering. On the aluminosilicate coating, the adsorption of the Grane oil also increased, whilst the Norne and Oseberg values decreased. For the crystals with the calcium carbonate coating, the Norne adsorption value increased, whilst the Oseberg and Grane values decreased. For all coatings, the Gullfaks A oil tended to change less than the other oil types when introduced to weathering

When Corexit 9500 were added, some trends were observed. The mass adsorption of the paraffinic Oseberg oil tended to decrease, whilst the asphaltic Grane oil tended to increase. The other oil types did not have as clear trends. The oil-in-seawater experiments did not give as clear tendencies as in the other experiments. The aluminosilicate coated crystals seemed to adsorb more than the other two crystal coatings, these two coatings tended to adsorb much less than in the other experiments.

Sammendrag

For å forbedre opprydningsoperasjoner i strandlinjen med den nåværende oljevernberedskapen, er det behov for en bedre forståelse av interaksjonene mellom råoljen i utslippet og overflatene i strandlinjen. Målet med denne undersøkelsen var å undersøke hvordan interaksjonene mellom modeller av kystlinjen og forskjellige råoljer påvirkes av forskjellen i kjemiske komponenter mellom oljene. Hvor lenge oljene har ligget i sjøen før de treffer strandlinjen, oljens forvitring, ble også undersøkt. Effekten av dispergeringsmiddel (Corexit 9500) og olje-i-sjøvann-emulgering vil også bli undersøkt.

De fire råoljene som ble undersøkt kom fra forskjellige oljefelt, og hadde ulik kjemisk sammensetning. De ulike oljene var en asfaltisk (asfaltholdig) olje (fra Granefeltet), en voksaktig olje (fra Norne), en naftensk olje (fra Gullfaks A) og en parafinsk olje (fra Oseberg). Ferske og forvitrede fraksjoner fra hvert felt ble undersøkt. Strandlinjen ble modellert med kvartskrystaller med forskjellig belegg; silika, kalsiumkarbonat og alumionsilikat. Parameterene som ble undersøkt i studiet var masseadsorpsjon av olje på krystallene, og fuktbarhet av sjøvann på de oljebelagte krystallene. Masseadsorpsjonen ble målt ved hjelp av quartz crystal microbalance with dissipation (QCM-D), og fuktbarheten ble funnet ved hjelp av måling av kontaktvinkelen av sjøvann på de oljebelagte krystallene.

Resultatene viser at den asfaltholdige Graneoljen adsorbte mest på den silicabelagte krystallen, mens aluminosilikatbelegget hadde en tendens til å også adsorbere mer av de andre oljetyperne. Den kalsiumkarbonatbelagte krystallen adsorbte også Graneoljen i stor grad, men adsorbte i tillegg mye av den parafinske Osebergoljen. Spredningen (dissipasjonen) som ble målt samtidig med masseadsorpsjonen viste at de fleste oljene adsorbte som et kompakt og fast lag. Når det gjelder fuktbarheten av oljetyperne, virket dette å følge masseadsorpsjonen; høy masseadsorpsjon ga lav fuktbarhet av sjøvann på de oljebelagte krystallene, spesielt for de silika- og kalsiumkarbonatbelagte krystallene.

Når det gjelder forvitring, ble det observert noen trender. For silikabelegget virket det som adsorpsjonen av Norne-, Oseberg-, og Graneoljene økte med økt forvitring. På aluminosilikatbelegget økte også adsorpsjonen av Graneoljen, mens Norne- og Osebergverdiene sank. For krystallene med kalsiumkarbonatbelegget økte Norneverdien for adsorpsjon, mens verdiene for Oseberg og Grane sank. For alle beleggene virket Gullfaks A-oljen å endre seg mindre enn de andre oljene under forvitring.

Da Corexit 9500 ble tilsatt, ble noen tendenser observert. Det virket som om masseadsorpsjonen av den parafinske Osebergoljen sank, mens Graneoljen økte. De andre oljetyperne hadde ikke så klare trender. Olje-i-sjøvann-eksperimentene ga ikke så klare tendenser som i de øvrige eksperimentene. Det virket som om de aluminosilikatbelagte krystallene adsorbte mer enn de to andre krystallbeleggene, det virket som disse to beleggene adsorbte mye mindre her enn i de øvrige eksperimentene.

Acknowledgements

I would like to thank my supervisor at NTNU, Professor Gisle Øye, for valuable guidance during the course of this thesis. I would also like to thank my other supervisor Umer Farooq, Research Scientist at SINTEF SeaLab, for guidance and help with interpreting my results, and for providing the quartz crystals, oil samples and seawater used in the thesis.

I declare that this is an independent work according to the exam regulations of the Norwegian University of Science and Technology (NTNU).

Jostein Kjemperud

Place and date

Table of contents

Introduction	1
1. Theory	2
1.1 Crude oils and weathering.....	2
1.2 Quartz Crystal Microbalance with Dissipation (QCM-D)	6
1.3 Contact angle/wettability	7
1.4 Emulsion production	8
1.5 Dispersants	8
2. Experimental	10
2.1 Crude oils and sample preparation	10
2.2 Emulsion production	11
2.3 QCM-D-measurements	12
2.3.1 Crystal cleaning methods.....	12
2.3.2 Oil-in-toluene experiments	13
2.3.3 Oil-in-seawater (emulsion) experiments.....	14
2.4 Contact angle measurements.....	16
3. Results and discussion	18
3.1 Results of experiments using oil-in-toluene without dispersants.....	19
3.1.1 Results of experiments using oil-in-toluene without dispersants – fresh oil samples	19
3.1.2 Results of experiments using oil-in-toluene without dispersants – weathered (200°C+) oil samples	23
3.1.3 Comparison of wettability.....	26
3.2 Results of experiments using oil-in-toluene with dispersants.....	27
3.2.1 Results of experiments using oil-in-toluene with dispersants – fresh oil samples ...	27
3.2.2 Results of experiments using oil-in-toluene with dispersants – weathered (200°C+) oil samples	31
3.3 Results of experiments using oil-in-seawater emulsions	36
3.3.1 Results of experiments using oil-in-seawater emulsions – fresh oil samples.....	36

3.1.2 Results of experiments using oil-in-seawater emulsions – weathered (200°C+) oil samples	40
3.4 Dissipation.....	45
3.5 Sources of error	45
4. Conclusion	46
References	48
Appendix A: Risk assessment	50
Appendix B: Sample calculation of mass adsorption	52
Appendix C: Quartz Crystal Microbalance with Dissipation (QCM-D) results.....	53
C.1 Oil-in-toluene without dispersants.....	53
C.2 Oil-in-toluene with dispersants.....	62
C.3 Oil-in-seawater experiments.....	71

Introduction

In order to mitigate or prevent the environmental impact of crude oil spill accidents, development of new oil spill response systems is essential. An efficient shoreline cleanup operation is an important feature in these kinds of systems, both to collect as much of the stranded oil from the shoreline as possible, and to prevent the oil from remobilizing into the sea and spread over a greater area of the affected coast. To develop a more effective shoreline cleanup operation, better understanding of the interactions between the spilled crude oil and the shoreline surface is required.

The aim of this thesis is to investigate how the interactions between different model shorelines and different crude oils are affected by the difference in chemical composition between the oils. The effect of weathering, i.e. how long the crude oil has been at sea before interacting with a model shoreline will also be investigated. The different types of crude oils studied are extracted from different oil fields, and have different contents of various chemical compounds; one of the oil types has a higher content of asphaltic components, one is more wax-like, one is more naphthenic and the last type is more paraffinic. Of each oil type, two fractions with different degrees of weathering has been studied, one fraction covers fresh oils, the other covers oils that have been altered to model a residence time of 24 hours at sea. The effect of adding dispersants to the crude oils has been studied, and the difference between oils emulsified in seawater and non-emulsified oils has also been investigated.

The parameters studied to investigate the interactions between the oils were mass adsorption of oil on the crystals, and the wettability of sea water on the oil covered crystals. The mass adsorption was found using Quartz Crystal Microbalance with Dissipation (QCM-D), which measures the change in frequency when an oil film is applied to an oscillating crystal. The different types of coating on different crystals correspond to the different shoreline compositions. The change in frequency measured is proportional to the mass adsorbed on the crystal. The QCM-D also measured dissipation, which indicates the rigidity of the different oil films. The wettability was studied by measuring the contact angle of sea water droplets on the different types of crystals using CAM 200, after the various oil films were applied.

1. Theory

In this chapter there will be given an introduction of the complex composition of crude oils and how these are affected by weathering at sea. Emulsions and how to produce these will be covered, along with a short introduction to dispersants and their use. The theory concerning the QCM-D will be explained, and the concept of finding wettability using contact angles will be described.

1.1 Crude oils and weathering

A crude oil is an extremely complex mixture, where the number of elemental compounds could be as many as several billion¹. The crude oils consist of hydrocarbons and hetero-compounds. Hydrocarbons consist only of compositions of hydrogen and carbon, whereas hetero-compounds also contain elements like e.g. nitrogen, oxygen, iron and sulfur¹. Crude oils are often separated into groups with respect to polarity, and one of these separation techniques is called the SARA-analysis, where SARA stands for the different separation groups; saturates, aromatics, resins and asphaltenes². Figure 1.1 shows how this kind of analysis separates the crude oil into groups. The different groups are described briefly on the next page, and example structures of the groups are displayed in figure 1.2.

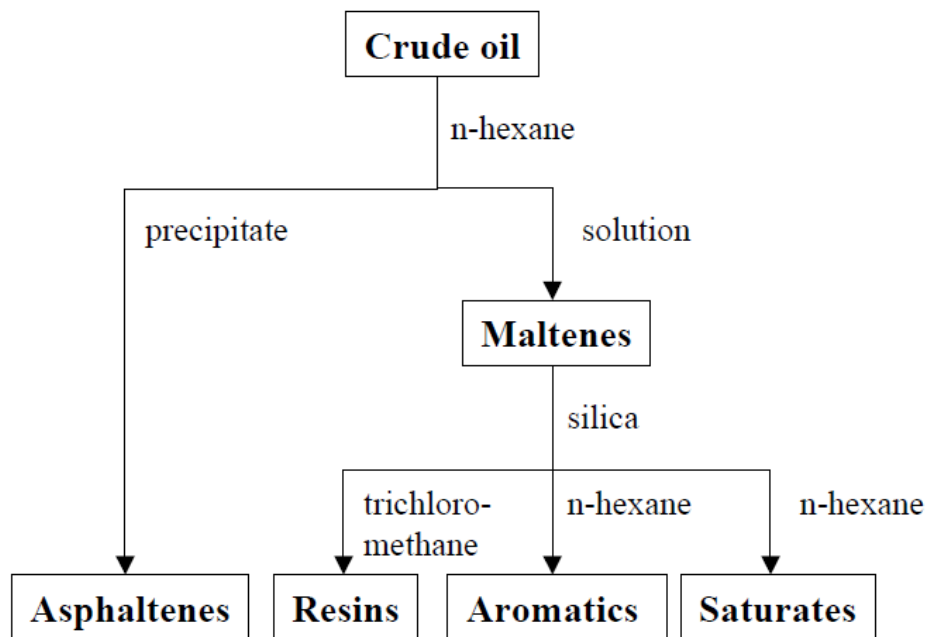


Figure 1.1: SARA-analysis of crude oils based on polarity, decreasing polarity from left to right².

Saturates: The saturate group contain alkane chains that are straight or branched (iso) which are called paraffins, and also cycloalkanes (naphthenes) with one or more rings. In this class waxy oils are also found, these are mostly built up by straight-chained alkanes, C₂₀ to C₃₀ in length.

Aromatics: As the name reveals, this group covers molecules containing aromatic rings. The compounds mostly consist of alkyl chains, cycloalkane rings and one or several aromatic rings. If aromatics have a high molecular weight or are polar, they may be classified as resins or asphaltenes.

Resins: In this group, we find hetero-compounds in addition to the hydrocarbons. The structures of the molecules are similar to those of surfactants³. The resins are characterized after their solubility, and will therefore overlap with the aromatic and asphaltene groups.

Asphaltenes: The asphaltene group also contains heteroatoms like oxygen, nitrogen and sulfur, in an even greater percentage than resins. In addition, this group also contains organometallic components like vanadium and iron. The molecules are formed by aromatic rings that have formed a cluster in the shape of a plate, with alkyl chains added in the periphery.

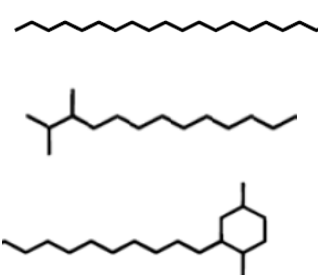
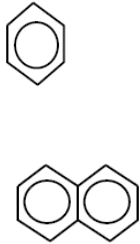
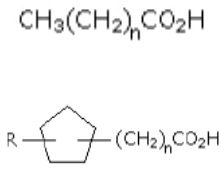
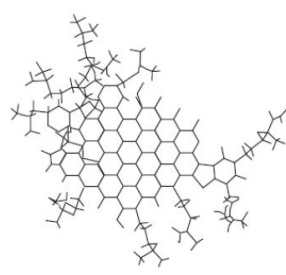
			
Saturates	Aromatics	Resins	Asphaltenes

Figure 1.2: Example structures of the four SARA-analysis groups used to classify crude oils³.

Weathering is the collective term for the processes that alter the properties of a crude oil when it is spilled at sea⁴. How weathering affects spilled oil is based on several factors, like the release conditions and ambient conditions, and the physicochemical properties of the oil that is spilled. The release conditions involve factors like the amount of the spill and if the spill was released under water or at the surface, whereas the ambient conditions deal with temperature, currents and sea-state. The physicochemical properties of a crude oil relates to how easily the oil is dispersed at sea, and its tendency to form water-in-oil (W/O) emulsions at the interface between sea and air.

Some of the most crucial weathering processes are the W/O and natural (oil-in-water, O/W) dispersion, evaporation of the more volatile components in the oil, diffusion, photolysis and sedimentation. These and other weathering processes are shown in figure 1.3. One way to simulate weathering is that the lighter components of oils are evaporated by distillation. The different examples of weathering fractions; 150°C+, 200°C+ and 250°C+, represent one half to one hour, one half to one day and one half to one week out at sea representatively, depending on the ambient conditions⁵.

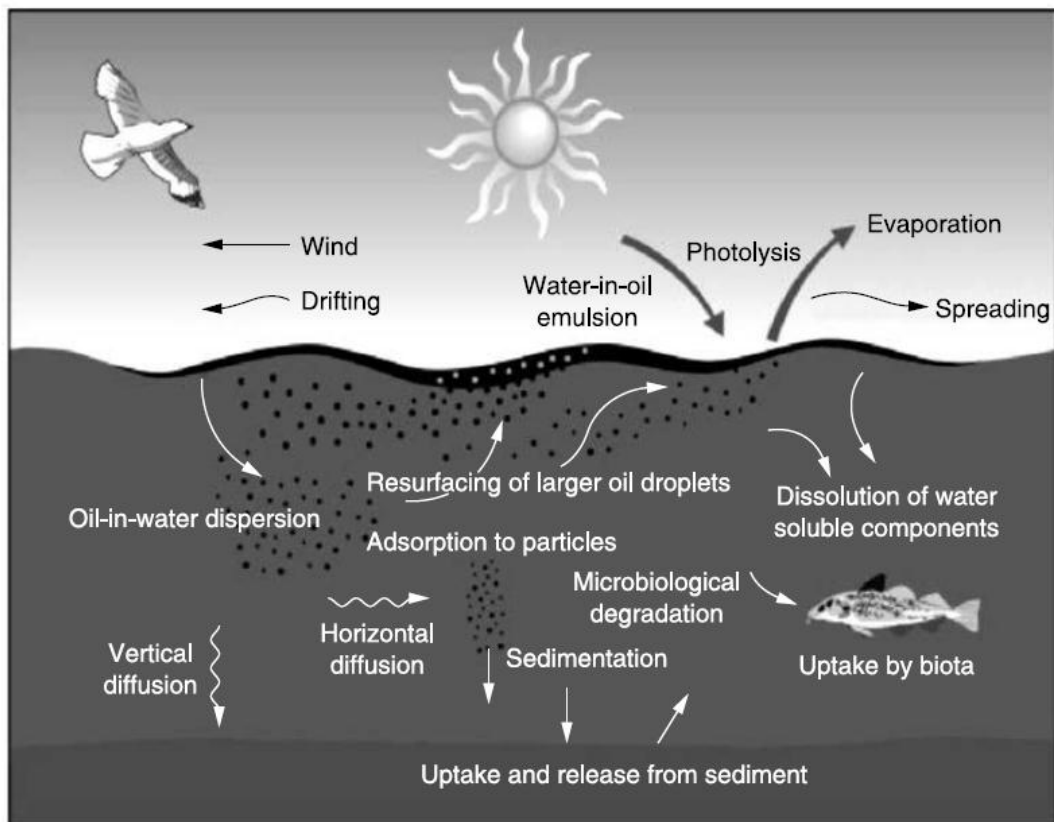


Figure 1.3: The effect of weathering processes on a spilt crude oil at the sea surface⁴.

When a spilt crude oil eventually hit a shoreline, both the physicochemical properties of the oil and how it has been weathered at sea will be of importance, regarding how the oil interacts with the materials of the shoreline. A way to measure this interaction, is to use a Quartz Crystal Microbalance which also measures dissipation (QCM-D) to measure how much of the oil in mass that is adsorbed by the shoreline surface, and to measure contact angle to investigate wettability. The theory of these two methods will be explained briefly in the following subchapters. After that, an explanation of emulsion production will be given, before chemical dispersants are described in the final subchapter.

1.2 Quartz Crystal Microbalance with Dissipation (QCM-D)

The quartz crystal microbalance technique dates back to the 1950s, where deposition of thin films in vacuum systems⁶. An electrical AC-field (alternating current) is applied to a crystal to make it oscillate. The crystals are made of quartz discs around 0.3 mm thick, this disc is sandwiched between two electrodes (see figure 1.4). The electrical field oscillates the crystal at a frequency (f) near the crystal's resonant frequency, and when a thin and rigid film is applied to the active electrode of the crystal, the decrease in frequency will be proportional to the mass of the film adsorbed. The active electrode can be a large number of materials, e.g. silica (SiO_2), gold, iron and polymers like nylon⁷.

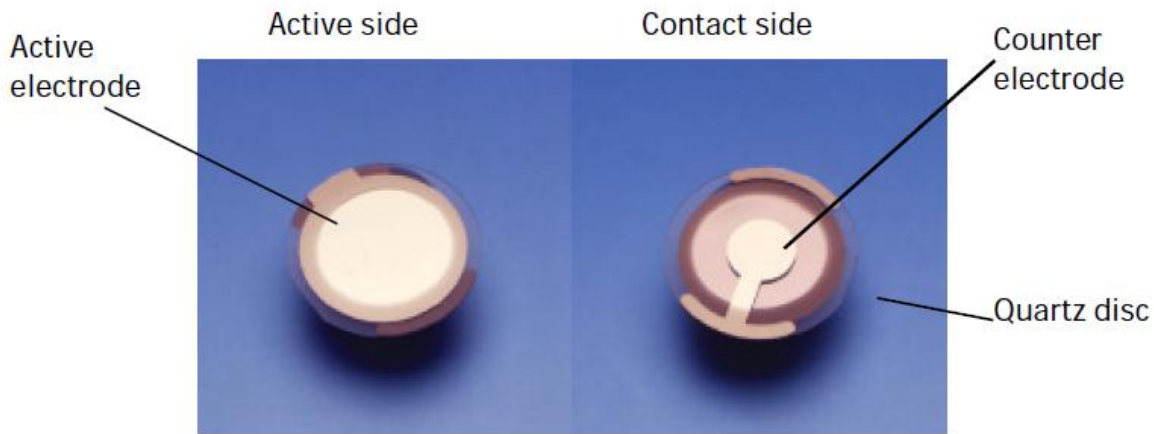


Figure 1.4: A quartz crystal used in the QCM-D measurements⁷.

When the film applied is rigid enough, the relation between the change in mass and change in frequency follows the Sauerbrey equation⁸, equation 1.1:

$$\Delta m = \frac{-C\Delta f}{n} \quad (1.1)$$

In this equation, Δm symbolizes change in mass, Δf change in frequency, C the proportionality constant and n the overtone or resonance number. This equation assumes three notions; the mass of the added film must be much smaller than the mass of the crystal, the film must distribute evenly across the electrode and the film must be rigid and unchanging during oscillation.

In many cases, the film coated over the crystal cannot be considered rigid. In these cases, when the crystal oscillates, the film will not follow the crystals oscillations as a rigid film would. This can be measured as dissipating energy due to frictional losses in the film. The QCM-D apparatus measures dissipation factor (D) or damping defined as in equation 1.2⁹.

$$D = \frac{E_{dissipation}}{2\pi E_{stored}} \quad (1.2)$$

Here, $E_{dissipation}$ is the total dissipated energy and E_{stored} is the total energy stored, both during one oscillation.

1.3 Contact angle/wettability

The wetting or wettability of a liquid on a solid surface is measured quantitatively by the contact angle (θ)¹⁰. This angle is geometrically defined as the angle formed where three phases intersect, e.g. vapor, liquid and solid like in figure 1.5¹¹.

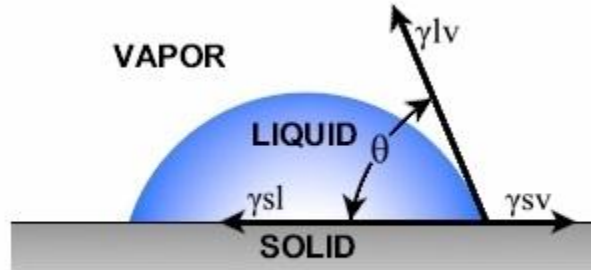


Figure 1.5: Contact angle and interfacial tensions in a three-phase intersection¹¹.

In figure 1.5, γ_{SL} , γ_{LV} and γ_{SV} symbolizes interfacial tension between solid and liquid, liquid and vapor and solid and vapor respectively. If these are known, the contact angle can be found via Young's equation, equation 1.3¹².

$$\cos(\theta) = \frac{\gamma_{SV} - \gamma_{SL}}{\gamma_{SV}} \quad (1.3)$$

The larger the contact angle, the less the liquid wets the solid surface. If the contact angle is zero, the liquid wets the solid completely.

1.4 Emulsion production

Emulsification, i.e. breaking down a bulk phase into small droplets, demands energy. After a time of added energy, a stationary condition will occur, where the rate of droplets breaking down into smaller drops equals the rate where droplets coalesce¹³. There are many different ways to create emulsions; some examples are homogenization, ultrasonic processing and apparatus based on the rotor-stator principle. A device that uses this principle is the Ultra Turrax. Figure 1.6 a) and b) show the head of the Ultra Turrax device and a cross-section of the head of an apparatus using the rotor-stator principle, respectively.

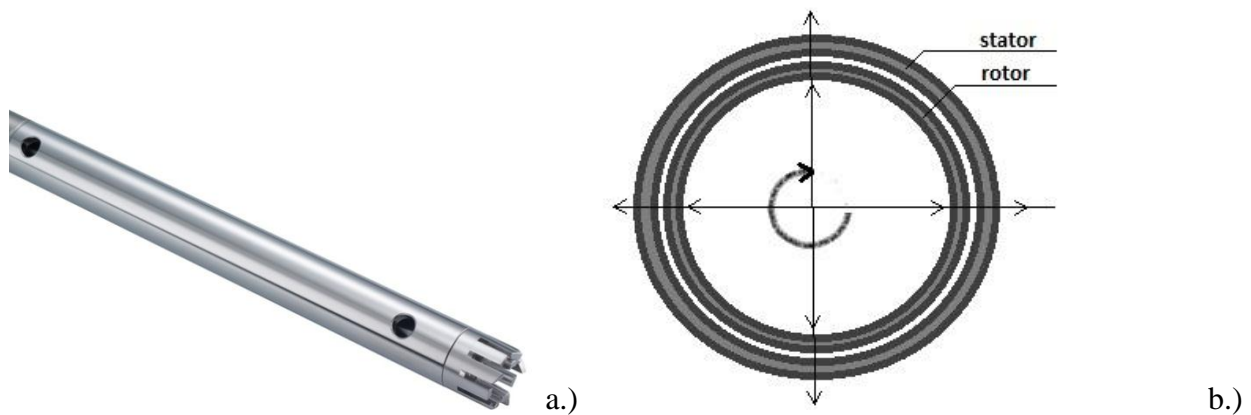


Figure 1.6: a.) Head of Ultra Turrax device¹⁴.

b.) Cross section of the head of an apparatus using the rotor-stator principle¹³.

When fluid is pressed through the narrow slits of the rotor part, droplet sizes of down to 1 μm can be obtained by the shear forces created¹³.

1.5 Dispersants

Dispersants consist of two main components; surfactants and solvents¹⁴. The solvents task is to distribute the surfactants over a large area, e.g. an oil spill. Surfactants, short for surface active agents, are amphiphilic components. This means that they, in aqueous solutions, contain both hydrophilic (water-loving) and oleophilic (oil-loving) groups. The surfactants are characterized by the fact that they, even in small concentrations, significantly reduce surface tension. Figure 1.7 shows how dispersants function when applied to an oil spill.

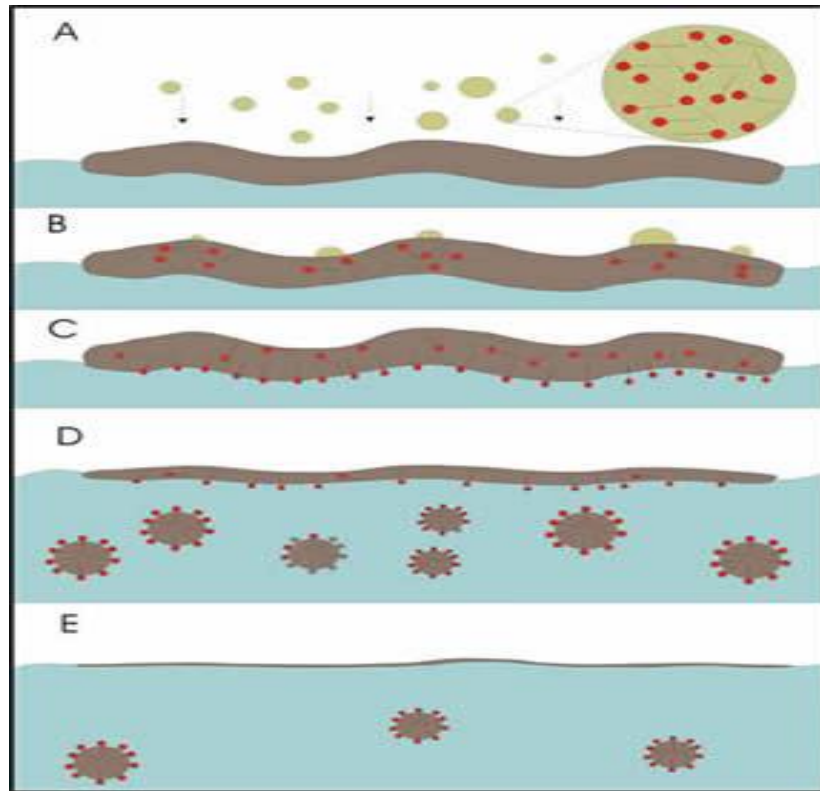


Figure 1.7: A: Dispersant is sprayed onto the oil spill. B: The solvent in the dispersion transports the surfactant into the oil. C: The surfactants migrate to the oil-water interface, where they reduce surface tension. D: The reduction of surface tension allows oil droplets to escape from the large slick of oil. E: The small droplets disperse by turbulent mixing, and are eventually bio-degraded¹⁴.

Image C of figure 1.7 shows how the hydrophilic surfactant head (red) is situated in the sea water, whereas the oleophilic tail (grey) is positioned in the oil slick. The way these molecules are positioned cause a reduction in the imbalance in the intermolecular forces that are usually found at these interfaces¹³. It will now take less energy to move an oil molecule to the interface (or to increase the surface of the oil), which means the surface free energy, or surface tension, has been lowered. This is the way dispersants make small droplets out of large oil slicks.

2. Experimental

This chapter will cover what samples are being examined and mixing of these samples, O/W emulsion formation, the use of the QCM-D apparatus and the measurement of contact angles, respectively. The cleaning procedures of the crystals and the devices used will also be mentioned. A risk assessment of the experiments was performed, this assessment is found in appendix A.

2.1 Crude oils and sample preparation

16 different crude oil samples were received from SINTEF SeaLab. The types of oils examined, if they contain dispersants, and to which extent they are weathered, is displayed in table 2.1. The types of oil are also marked with what type of compounds they contain more of than other oils (e.g. asphaltic or paraffinic).

Table 2.1: Oil fractions used in experiment.

Weathering Oil type	Fresh	200°C+ (up to 24 h at sea)	Fresh containing dispersant	200°C+ (up to 24 h at sea) containing dispersant
Grane (Asphaltic)	X	X	X	X
Norne (Waxy)	X	X	X	X
Gullfaks A (Naphthenic)	X	X	X	X
Oseberg (Paraffinic)	X	X		
Sture blend (Paraffinic)			X	X

The dispersant used was Corexit 9500, which contains both nonionic and anionic surfactants¹⁵. The oil samples were firstly heated to 50°C, shaken, allowed to cool to room temperature and then shaken once more. This was done to make sure the oil mixes were homogenous. The oil fractions were diluted to 10 weight percent (wt%) oil with toluene, a nonpolar (oleophilic) solvent. This was done to decrease the effect of difference in viscosity between the oils, and to make the samples more manageable when used in the QCM-D apparatus. For each sample, 2.0 grams of oil were added to a glass vile, before toluene was added until the vile contained 20.0 grams of solution. A screw-on cap was put on the vial immediately after the sample was prepared to prevent volatile components of the oil or toluene from evaporating.

2.2 Emulsion production

The oil-in-seawater emulsions were mixed using the Ultra Turrax T25 device, shown in figure 2.1.



Figure 2.1: Dispersing instrument Ultra Turrax T25¹⁶.

At first, 1 wt% oil was mixed in seawater at 1400 revolutions per minute (rpm) for ten minutes. This amount of oil did not mix well for most of the oil types, and coalesced over the sea water immediately after the device was switched off. An increase in rpm and an increase of mixing time were attempted, but neither of these actions created stable emulsions. The same was experienced for most oil types when 0.5 wt% oil was utilized. When 0.1 wt% was used, all of the oil types mixed completely with the sea water, and did not separate for over four hours. This was a sufficient time span for the emulsions to be used in the QCM-D experiments.

2.3 QCM-D measurements

2.3.1 Crystal cleaning methods

The quartz crystals used to model the shoreline in this experiment had an active side of either silica (SiO_2), aluminosilicate ($\text{AlSi}_2\text{O}_6^-$) or calcium carbonate (CaCO_3). To get a decent result of the QCM-D, the crystals used had to be cleaned⁶. The crystal cleaning procedure for the silica and aluminosilicate crystals is shown in table 2.2. The calcium carbonate crystals were cleaned using only points 1, 2, 3 and 6 in the table below. These crystals are more sensitive to cleaning than e.g. the silica crystals, and were not treated with SDS since this could have degraded the crystal coating, after recommendation from the crystal manufacturers, q-sense.

Table 2.2: Cleaning procedure of quartz crystals with silica or aluminosilicate coating.

Cleaning method	Time [minutes]
1. Washing with Milli-Q water, ethanol and Milli-Q water again, then blow dried	5-10
2. Treatment in UV chamber	10
3. Washing with Milli-Q water, ethanol and Milli-Q water again, then blow dried	5-10
4. Treatment in 2 wt% sodium dodecyl sulfate (SDS) in Milli-Q water	30
5. Washing with Milli-Q water, ethanol and Milli-Q water again, then blow dried	5-10
6. Treatment in UV chamber	10

2.3.2 Oil-in-toluene experiments

After being cleaned, a crystal was mounted into the QCM-D apparatus. To get a stable baseline for the actual measurements, toluene was added to the machine first. A stable baseline is important to get stable results, and toluene was used since this is also the solvent the oil samples are diluted with. The temperature for the execution of all experiments was room temperature, $21 \pm 0.5^\circ\text{C}$. First, about 3 ml of toluene was added through the loop, seen in figure 2.2, to stabilize the temperature of the sample. The apparatus was initiated, and the initial f and D (frequency and dissipation) of the crystal were found. Then, 2 ml of toluene was added through the sensor. A significant drop in frequency and increase in dissipation occurred, and after 15-20 minutes, both of the parameters usually stabilized. These parameter values were to be used as the baseline, so the f and D values of the crystal were found once more. The baseline varied with about ± 3 Hz as the actual experiments were started.

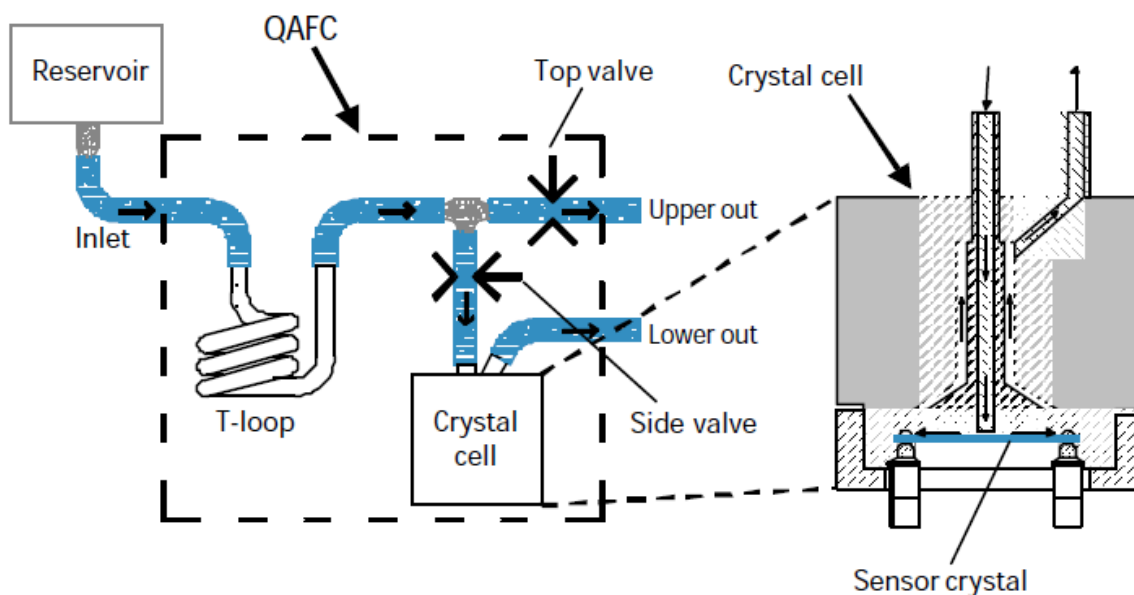


Figure 2.2: Schematic illustration of a QCM-D apparatus. QAFQ stand for Q-sense Axial Flow Chamber⁶.

The oil sample was added to the syringe, and 3 ml were added through the loop of the apparatus. The measurement of the sample was started. The few first minutes, no oil sample was added; this is to make sure that the baseline is stable. This can be seen in figure 2.3, which is a sample result from a QCM-D measurement.

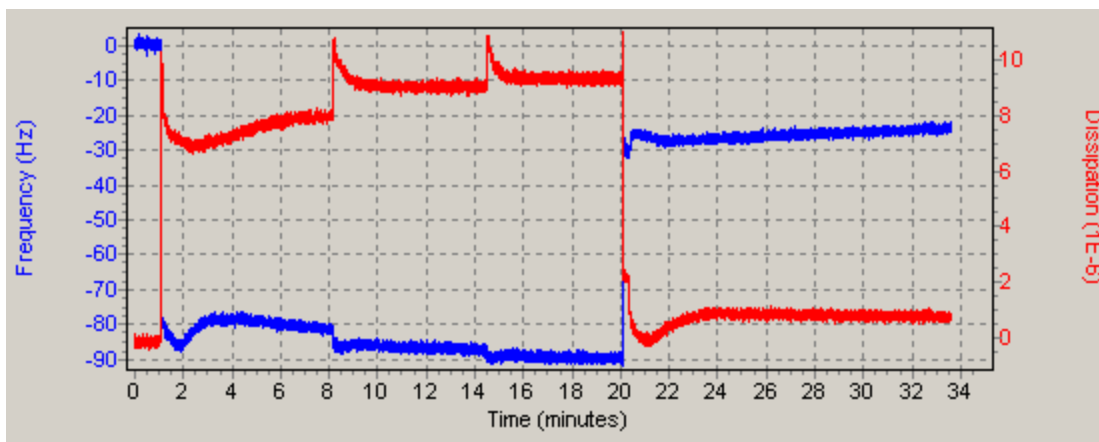


Figure 2.3: Sample result of an oil-in-toluene QCM-D measurement.

After the first few minutes, 2 ml of oil is added through the sensor crystal. A drop in frequency and increase in dissipation were noted, and the parameters stabilized after about ten minutes. Again, 2 ml of sample was added, the frequency decreased further whilst the dissipation increased. The oil sample was added four times to get a stable frequency and dissipation values although oil was still being added. Between the third and fourth addition, there was usually little change in both parameters. Lastly, 2 ml of toluene was added to wash excess oil off the crystal (after 20 minutes in figure 2.3), so that the only components of the oil remaining are the ones that have attached to the crystal. The now oil coated crystal was washed with some Milli-Q water (ultra-pure deionized water) and blown dry, before the contact angle of the crystal was measured. The QCM-D apparatus was rinsed with ethanol and Milli-Q water before it was blown dry, as described in the Q-sense manual⁶.

2.3.3 Oil-in-seawater (emulsion) experiments

In the emulsion experiments as in the oil-in-toluene experiments, a stable baseline is required to obtain usable results. Here, seawater was used as a baseline instead of toluene. The procedure of making a stable baseline was the same as when the toluene baseline was made for oil-in-toluene samples, with the exception that the seawater was left to stabilize for a slightly longer time, 25-30 minutes. The frequency drop from air to seawater was somewhat larger than from air to toluene, and the stabilized baseline was a bit more unstable than the toluene baseline, up to ± 5 Hz as the oil-in-seawater experiments were started.

The emulsion experiments were performed as the ones with oil-in-toluene samples. Figure 2.4 shows that an oil emulsion was added four times, 2 ml each time, with time to stabilize in-

between. However, after the last 2 ml of emulsion were added and was given time to stabilize, Milli-Q water was added instead of seawater to wash away the excess oil on the crystal, after about 29 minutes in figure 2.4. This was done because an addition of seawater to the oil coated crystal caused the frequency to drop critically, which could be an effect of the seawater bonding to the components of the oil adsorbed onto the crystal. The difference between seawater and Milli-Q water was made up for by measuring the frequency increase when adding 2.0 ml of Milli-Q water to the seawater baseline, and including this difference when calculating the mass adsorption of the emulsified oils on the crystals. An example calculation of the mass adsorbed onto a crystal from an oil-in-seawater emulsion can be found in appendix B.

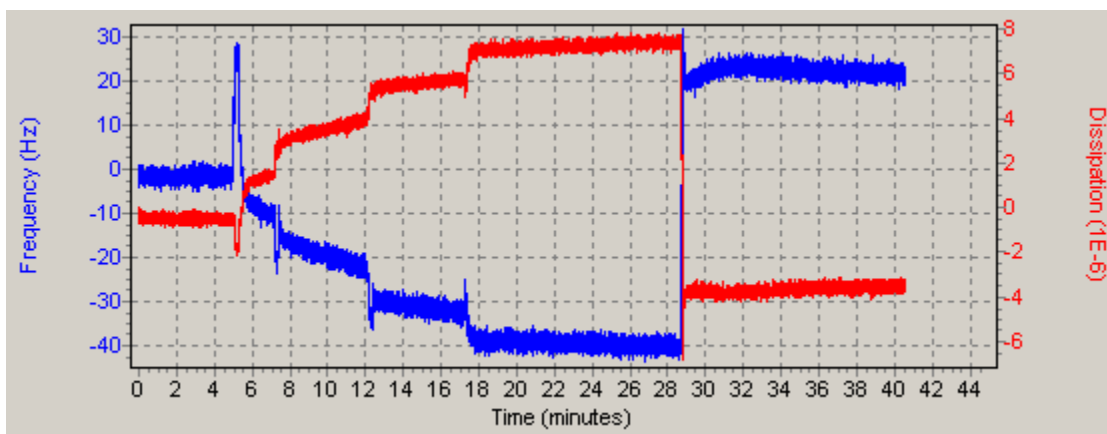


Figure 2.4: Sample result of an oil-in-seawater QCM-D measurement.

2.4 Contact angle measurements

The CAM200 apparatus is set up as seen in figure 2.5, and this apparatus is connected to a computer containing software which analyzes the contact angle. The room containing the apparatus was kept dark, so that no external light would afflict the measurements.

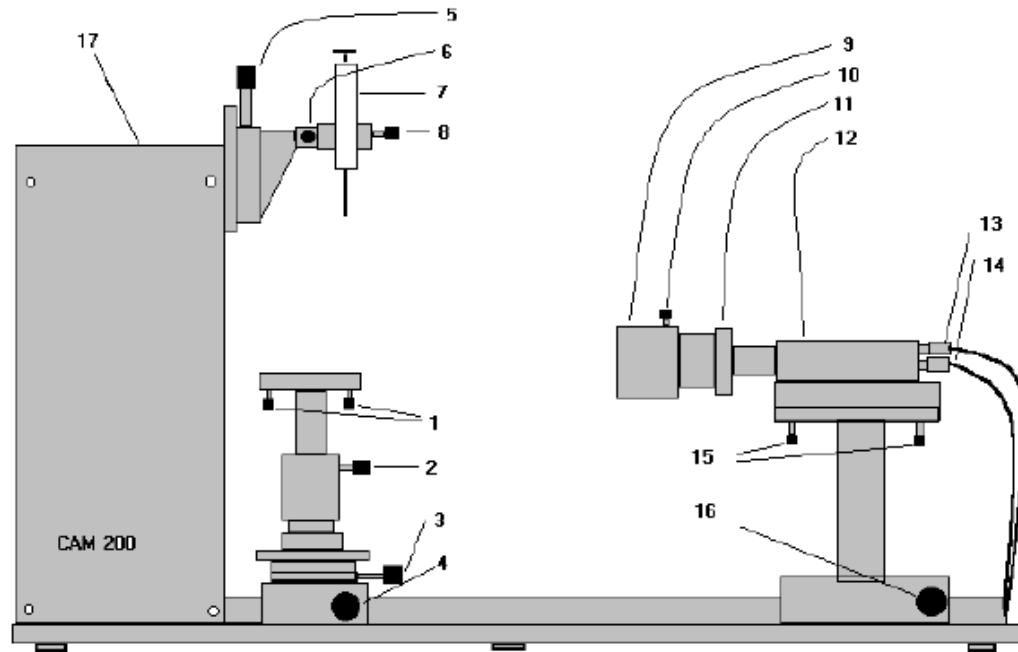


Figure 1.

- | | |
|-------------------------------|-------------------------------------|
| 1) Stage level adjustment | 9) Camera lens zoom |
| 2) Stage height adjustment | 10) Camera zoom lock |
| 3) Stage lateral adjustment | 11) Lens aperture adjustment |
| 4) Stage linear adjustment | 12) CCD Camera |
| 5) Syringe height adjustment | 13) Light Synchronizing cable |
| 6) Syringe lateral adjustment | 14) Video Out cable |
| 7) Syringe | 15) Camera level adjustment |
| 8) Syringe clamp | 16) Camera Linear Adjust (focus) |
| | 17) Light source and Interface Unit |

Figure 2.5: Experimental setup of the contact angle measurement¹⁰.

A clean syringe was filled with sea water which held room temperature, provided by SINTEF SeaLab. A quartz crystal coated with an oil film in the QCM-D was placed on the stage of the apparatus. The crystal had previously had its contact angle measured, before oil coating was applied. This way, the change in contact angle before and after application of oil could be calculated. The QCM-D and contact angle measurements were performed on the same day, so

that the oil coating on the crystal would have little time to deteriorate. The syringe of the CAM 200 apparatus was brought much closer to the stage than shown in figure 2.5. This was done to place the droplets gently onto the crystal, to be able to do multiple measurements on the small area of the crystal. A droplet of sea water was added gently to the crystal, and the contact angle of the droplet was measured by the camera. Three or four droplets of sea water were added, depending on how much the droplet wet the crystal. If the droplets wet the crystal greatly, there was no room for a fourth measurement. The contact angle measurements were done in the exact same way for oil-in-toluene and oil-in-seawater experiments. After the measurements, the crystals were cleaned as described as in subchapter 2.2.1. The syringe was cleaned with Milli-Q water and toluene, and then blown dry.

3. Results and discussion

In this chapter, the results from all the fresh and weathered oils from each oil field mixed in toluene without dispersants for all three crystal types will be presented, compared and discussed. Then, all fresh and weathered fractions of oil types containing dispersants (also mixed in toluene) will be presented and discussed. These results will also be compared with the oil types not containing dispersants. All of the results from the oil-in-seawater experiments will then be presented, compared internally and discussed, before they are compared with the results from the oil-in-toluene experiments. The results will be presented in the crystal coating order *silica – aluminosilicate – calcium carbonate* for each experiment, to easier find and compare results.

Since many parameters were varied, giving 72 different experiments (four oil types with two different weathered fractions, three different crystals and three types of experiments), and all experiments were measured both in the QCM-D and the CAM 200 devices, there were not performed three parallels of each experiment. To investigate the reproducibility of the experiments, one of each of the experiments; oil-in-toluene without dispersants, oil-in-toluene with dispersant and oil-in-seawater, were each performed three times on the same crystal with the same fraction of the same oil. That is, the same experiment used the exact same crystal and crude oil for the three reproducibility trials, but when the experiment was changed (from e.g. oil-in toluene without dispersant to oil-in toluene with dispersant), the crystal type and oil type were also changed. This way, reproducibility was tested on all crystals and most of the oil types. The graphs of the reproducibility experiments are found in appendix C (figures C.1.6 a-c, C.2.19 a-c and C.3.13 a-c). Table 3.1 shows the reproducibility of the experiments, and which oil samples and crystal coatings that have been tested.

Table 3.1: Reproducibility of each experiment, showing oil sample and crystal coating used.

Experiment	Oil-in-toluene without dispersant	Oil-in-toluene with dispersant	Oil-in-seawater Emulsion
Sample	Oseberg, 200°C+	Gullfaks, fresh	Norne, 200°C+
Crystal coating	Silica	Calcium carbonate	Aluminosilicate
Mass adsorbed (mg/m ²)	2.242±0.944	2.006±0.649	0.512±1.121

The mass adsorbed is calculated with the Sauerbrey equation (equation 1.1), and sample calculations for the different experiments are found in appendix B. In the calculations, the proportionality constant C used is $0.177 \text{ mg}/(\text{Hz m}^2)^{17, 18}$ and the overtone number considered in the QCM-D measurement is the third one, so n equals three. This overtone number was chosen since it was found to be more easily stabilized in comparison to the fundamental frequency.

3.1 Results of experiments using oil-in-toluene without dispersants

3.1.1 Results of oil-in-toluene without dispersants – fresh oil samples

Figure 3.1 shows the values from when the fresh oil samples from the four oil fields Norne, Oseberg, Gullfaks A and Grane were applied to the silica crystals. The blue columns along with the leftmost axis show the contact angle of the crystals after the different oil coatings were applied. The masses adsorbed calculated from the changes in frequency are found from the red columns, using the rightmost y-axis.

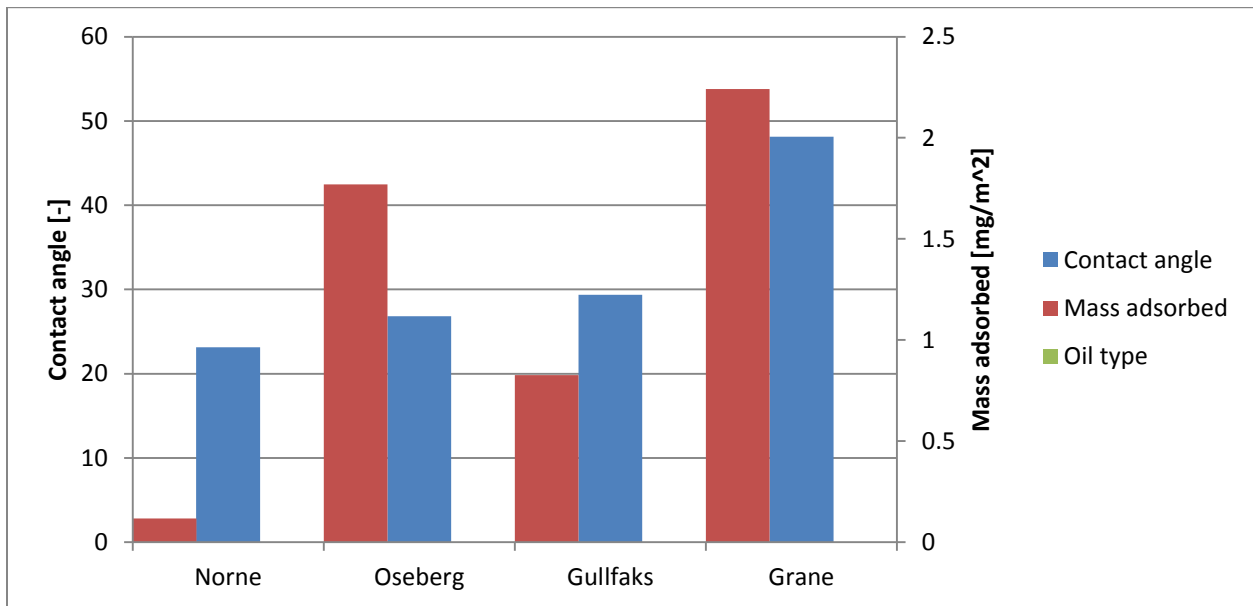


Figure 3.1: Contact angle and adsorbed mass of the four fresh samples of the Norne, Oseberg, Gullfaks A and Grane oil types on a silica crystal.

Figure 3.1 shows that the fresh oil from the Grane oil field, an oil type with high content of asphaltic components, has high values of both adsorbed mass (2.242 mg/m^2) and contact angle (48.13 degrees) on the silica crystal. The figure also shows that the three other oils are all in the same area with respect to contact angle value, around half of the value of the Grane oil. This means that salt water coming in contact with silica with these oil types covering it, will wet the silica more than it would the asphaltic oil. From equation 1.3, since γ_{LV} and γ_{SV} stays the same for the experiments, an increase in contact angle equals an increase in interfacial tension between the seawater and the oil coated crystal, γ_{SL} . The paraffinic Oseberg oil has a higher adsorbed mass than the naphthenic Gullfaks oil, and the waxy Norne oil has a very low adsorbed mass compared to the other samples.

As mentioned in the theory, the asphaltene group contains heteroatoms like oxygen, nitrogen and sulfur. The high percentage of heteroatoms shows that asphaltenes are highly polar compounds, and contain numerous functional groups¹⁹. Some compounds where these heteroatoms are included are carboxylic acids and hydroxyls for oxygen, pyridine and NH for nitrogen, different sulphide groups for sulfur, and heterocycles for both oxygen and sulfur¹⁹. When dissolved in toluene, the asphaltenes will form molecular aggregates. The silica coated crystal surface consists of siloxane and silanol, the latter of which can occur as silanol groups or as SiOH pairs which are hydrogen bonded. These polar sites of silanol may have acted as adsorption sites for the polar asphaltic aggregates, where van der Waals forces and hydrogen bonds are the major interactions¹⁹. The lower adsorption values of the oil samples containing more resins fits well with the theory that the resins form a rigid monolayer, and that individual molecules are present on the crystal surface rather than molecular aggregates²⁰. However, in solutions where both resins and asphaltic complexes are present, these two types of compounds may adsorb to the crystal surface as mixed aggregates, which might be the case for the Grane sample especially²¹.

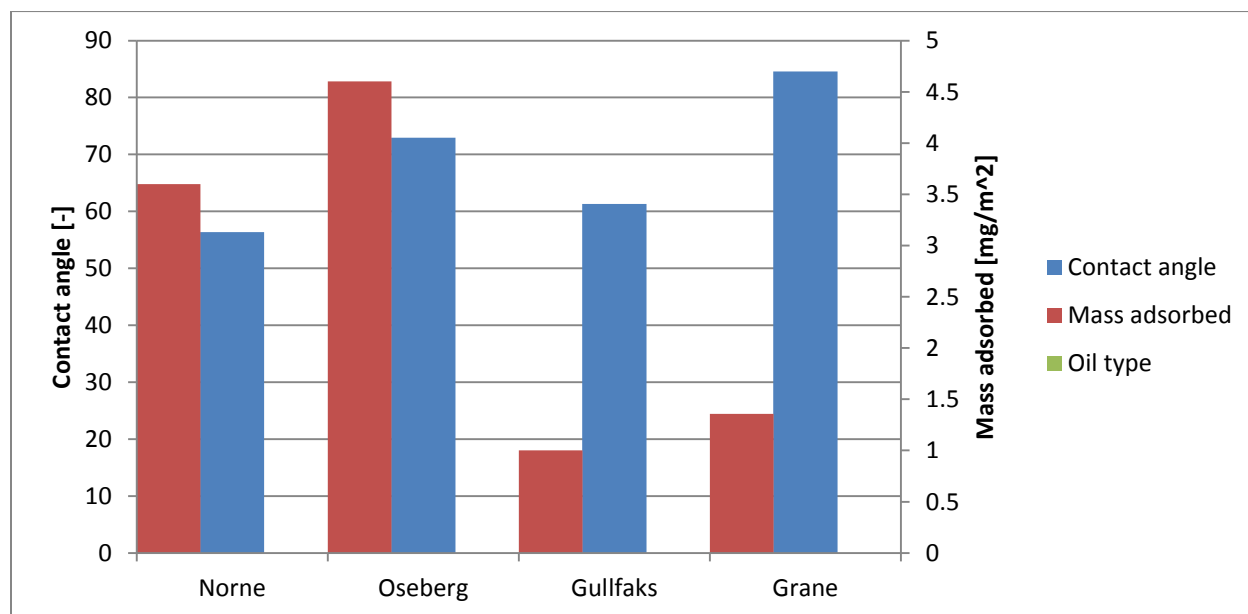


Figure 3.2: Contact angle and adsorbed mass of the four fresh samples of the Norne, Oseberg, Gullfaks and Grane oil types on an aluminosilicate crystal.

For the fresh oil samples on the aluminosilicate crystal, figure 3.2 shows that the paraffinic Oseberg oil has the highest adsorbed mass on this kind of crystal coating, with 4.602 mg/m². The Norne oil also adsorbs a great deal on the crystal, whilst the Gullfaks A and Grane oil adsorbs to a lesser extent. Comparing these mass adsorption values to the ones found on the silica coated crystal, it is seen that the Oseberg and Norne oil samples adsorb a great deal more on the

aluminosilicate crystal than on the silica crystal, whilst the Grane sample adsorbs less. The Gullfaks oil sample has a similar value for both crystal coatings.

When observing the contact angle values, it is noted that the Grane oil has the highest value in figure 3.2 as in figure 3.1, but that the value for the Oseberg oil is not as low and similar to the Norne and Gullfaks values. The contact angle values are in general much higher for the aluminosilicate coating than for the silica coating; this is due to the fact that a clean aluminosilicate crystal has a contact angle of 43.06 degrees, whilst a clean silica crystal has a contact angle of 14.21 degrees. A comparison of the change in contact angle (from clean to oil coated crystal) of these two crystal coatings as well as the calcium carbonate coating, with a clean crystal contact angle of 60.12 degrees, is found in table 3.2. This comparison is done to see the effect the oil coating has on the wettability of the different crystal coatings.

The fact that the aluminosilicate coating adsorbs less of the asphaltic oil than the silica coating, could be because the anionic sites of this coating makes it less reactive with hydrogen-bonding compounds²². The anionic sites may bond with another compound found in the crude oil, which may work as a cationic counter-ion and hinder the molecular aggregates that form hydrogen bonds from reaching the crystal surface. The waxy and paraffinic oils, Norne and Oseberg, adsorb much more on the aluminosilicate coating than the silica coating. This might be explained with the fact that aluminosilicate may be more hydrophilic than silica, and adsorption of a more tightly packed monolayer of resins might be a possibility, but there has been found little in the literature confirming this.

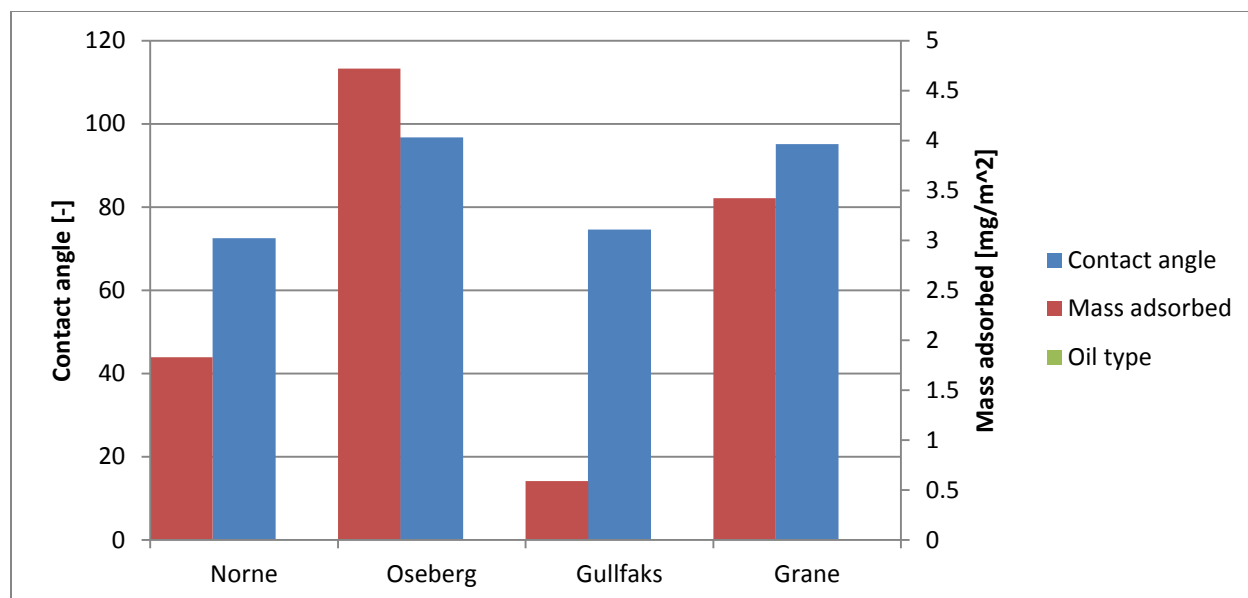


Figure 3.3: Contact angle and adsorbed mass of the four fresh samples of the Norne, Oseberg, Gullfaks and Grane oil types on a calcium carbonate crystal.

Figure 3.3 shows the mass adsorbed and change in contact angle for the fresh samples of the waxy, paraffinic, naphthenic and asphaltic oil types, respectively from left to right. The mass adsorption value of the Grane oil sample on the calcium carbonate coating is higher than the values for the two previous coatings, whilst the Gullfaks A oil sample value is a bit lower. The Oseberg value is the about the same as for the aluminosilicate coating, more than double the value of the silica coating. The Norne value in figure 3.3 lies between the values of the two other coatings. As in figure 3.2, the Oseberg and Grane oil samples have the highest contact angle values, with similar lower values for the Norne and Gullfaks samples. The contact angles in figure 3.3 are in general higher than for the values of the other crystal coatings, this could be because the clean calcium carbonate crystal has a higher contact angle than the other two crystal coatings, as seen in table 3.2.

The fact that all mass adsorption values, except for the Gullfaks A sample, are much larger for the samples in figure 3.3 than in figure 3.1, could be explained by the fact that the calcium carbonate coating is more hydrophilic than the silica coating²³. Adsorption of surfactants from nonaqueous solutions like in this experiment seems to mainly be governed by polarity differences between the solution and the crystal surface.

3.1.2 Results of oil-in-toluene without dispersants – weathered (200°C+) oil samples

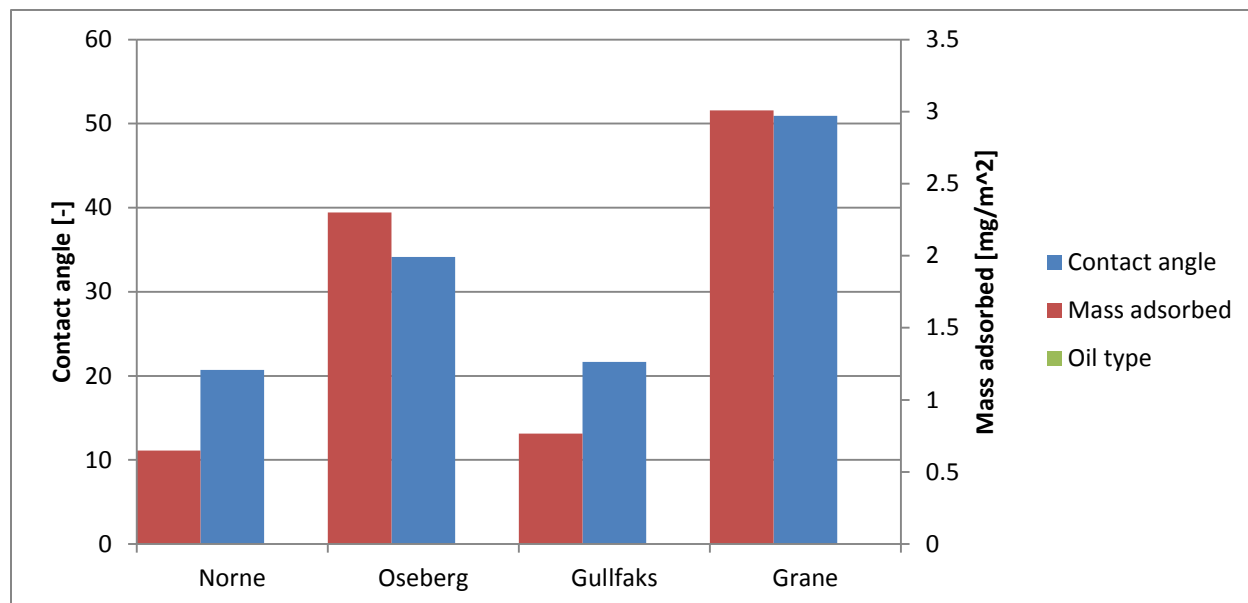


Figure 3.4: Contact angle and adsorbed mass of the four weathered (200°C+) samples of the Norne, Oseberg, Gullfaks and Grane oil types on a silica crystal.

In figure 3.4, the mass adsorption for the Grane oil sample at 200°C+ (up to 24 hours at sea) on a silica crystal has a higher value than the other three oil types. The Oseberg oil sample adsorbs the second most, not as much as the Grane sample, but over twice as much as the Norne and Gullfaks A samples. These trends are very similar to the fresh oil samples on the same crystal coating shown in figure 3.1, although all of the mass adsorption values have increased except the Gullfaks sample value which has decreased slightly. The contact angle values seem to follow the mass adsorption values somewhat more in figure 3.4 than in figure 3.1, but the values are quite similar for the fresh and weathered samples of each crude oil.

In an earlier study, crude oils had large losses of light components like alkanes with low molecular weight and monoaromatic hydrocarbons as a result of weathering²⁴. An explanation of the increase in mass adsorption from figure 3.1 to figure 3.4 could be that since these light components have been removed, the heavier components that bond with the silica surface have better access to the binding sites (SiOH pairs).

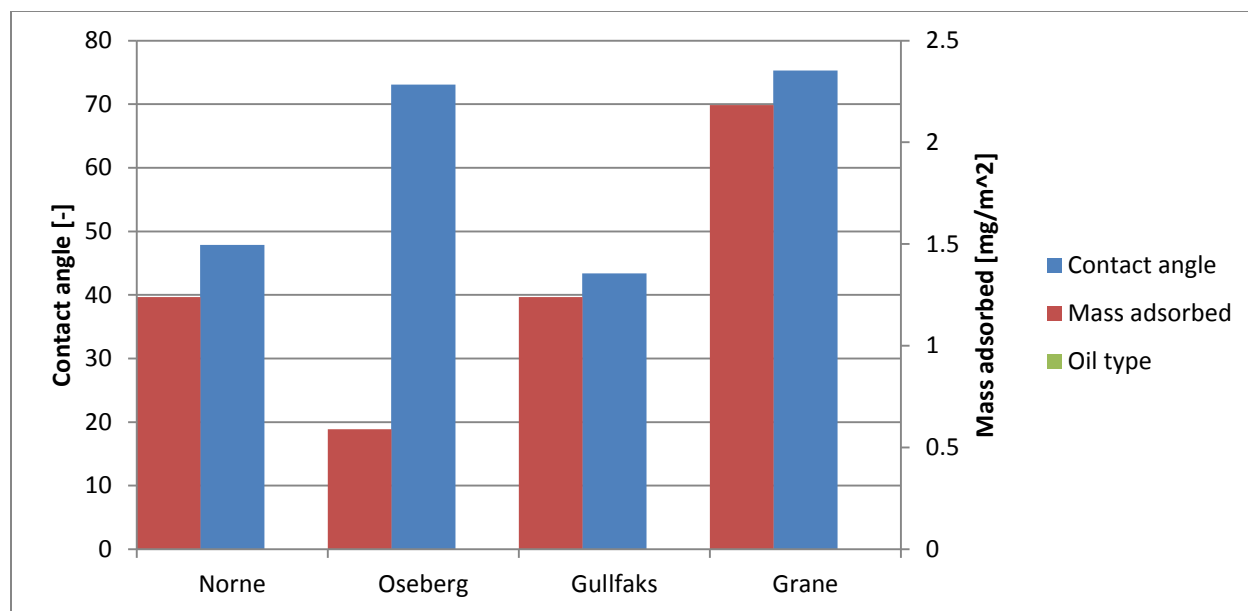


Figure 3.5: Contact angle and adsorbed mass of the four weathered (200°C+) samples of the Norne, Oseberg, Gullfaks and Grane oil types on an aluminosilicate crystal.

The values of mass adsorption on the aluminosilicate crystal of the weathered fractions of the different oil types in figure 3.5 are quite dissimilar to the values of the fresh fraction found in figure 3.2. The values of Norne and Oseberg samples decrease greatly, from 3.599 and 4.602 mg/m² in figure 3.2, to 1.239 and 0.590 mg/m² in figure 3.5. The Grane sample value increases, whilst the Gullfaks A sample value stays fairly similar for the two fractions.

Comparing the mass adsorption values in figure 3.5 to the ones for the same oil types on silica coated crystals in figure 3.4, it is seen that the Grane sample adsorbs the most for both types of coating, and the Norne and Gullfaks A sample values are similar to each other. The greatest difference in trends between these two figures is that the Oseberg oil sample value is much lower than the other samples in figure 3.4, whilst it in figure 3.5 this value is the second largest. The contact angle values in figure 3.5 seem to follow the mass adsorption values, except the Oseberg sample value which has a much higher contact angle compared to mass adsorption than the other oil samples.

An explanation of why the mass adsorption values of Norne and Oseberg decrease from figure 3.2 to figure 3.5 could be that the compounds that bind to the aluminosilicate crystal surface of are removed during weathering. The explanation for the Grane value increasing, could be the

same as for the results in figure 3.4; the compounds binding to the surface have better access to it after the low molecular weight alkanes are removed.

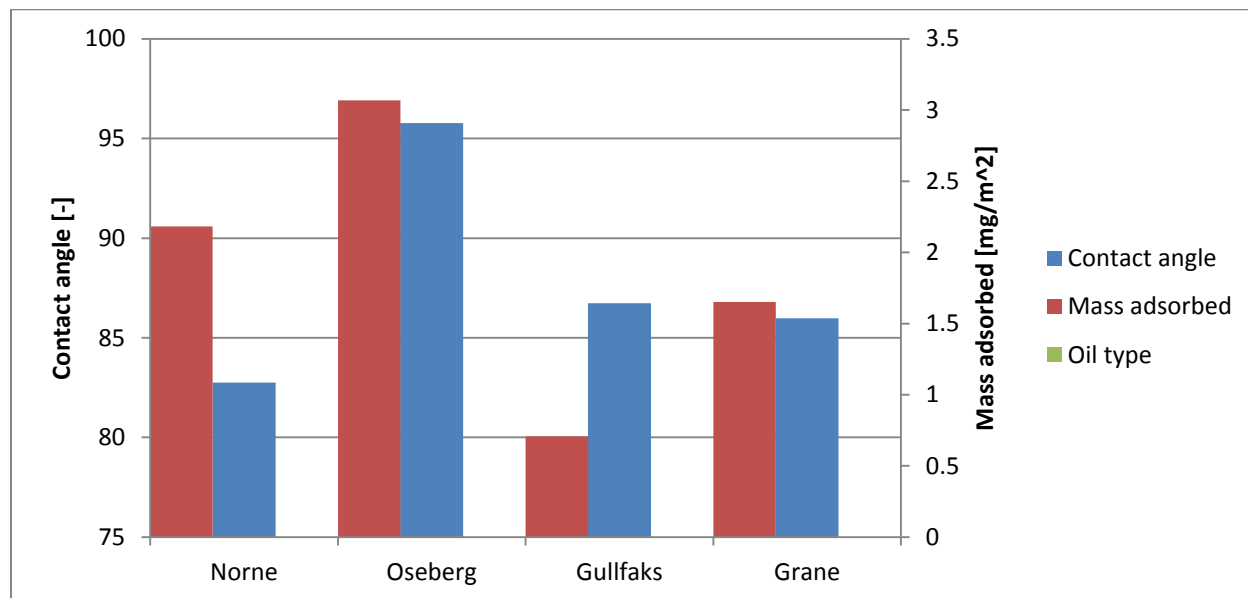


Figure 3.6: Contact angle and adsorbed mass of the four weathered (200°C+) samples of the Norne, Oseberg, Gullfaks and Grane oil types on a calcium carbonate crystal.

Comparing the weathered fractions of the different oil types on the calcium carbonate coated crystal in figure 3.6 to the fresh fractions in figure 3.3, it is seen that the mass adsorption values are in the same order, except that the value of the Grane is lower than the Norne sample value in figure 3.6. The Grane and Oseberg sample values decrease greatly from fresh to weathered fractions, whilst the value of the Norne sample decrease. The Gullfaks A sample value increases slightly, but the value stays in the same area as for all oil-in-toluene mass adsorption without dispersants (from 0.590 to 1.239 mg/m²). The contact angle values are similar for the oil samples in figure 3.3, except for the high value of the Oseberg sample, which also has the highest mass adsorption value.

Comparing the mass adsorption values of the weathered fractions on the calcium carbonate crystal to the values on the other crystal coatings, there are not many similar trends. The Gullfaks A sample has a quite low value on all three coatings, but the Grane sample is the highest on silica and aluminosilicate, not on calcium carbonate, the Oseberg sample has a high value on the silica and calcium carbonate coatings but not on the aluminosilicate, and the Norne sample has a low value on the silica coating, medium on the aluminosilicate, and quite large on the calcium

carbonate. The contact angle values tend to follow the mass adsorption for most of the samples of weathered fractions.

The high mass adsorption values of Norne and Oseberg may be explained with the fact that the calcium carbonate coating is, as mentioned, highly hydrophilic²³. It is observed that the Oseberg and Grane sample values drop from fresh to weathered samples, which could be explained by the loss of components that binds to this type of crystal coating during weathering, but this is not the case for the Norne sample.

3.1.3 Comparison of wettability

As previously mentioned, the contact angles of the clean crystal of the silica, aluminosilicate and calcium carbonate coatings when seawater droplets are applied to them are 14.21, 43.06 and 60.12 degrees, respectively. Subtracting these clean contact angles from the contact angles measured when oil is coated onto the crystals, the difference in wettability is found. The changes in contact angle are found in table 3.2.

Table 3.2: Changes in contact angle from clean to oil coated crystal for all oil-in-toluene experiments without dispersants.

Oil type \ Crystal coating	Norne Fresh	Oseberg Fresh	Gullfaks Fresh	Grane Fresh	Norne 200°C+	Oseberg 200°C+	Gullfaks 200°C+	Grane 200°C+
Silica	8.93	12.62	15.16	33.92	6.48	19.94	7.46	36.73
Aluminosilicate	13.28	29.88	18.22	41.54	4.83	30.02	0.33	32.22
Calcium carbonate	12.36	36.62	14.47	34.99	22.63	35.65	26.61	25.86

The contact angles in table 3.2 shows that the wettability of the crystal coatings tends to follow the mass adsorption values found in figures 3.1 to 3.6, especially for the silica and calcium carbonate crystal coatings. In general, the Grane oil type has a high change in contact angle, which means that the seawater does not wet the Grane covered crystals as much as the other oil covered crystals, and that the interfacial tension between the solid and liquid phase is higher. The Oseberg oil also has high contact angle values, whilst the Norne and Gullfaks values are usually lower. The change in contact angle for the experiments containing dispersants and for the emulsion experiments did not follow mass adsorption to the same extent and often gave negative results, which would suggest that the oil coatings reduce the interfacial tension beyond that of a clean crystal coating.

3.2 Results of experiments using oil-in-toluene with dispersants

3.2.1 Results of oil-in-toluene with dispersants – fresh oil samples

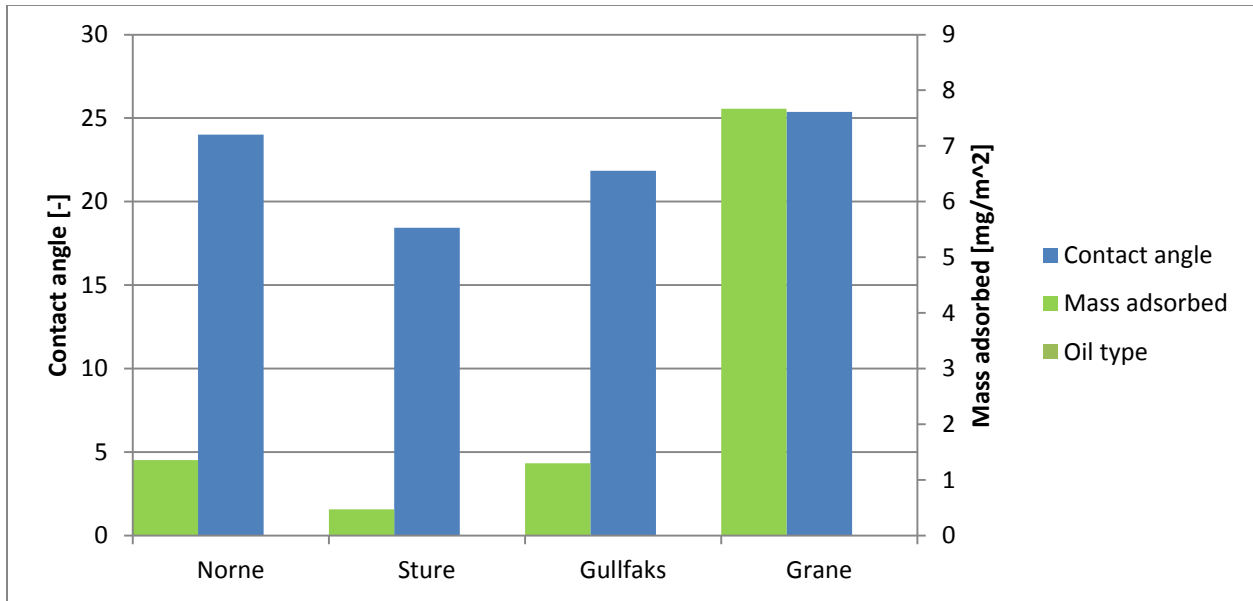


Figure 3.7: Contact angle and adsorbed mass of the four fresh samples of the Norne, Sture, Gullfaks and Grane oil types containing Corexit 9500 on a silica crystal.

Figure 3.7 shows the values of the contact angle (blue polls, leftmost y-axis) and mass adsorption (green polls, rightmost y-axis) for the fresh fractions of the four crude oils Norne, Sture, Gullfaks and Grane on silica coated quartz crystals. The oils contain 1:100 of the dispersant Corexit 9500, and are diluted to 10 wt% oil with toluene as the samples without dispersant. The figure shows that the mass adsorption value of the Grane oil sample is much higher than the value of the other three oil samples. The Norne and Gullfaks sample mass adsorption values are quite similar, whilst the Sture sample value is under half of these two values. The contact angle values are quite similar for all four oil samples, ranging from 18.44 to 25.38 degrees.

Comparing the oil samples with dispersants to the same oil types without dispersants in figure 3.1, the fact that the Grane oil adsorbs the most is the same for both experiments, but the difference in value between this oil and the other three is much more significant where dispersant is added. The Gullfaks oil sample increases from figure 3.1 to figure 3.7, and the Norne oil increases greatly. The contact angle values for oil samples both with and without dispersants lie in the same area, except for the high value of the Grane oil sample in figure 3.1.

The fact that some oil types decrease and some increase, might be because the effectiveness of the dispersant is dependent on the composition of the oil. In literature, the dispersant effectiveness is found to correlate positively with high saturate concentration, and correlate negatively with high concentration of asphaltic and aromatic compounds²⁵. It is also written that some components of crude oils, such as asphaltenes, large waxes and large aromatics, are barely or possibly not at all dispersible, whilst oils containing mainly saturates are easier to disperse, naturally and using dispersants²⁶. This information fits well with the strong decrease of the paraffinic Oseberg oil and the strong increase of the asphaltic Grane oil from figure 3.1 to figure 3.7, and could possibly explain the increases in both the waxy Norne oil and the naphthenic Gullfaks A oil.

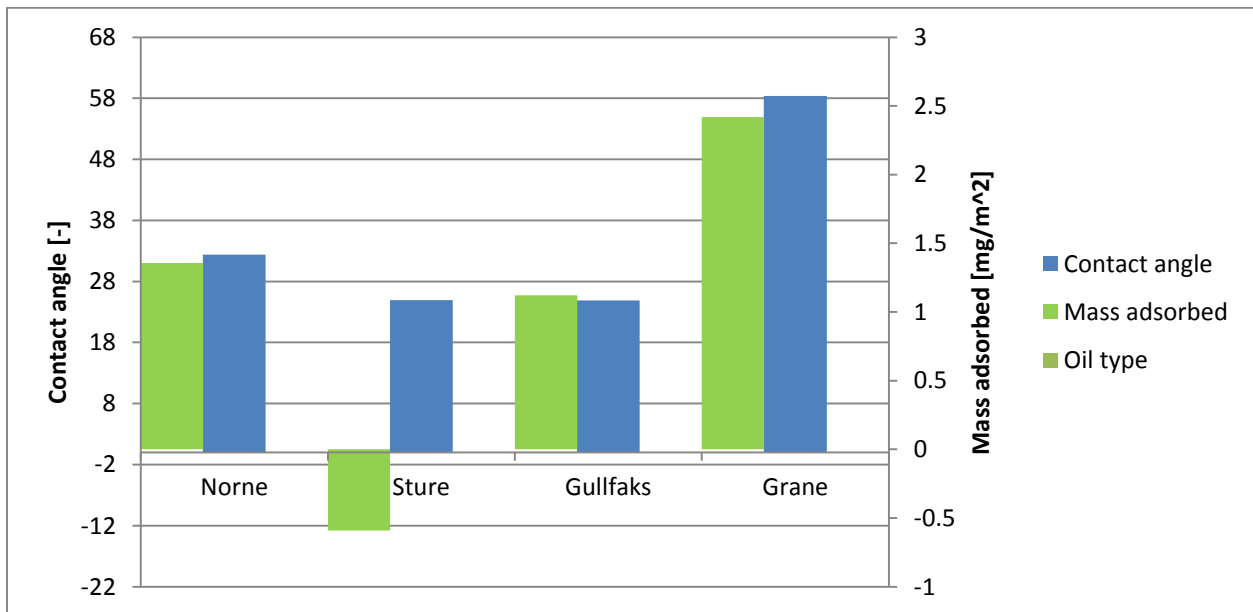


Figure 3.8: Contact angle and adsorbed mass of the four fresh samples of the Norne, Sture, Gullfaks and Grane oil types containing the dispersant Corexit 9500 on an aluminosilicate crystal.

In figure 3.8, the values of the fresh oil samples containing dispersants on aluminosilicate coated crystals are shown. The mass adsorption value of the Grane sample is higher than the other sample's values, but not to the great extent as for the silica crystal in figure 3.7. The adsorption values of the Norne and Gullfaks A samples are equal, and very similar to the values for these

samples in figure 3.7. The Sture sample again has the lowest mass adsorption value, but in figure 3.8, this value is negative, an explanation for this negative value for an oil-in-toluene experiment has not been found. The contact angle values for the oil samples in figure 3.8 are similar and in the same area as the values in figure 3.7 (somewhat higher), except for the Grane sample value, which is twice the value of the others and seem to follow the mass adsorption.

Comparing the same oil samples on the aluminosilicate coated crystals with and without dispersants (figure 3.8 and figure 3.2 respectively), there is hard to find similarities or trends. Of the three oil samples found in both figures, Norne adsorbs the most mass without dispersant, with dispersant Grane adsorbs the most. Neither of the values are close to each other between the figures. The only similar mass absorption value between these two graphs is the Gullfaks A sample value, which lies in the same area for all of the figures 3.1-3.8. The contact angle values in figure 3.2 are much higher than in figure 3.8, with the similarities that the Grane sample value is the largest one, and the Norne and Gullfaks values are quite similar. The lower values in figure 3.8, even lower than the clean coating for three oil samples, could be explained by the fact the dispersant is applied to reduce interfacial tension, and lower contact angle values equal a lower tension between the oil coating and the seawater, γ_{SL} .

The changes in mass adsorption from figure 3.2 to figure 3.8 seem to be somewhat similar to the changes for the silica coating (figure 3.1 to figure 3.7); the Corexit 9500 seems to disperse the paraffinic Oseberg oil, but have a negative effect on the dispersing of the naphthenic Gullfaks and asphaltic Grane oil types. This seems to fit with what found in literature^{25, 26}. However, the Norne oil decreases from figure 3.2 to figure 3.8, unlike for the silica coating. This may be because of the difference in hydrophobicity, aluminosilicate being more hydrophilic, and the fact that the components of the crude oils bond differently to the two crystal surfaces.

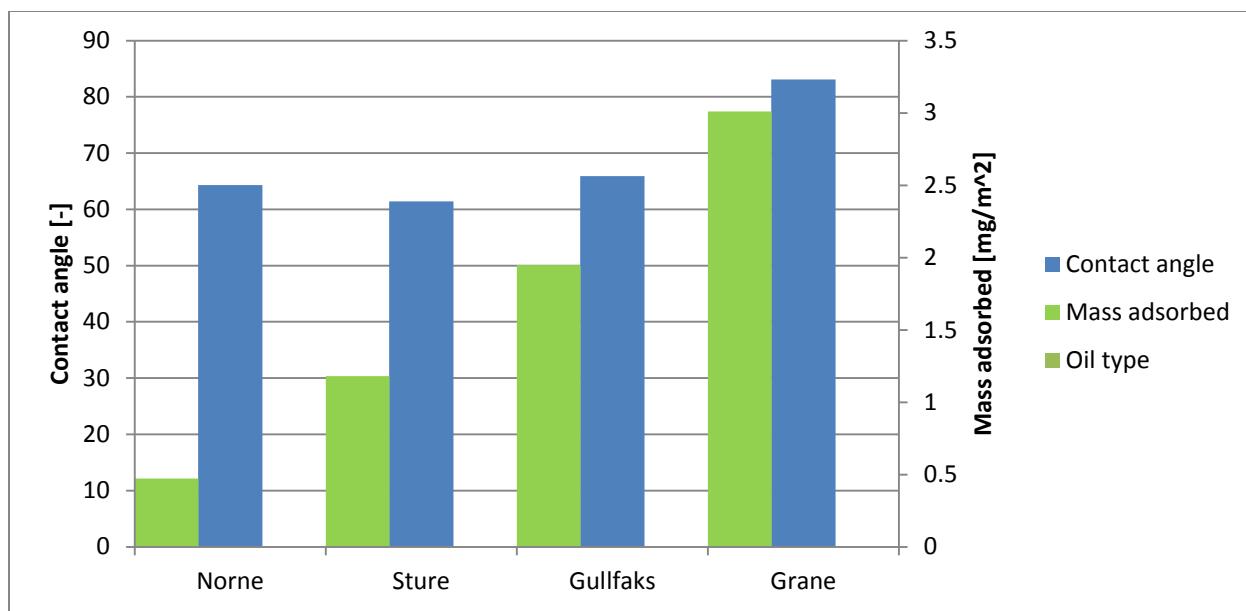


Figure 3.9: Contact angle and adsorbed mass of the four fresh samples of the Norne, Sture, Gullfaks and Grane oil types containing the dispersant Corexit 9500 on a calcium carbonate crystal.

As for the silica and aluminosilicate coated crystals, the mass adsorption value of the Grane sample containing dispersants is the highest for the calcium carbonate coated crystal, as seen in figure 3.9. This value is somewhat higher than the value of the same sample in figure 3.8. The mass adsorption value of the Norne sample is lower, and the Sture and Gullfaks sample values are higher than the values of the same samples in both figure 3.7 and 3.8. The contact angle value of the Grane sample is higher than the other three contact angle values, which seem similar to each other. This tendency is found in both figure 3.8 and figure 3.9.

There are found few similarities when comparing the oil samples with and without dispersants on calcium carbonate crystals (figure 3.9 and figure 3.3, respectively). The Grane sample has the highest mass adsorption value of the three oil samples found in both figures, and the value is quite similar with and without dispersants. The Norne value is much higher in figure 3.3, whilst the Gullfaks value is much higher in figure 3.9. In both experiments, the contact angle value of the Grane sample is higher than the Norne and Gullfaks sample values, these two being similar to each other. All three contact angle values are around ten degrees lower when dispersants are added, a result that shows the reduction of interfacial tension.

The mass adsorption value paraffinic oil decreases when the dispersant is added (figure 3.3 to figure 3.9), and the naphthenic oil increases. This is what is expected from literature^{25, 26}, but the waxy Norne oil decreases as it does for the aluminosilicate coated crystal, which is opposite as for the silica coating and literature findings. Also, the Grane adsorption value decreases slightly, which is opposite behavior from the other crystal coatings.

3.2.2 Results of oil-in-toluene with dispersants – weathered (200°C+) oil samples

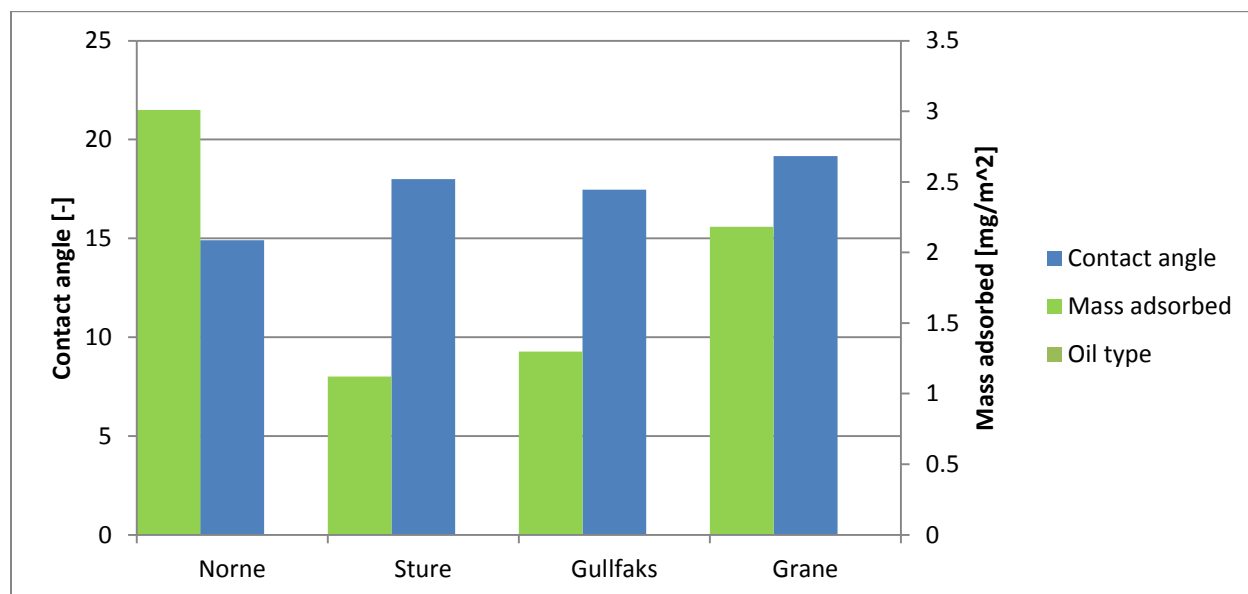


Figure 3.10: Contact angle and adsorbed mass of the four weathered (200°C+) samples of the Norne, Sture, Gullfaks and Grane oils types containing the dispersant Corexit 9500 on a silica crystal.

The values of mass adsorption and contact angle on silica coated crystals of the four weathered (200°C+) crude oils containing dispersant is found in figure 3.10. In this figure, the mass adsorption value of the Norne sample is the highest, whilst Grane is the second highest. The adsorption value of the Gullfaks A sample is in the same range as in all of the previous figures, and the Sture sample again has the lowest value. The contact angle values in figure 3.10 are quite similar, with the Grane sample having the highest value.

Compared to the values of the fresh oil fractions with dispersants on silica coated crystals in figure 3.7, the largest differences is that the mass adsorption value of the Grane sample in figure 3.10 is much lower than in figure 3.7, even lower than the Norne sample value, which is almost

three times larger in figure 3.10 than in figure 3.7. The Gullfaks A sample adsorption value is equal for both these experiments, and the Sture sample has a higher value with dispersants than without, as the Norne sample.

Comparing the values in figure 3.10 to the values of the same oil samples where dispersants are not added, in figure 3.4, there are big differences. The mass adsorption value of the Norne samples in figure 3.10 is much larger than the value in 3.4, the Gullfaks sample is also higher, but the Grane sample has a lower value. In figure 3.4, the contact angle values seem to follow the mass adsorption values of the different oil samples, this is not the case in figure 3.10, where the contact angle values are gathered in the same range.

The weathered oil samples on silica act mostly as the fresh samples with addition of dispersant (figure 3.4 to figure 3.10); an increase in mass adsorption for the waxy and naphthenic oils, and a decrease for the paraffinic oil type. These changes are expected from literature^{25, 26}, but the slight decrease of the asphaltic oil is not.

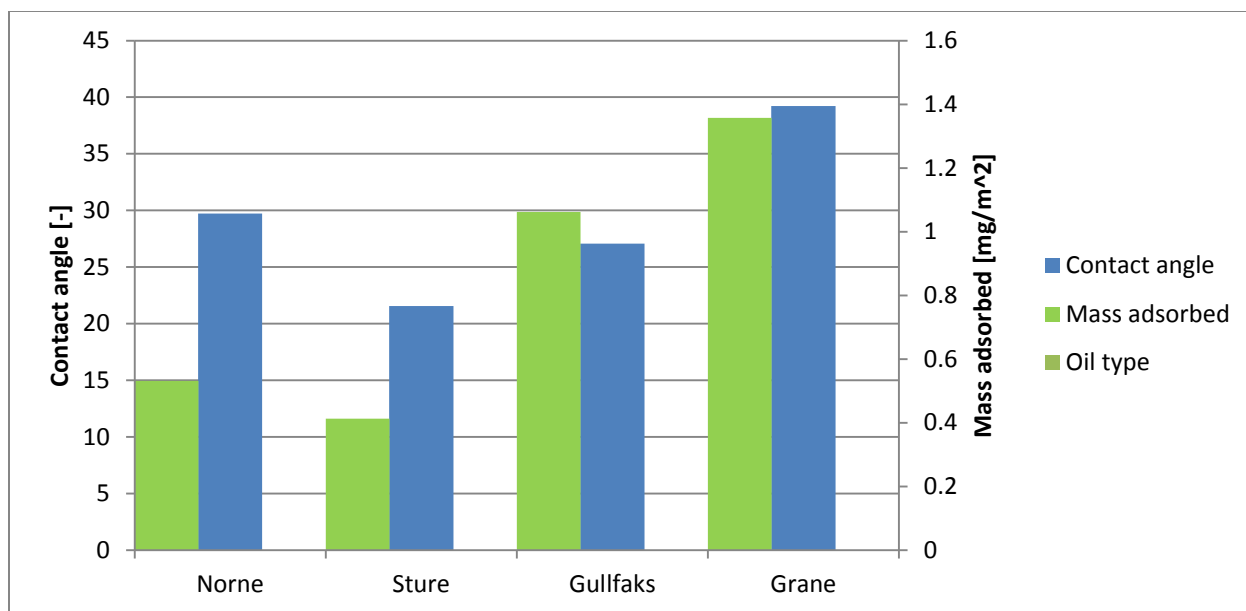


Figure 3.11: Contact angle and adsorbed mass of the four weathered (200°C+) samples of the Norne, Sture, Gullfaks and Grane oils types containing the dispersant Corexit 9500 on an aluminosilicate silicate crystal.

In figure 3.11, the values of contact angle and mass adsorption measured for four weathered crude oil samples on aluminosilicate crystals are found. The Grane sample has the highest mass adsorption value, followed by the Gullfaks sample. The Norne and Sture samples have low and quite similar values of mass adsorption. The contact angle values are quite similar for three of the oil samples, whilst the value of the Grane sample is somewhat higher. Compared to the same oil types (Norne, Gullfaks and Grane) on aluminosilicate crystals without dispersants in figure 3.5, the tendencies are similar; Grane adsorbs more than Gullfaks and Norne, and also has a higher contact angle value than the two. All values of the two parameters drop when dispersant is added. In figure 3.5, Norne and Gullfaks adsorb equally onto the crystal, in figure 3.11 the Norne value has dropped more.

When comparing the weathered oil samples to the same samples when fresh (figure 3.8), the tendencies are also quite similar. The Grane sample both adsorbs more and has a higher contact angle value for both experiments. All values of both parameters drop from fresh to weathered oil samples, except the adsorption of Sture oil, and the contact angle of the Gullfaks sample which increases slightly. The mass adsorption value of the Gullfaks oil is also the one to drop the least from fresh to weathered sample.

The weathered paraffinic and waxy oil samples decrease when dispersant is added (figure 3.5 to figure 3.11), as the fresh samples do. The naphthenic and asphaltic samples also decrease, which is not expected. An explanation could be that the components in these samples that bond to the aluminosilicate surface are removed by Corexit 9500. However, this should give a decrease for these oil types when the fresh samples are added dispersants, but the values of these samples increase.

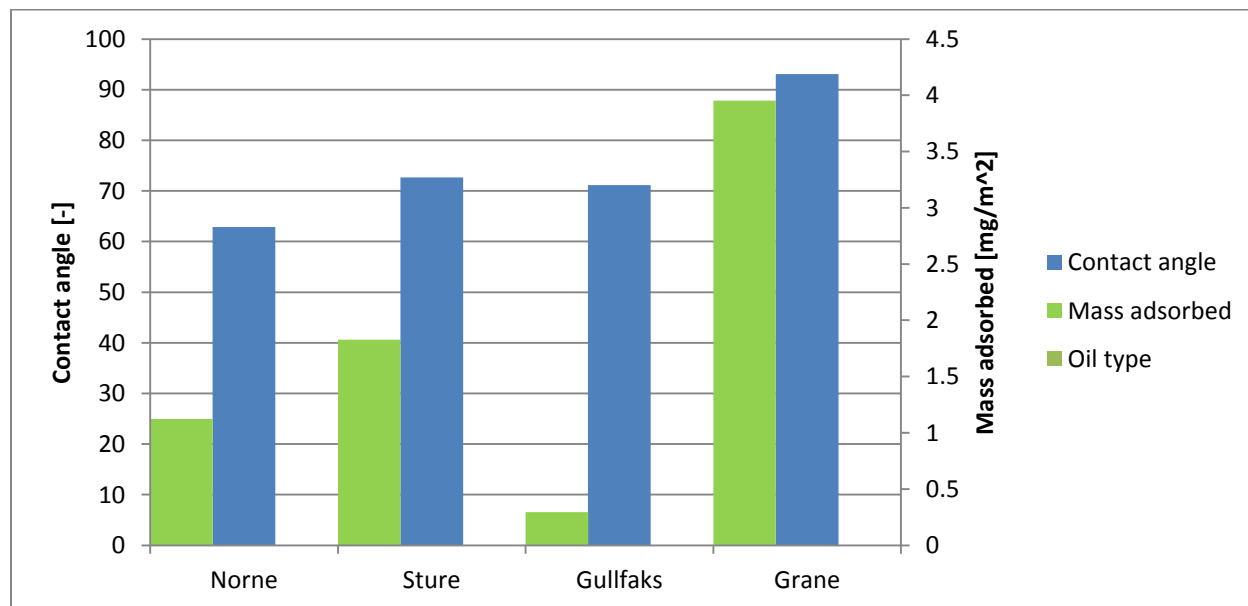


Figure 3.12: Contact angle and adsorbed mass of the four weathered (200°C+) samples of the Norne, Sture, Gullfaks and Grane oils types containing the dispersant Corexit 9500 on a calcium carbonate crystal.

Figure 3.12 shows the mass adsorption and contact angle values measured on four weathered oil samples with dispersants on a calcium carbonate coated crystal. The mass adsorption values have quite similar tendencies to the other oil samples containing dispersants; the Grane sample adsorbs the most on the calcium carbonate coating, whilst the other samples adsorb less. The contact angle values are also similar to the other graphs; the Grane sample has the highest value, and the other three values are lower and quite similar to each other.

Comparing the same oil types on the same crystal with and without dispersants, figures 3.12 and 3.6, the mass adsorption values of all oil types are quite different. The Norne and Gullfaks samples adsorb about half as much when dispersants are added, whilst the Grane sample adsorbs more than twice as much. The contact angle values for the three oil types are quite similar to

each other in figure 3.6, in figure 3.12 the Norne and Gullfaks value have decreased whilst the Grane value has increased, this is in line with the change in mass adsorption. The increase in mass adsorption for the Grane oil, and the decrease for the paraffinic oil are both according to literature^{25, 26}. The decrease for the Norne and Gullfaks values from figure 3.6 to figure 3.12 are unexpected, but could have something to do with the fact that calcium carbonate is more hydrophilic than silica²³, and the components of these two oils that bonded to the crystal surface in figure 3.6, are removed with Corexit 9500.

From fresh to weathered oil samples, figure 3.9 to figure 3.12, the mass adsorption values of the Norne, Sture and Grane samples increase, whilst the Gullfaks sample value decrease greatly, especially. The contact angle values have equal trends in both figures with the Grane sample value being higher than the others, the other sample values being quite equal to each other.

3.3 Results of experiments using oil-in-seawater emulsions

3.3.1 Results of oil-in-seawater emulsions – fresh oil samples

The fresh crude oils of Norne, Oseberg, Gullfaks and Grane were emulsified with seawater using the Ultra Turrax device, and mass adsorption and contact angle values were found using the QCM-D and CAM 200 devices, respectively. The values of these measurements on a silica coating are found in figure 3.13. The mass adsorption value (yellow) of the Norne sample is the highest, the Oseberg and Gullfaks are quite low and similar to each other, and the Grane value is negative. The contact angle values in figure 3.13 are low and quite similar for all samples except the Oseberg sample, where the value is half of the others.

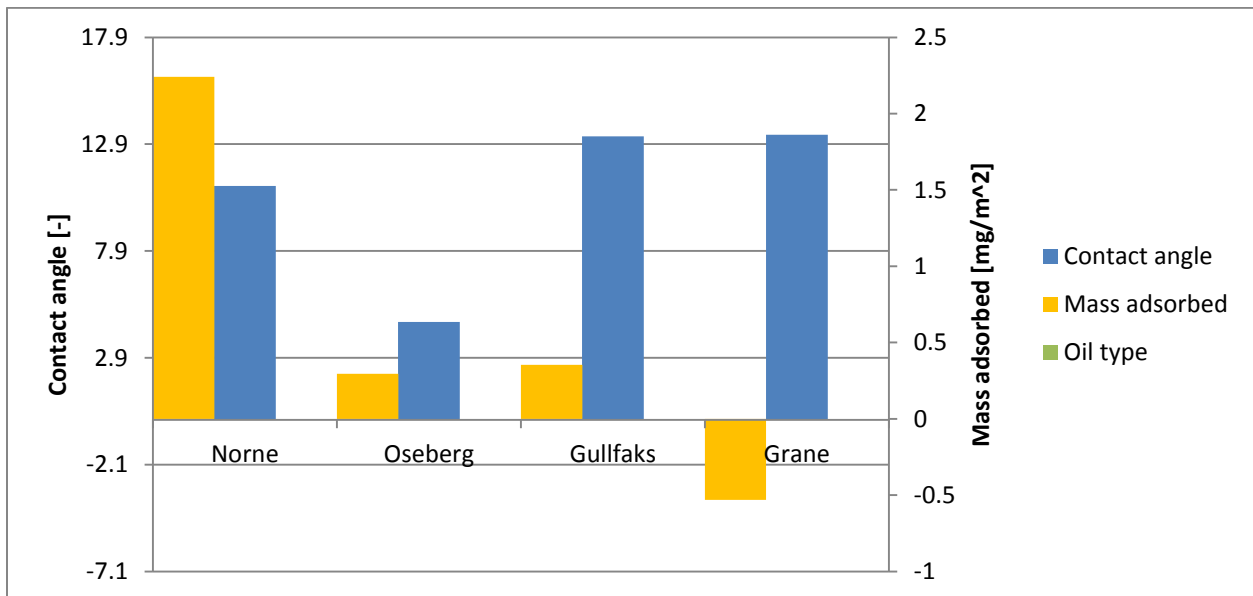


Figure 3.13: Contact angle and adsorbed mass of the four fresh samples of the Norne, Oseberg, Gullfaks and Grane oils types emulsified with seawater on a silica crystal.

The mass adsorption values in figure 3.13 are quite dissimilar from the values found in the oil-in-toluene experiments using the same oil types, found in figure 3.1. For the oil-in-toluene experiments, the Grane and Oseberg sample values are highest, whilst the Norne value is low. This is quite opposite in figure 3.13, and the value of the Gullfaks sample is also more than halved, lower than for all of the oil-in-toluene experiments. The contact angle values are in general much lower for the emulsions, several times lower than the values in figure 3.1. An explanation for the low values of mass adsorption could be that the oil droplets mixed in

seawater have less access to the crystal surface than in the oil-in-toluene experiments. The two types of experiments are quite different; The molecular aggregates in the oil-in-toluene experiments and the oil droplets in the oil-in-seawater experiments will most likely bond with the crystal surfaces in different manners, so dissimilar results are expected. Since the binding sites of the crystal surface are the polar silanol, these might have already bonded with seawater, which could be why the oil-in-seawater emulsions cause little change in mass adsorption. An exception for this theory is the waxy Norne oil, an explanation for this exception has not been found. A negative mass adsorption value in these experiments could possibly mean that components of the seawater have connected to the surface during stabilization of the seawater baseline, and is in some way desorbed as the oil sample is added.

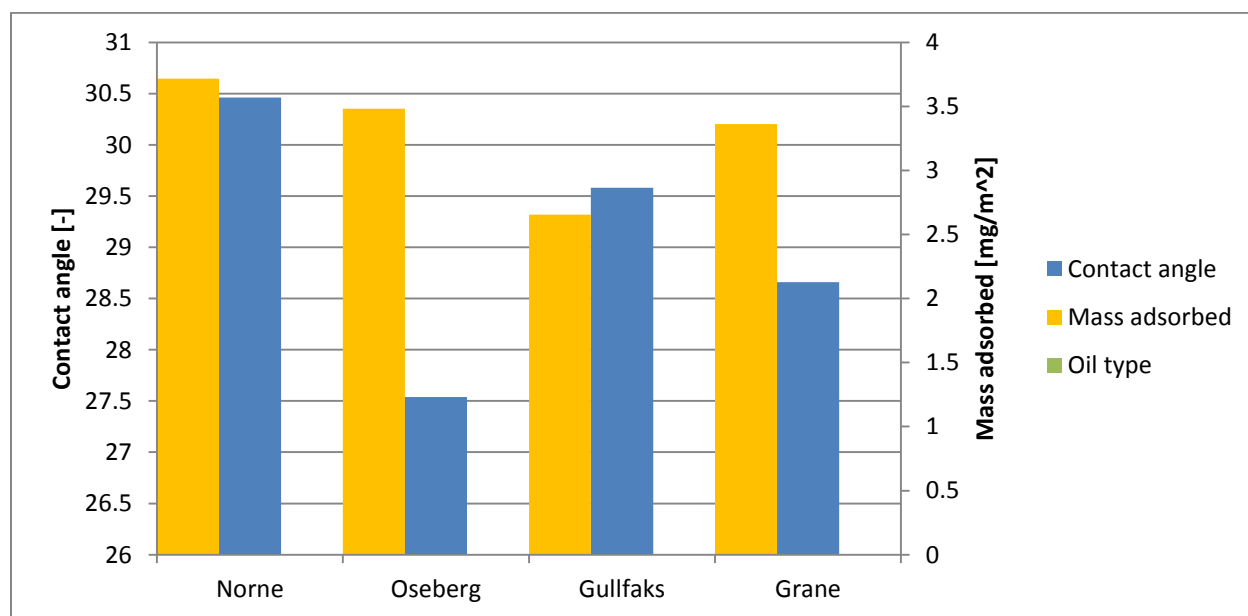


Figure 3.14: Contact angle and adsorbed mass of the four fresh samples of the Norne, Oseberg, Gullfaks and Grane oils types emulsified with seawater on an aluminosilicate crystal.

For the fresh oil-in-seawater emulsions on the aluminosilicate crystals, with values of contact angle and mass adsorption found in figure 3.14, the oil samples tend to adsorb significantly. Norne, Oseberg and Grane adsorb quite similarly, around 3.3 to 3.7 mg/m², Gullfaks adsorbs a bit less. The contact angle values of all samples are quite similar to each other, with the Norne sample having the highest value at 30.46, and Oseberg the lowest at 27.54. All contact angle values are smaller than for an original clean aluminosilicate crystal, which means that the interfacial tension between the seawater and the oil covered crystal surface has decreased with addition of emulsion. An explanation for this could be that the oil coating is now several oil

droplets on the surface, instead of a continuous layer for the oil-in-toluene experiments, and the uneven surface causes the drop in contact angle.

Comparing the oil-in-toluene and emulsion experiments with the same oil types and the same type of crystal (figure 3.2 and 3.14, respectively), some similarities and some differences are found. The adsorption values of The Norne and Oseberg samples are high and quite similar for both experiments, but the Gullfaks and Grane samples have much lower values in figure 3.2. The contact angle values have few similarities between the figures; the values in the oil-in-toluene experiments are high and not very similar to each other, whilst the emulsion experiment values are lower and similar between the samples.

The fact that the aluminosilicate coating adsorbs a great deal more than the silica coating for all fresh oil samples in emulsion, could be that the anionic binding sites of the aluminosilicate coating is less reactive with hydrogen-bonding compounds²², and therefore does not bond with the seawater, which could be an explanation for the low mass adsorption on the silica coating. The anionic sites may therefore be more available to adsorb droplets of the oil samples, but since the adsorption values in figure 3.14 differ from the ones in figure 3.2, the components adsorbed might not be the same for the oil-in-toluene and the emulsion experiments, or the components bonding might be the same ones, but they are bonded differently to other components in the emulsion.

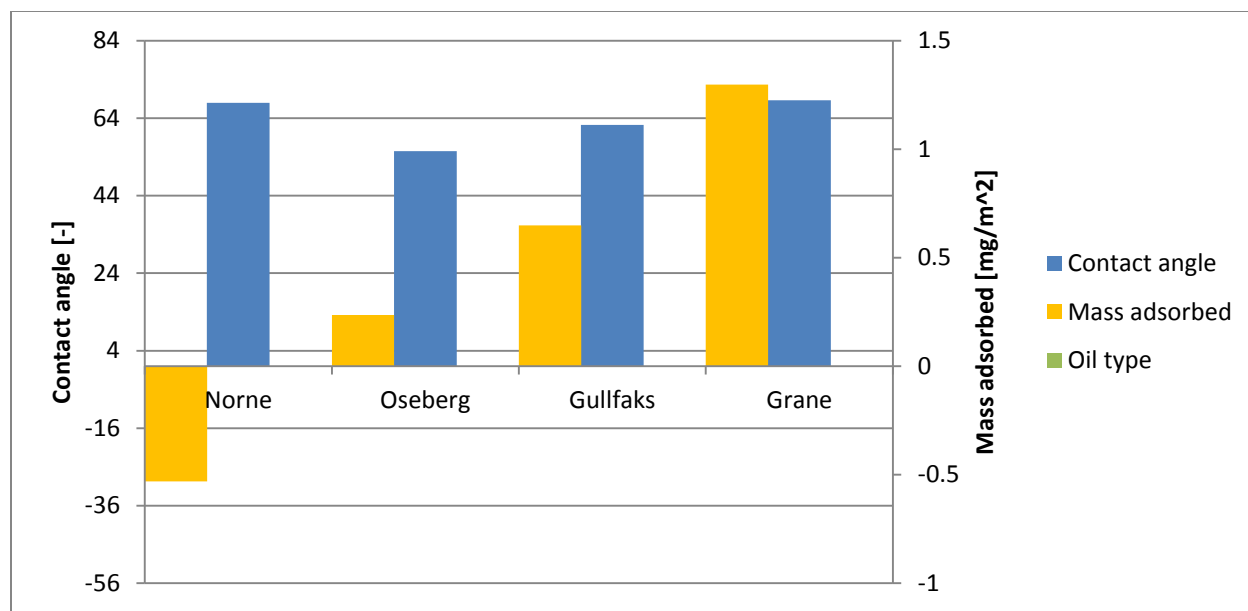


Figure 3.15: Contact angle and adsorbed mass of the four fresh samples of the Norne, Oseberg, Gullfaks and Grane oils types emulsified with seawater on a calcium carbonate crystal.

In figure 3.15, the values of mass adsorption and contact angle for the fresh samples of the crude oils Norne, Oseberg, Gullfaks and Grane on calcium carbonate coated crystals are found. The adsorption values are quite low, with Grane having the highest sample, then Gullfaks, then Oseberg quite close to zero, and Norne having a negative value. The contact angle values are quite similar to each other around 65 degrees, with Oseberg somewhat lower at 55.5 degrees.

When comparing the oil-in-toluene and emulsion experiments with the same oil samples on the calcium carbonate crystals, figure 3.3 and 3.15, few similarities are found. The samples that adsorbed the most in figure 3.3, Oseberg and Grane, has much lower values in figure 3.15. The Norne sample also has a quite high adsorption value in the oil-in-toluene experiment, but has a negative value for the emulsion experiment. The Gullfaks A adsorption value is similar for both experiments. The contact angle values in the two figures have some similarities, in figure 3.15 the values are quite similar to each other, in figure 3.3 the Norne and Gullfaks samples are still somewhat similar to each other, slightly higher than in figure 3.15. The Oseberg and Grane values are also similar to each other in figure 3.3, but about 30 degrees higher than in figure 3.15.

Comparing the emulsions of the fresh oil samples on the different crystal coatings, figure 3.13- figure 3.15, the values give few tendencies. The silica and calcium carbonate coatings give basically opposite tendencies for the values for mass adsorption, whilst the aluminosilicate

coating gives higher values than the other coatings. There are no apparent trends found in the contact angle values. The differences between the silica and calcium carbonate coatings could be explained by the difference in hydrophobicity²³, and that the compounds binding to the surface in figure 3.15, are not the same as the compounds in figure 3.13. The low adsorption in figure 3.15 compared to the adsorption in figure 3.3 may be explained by the fact that the binding sites of the surface are occupied with components of the seawater, which do not cause a large frequency shift as the crude oil components do.

3.3.2 Results of oil-in-seawater emulsions – weathered (200°C+) oil samples

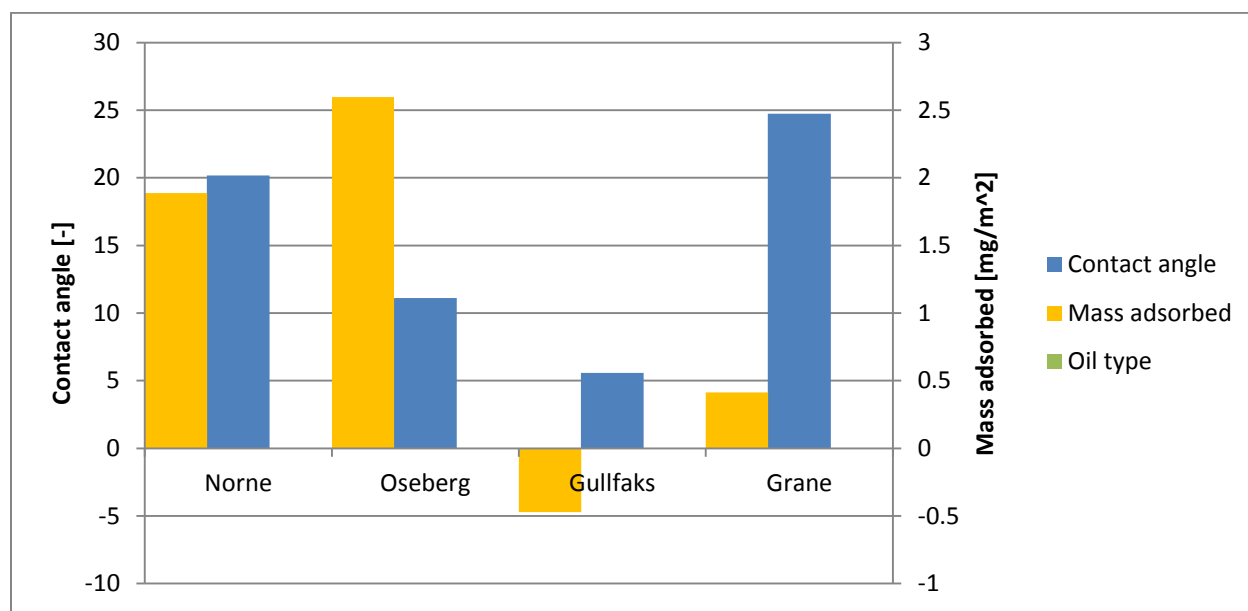


Figure 3.16: Contact angle and adsorbed mass of the four weathered (200°C+) samples of the Norne, Oseberg, Gullfaks and Grane oils types emulsified with seawater on a silica coated crystal.

Figure 3.16 shows the weathered (200°C+) oil samples of the four oil-in-seawater emulsions tested on silica coated crystals. The Oseberg sample shows the highest adsorption, followed by the Norne sample. The Grane sample has a low mass adsorption value, and the Gullfaks sample has a slightly negative value. The contact angle values of the samples do not seem to follow mass adsorption, since the Grane and Norne values are the largest, and the Oseberg and Gullfaks values are lower.

Compared to the emulsions of the fresh samples of the same oils on silica crystals (figure 3.13), there are not many similarities. The Norne sample mass adsorption values are similar in figures 3.13 and 3.16, but the Grane oil decreases from fresh to weathered samples, and the Oseberg and Gullfaks oil increases. The contact angle values are also dissimilar, lower for most of the fresh samples, except for the Gullfaks oil. The values decrease in different extents for the other three oils. The adsorption value changes could mean that the low molecular components of the Oseberg and Gullfaks oils are removed during weathering, and heavier components now have access to the crystal surface.

When comparing the values in figure 3.16 to its oil-in-toluene equivalents in figure 3.4, there are few observed similarities. All crude oils have a lower mass adsorption value in figure 3.16, but where the Grane oil is around 1.8 mg/m^2 lower in figure 3.16 than in figure 3.4, the Oseberg oil is merely 0.3 mg/m^2 lower. The Norne and Grane oils both reduce their values with about 1.2 mg/m^2 . The contact angle values are higher for the oil-in-toluene samples than the emulsion samples, and these values seem to follow the mass adsorption values in figure 3.4, but not in figure 3.16.

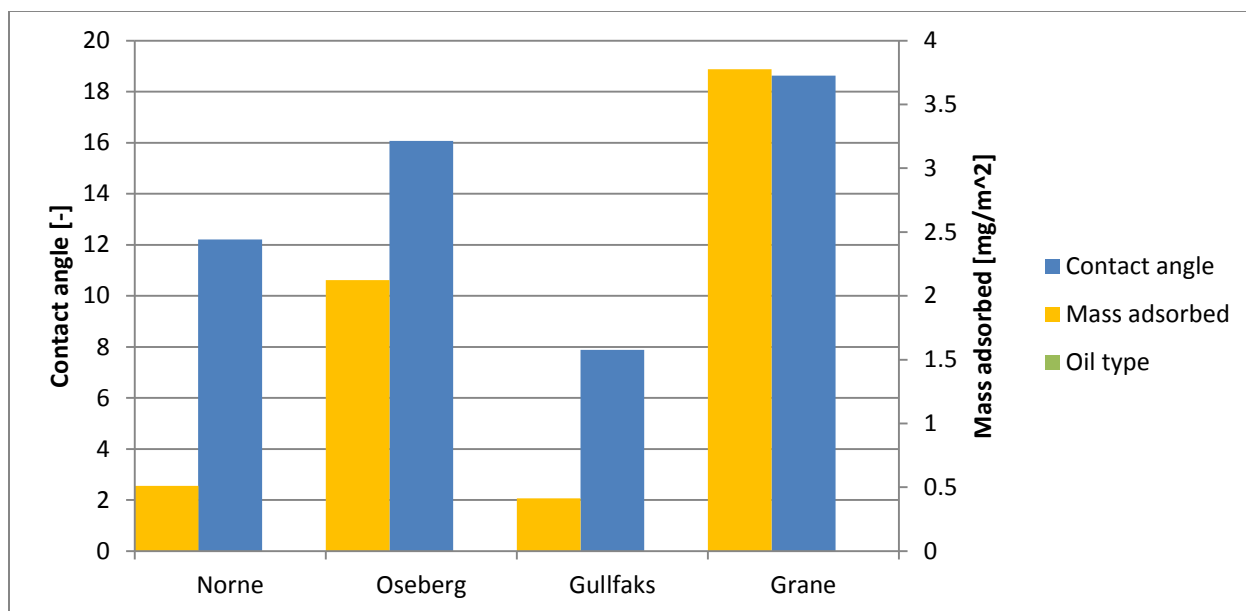


Figure 3.17: Contact angle and adsorbed mass of the four weathered (200°C+) samples of the Norne, Oseberg, Gullfaks and Grane oils types emulsified with seawater on an aluminosilicate crystal.

For the weathered samples of the emulsion experiments on an aluminosilicate coating, the values of contact angle and mass adsorption are found in figure 3.17. The figure shows that the Grane sample adsorbs more than the other samples, and the Gullfaks sample adsorbs the least, slightly below the Norne sample. The contact angle values seem to follow the adsorption values somewhat, with the Grane sample having the highest value followed by Oseberg. The Norne and Gullfaks sample values are not as similar regarding contact angle.

Compared to the values of the fresh samples of the same experiments found in figure 3.14, the adsorption onto the crystals is lower for all oils except Grane, where this value rises slightly. The Norne and Gullfaks sample adsorption values decrease greatly, more than the value of the Oseberg sample. The contact angle values of the samples are higher and more similar to each other in figure 3.14, in figure 3.17 they seem to follow the mass adsorption values to some extent.

The values of mass adsorption and contact angle of the oil-in-toluene and emulsion experiments for weathered samples on aluminosilicate crystals can be compared by studying figures 3.17 and 3.5. The mass adsorption values of the Norne and Gullfaks samples are similar to each other in

both figures, and both values decrease from figure 3.5 to figure 3.17. The Oseberg and Grane samples, however, increase, both with about the same amount. The contact angle values are much larger in figure 3.5, and more similar to each other in figure 3.17. In both figures, Grane and Oseberg hold the highest contact angle values.

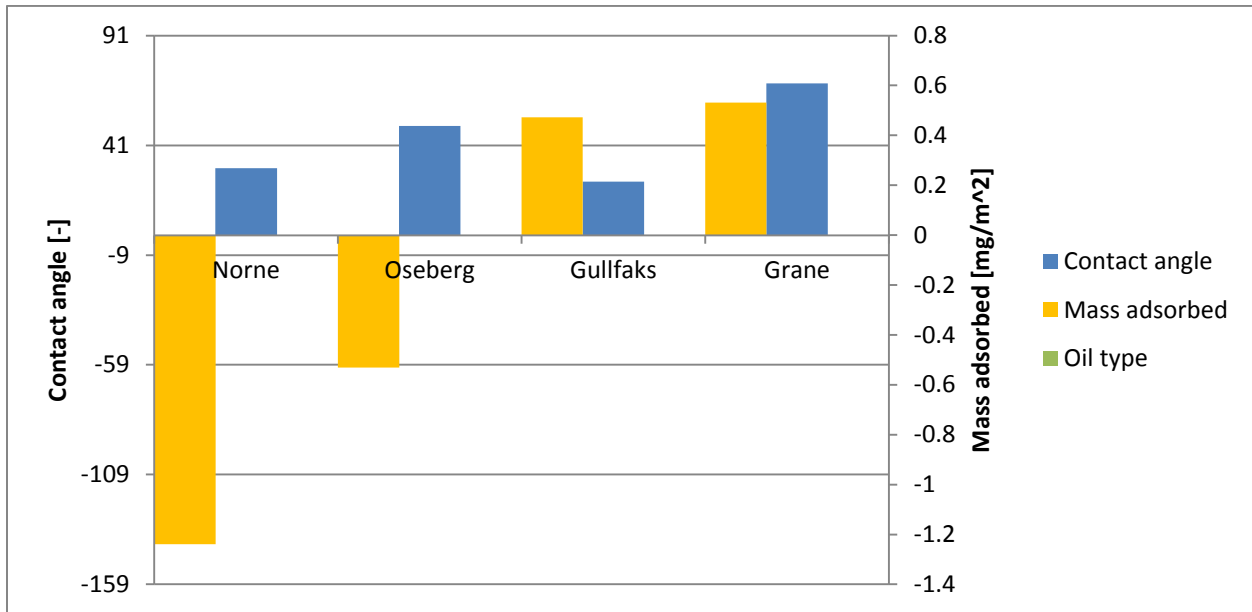


Figure 3.18: Contact angle and adsorbed mass of the four weathered (200°C+) samples of the Norne, Oseberg, Gullfaks and Grane oils types emulsified with seawater on a calcium carbonate crystal.

In figure 3.18, the contact angle and mass adsorption values of the emulsion experiments using the weathered oil samples on calcium carbonate coated crystals are presented. The Norne and Oseberg samples have negative adsorption values, whilst the Gullfaks and Grane sample values are positive but low, and similar to each other. Because of the negative values of mass adsorption, the contact angle values might be hard to observe in the figure. The Grane sample value is highest at 69.26 degrees, followed by Oseberg at 49.89. The Norne and Gullfaks sample values are lower and quite similar, at 30.52 and 24.51 degrees respectively.

The contact angle and mass adsorption values of the fresh and weathered samples of the emulsions experiments on calcium carbonate coated crystals are found in figures 3.15 and 3.18, respectively. The adsorption values seem to follow the same trend, with the Grane sample having the highest value, then Gullfaks, Oseberg and Norne. All oil types decrease with approximately

0.7-0.8 mg/m² from fresh to weathered sample, except the Gullfaks oil which only decreases with 0.18 mg/m². The contact angle values of the Norne and Gullfaks oils decrease greatly from figure 3.15 to figure 3.18, both with around 37 degrees, the Oseberg value decreases somewhat, and the Grane value increases slightly, with 0.63 degrees.

Comparing the values of the emulsion experiments in figure 3.18 to the values of the oil-in-toluene experiments with the same oil types in figure 3.6, few similarities are found. The Norne and Oseberg mass adsorption values are large and positive in figure 3.6, both are negative in figure 3.18. The Gullfaks value decrease somewhat from the oil-in-toluene to the emulsion experiment, whilst the Grane value decreases to under one third of the value in figure 3.6. All contact angle values decrease from figure 3.6 to figure 3.18; the Norne, Oseberg and Gullfaks values decrease greatly, with the reduction of 52.23, 45.88 and 62.22 degrees respectively, whilst the Grane value decreased with 16.72 degrees.

Some of the values of mass adsorption of the emulsions are measured to be negative. This is previously discussed by the possibility that components of seawater bond to the crystal surface during the stabilization of the baseline, and are removed somehow when the oil sample is added. Different oil types have negative values for different crystal coatings, which coincides with the fact that different components may bond with the different coatings. However, the negative values are quite small, and the seawater baseline is found to be somewhat more unstable than the toluene baseline, so these negative values could be a factor of disturbance in the measurements.

3.4 Dissipation

The main tendency of the dissipation values is that they seem to negatively correlate to the frequency values. Figures 2.2 and 2.3 show that when mass is added to a crystal and the frequency drops, the dissipation value increases. This shows that more mass added equals a less rigid layer. This tendency is found for most of the 78 figures in appendix C, with the exception of a few of the figures. Most of the dissipation values in appendix C are quite small; for the oil-in-toluene experiments, 43 out of 52 values are in the range $\pm 5 \times 10^{-6}$, and of the nine not in this range, only three lie outside the range $\pm 10 \times 10^{-6}$. According to literature⁸, a dissipation of 5×10^{-6} should be low enough for the film to be rigid and unchanging, an assumption for the use of the Sauerbrey equation as stated in subchapter 1.2.

3.5 Sources of error

During the experiments, some outside disturbances might have influenced the measurements. For the QCM-D measurements, air could have been trapped in the chamber when mounting the crystal, causing unstable results. Contamination of the oil-in-toluene emulsion samples might have occurred before measurements, by e.g. glassware or pipettes used for sample mixing not being sufficiently clean. For the emulsion experiments, a source of error could be that the emulsions were mixed at the same rpm for the same amount of time. Since the oil types have different compositions, some oils could have emulsified to a greater extent than others, and e.g. have different oil droplet size when measured in the QCM-D. There were also found some signs of corrosion on the Ultra Turrax device; if some corroded particles were mixed into some of the emulsion, this could have affected the measurements. Outside disturbance like people working around the QCM-D apparatus or construction work outside the building could possibly have affected the frequency measurements.

For the contact angle measurements, outside light could have affected the CAM 200 camera used to measure the contact angle. This was mitigated by keeping the measurement room as dark as possible. The crystals used are sensitive, and continued use might have caused the crystals to deteriorate. The crystals were cleaned as described in the Q-sense manual, but this may not have been sufficient. Additional cleaning was attempted (additional time in UV-chamber and in SDS solution, use of more toluene, Milli-Q water and ethanol), but this did not give different results. Another source of error is that the room temperature could have changed for the experiments, and affected the sea water or crystals. These sources of error mentioned were mitigated or prevented as far as possible.

4. Conclusion

The aim of this thesis was to investigate how the chemical composition of different model shoreline surfaces and different crude oils affect the interactions between the two phases, and how this influence wettability alterations. The interactions were studied by the Quartz Crystal Microbalance with Dissipation (QCM-D) technique, whilst the wettability alterations were investigated by contact angle measurements using the CAM 200 device. The shoreline surfaces were modeled by different coatings on the quartz crystals used; the surfaces investigated were silica, aluminosilicate and calcium carbonate. The crude oils investigated were the waxy Norne oil, the paraffinic Oseberg oil, the naphthenic Gullfaks A oil and the asphaltic Grane oil. The effect of weathering, the addition of the dispersant Corexit 9500 and the effect of emulsifying the crude oils in seawater were also investigated. For the experiments where dispersants were added, a paraffinic Sture blend was used in place of the Oseberg oil.

For the silica coated crystals, the asphaltic Grane oil tended to adsorb more than the other oils. This can be explained by the silanol groups of the silica coating forming hydrogen bonds with the polar asphaltic compounds of the Grane oil. The aluminosilicate coated crystals seemed to adsorb more of the other oil types than the silica coated crystals. The anionic binding sites of this coating may have bonded with other compounds found in these crude oils instead of the asphaltic compounds. The calcium carbonate coating tended to adsorb the asphaltic Grane oil, but also the paraffinic Oseberg oil to a great extent. The fact that the different coatings adsorb the crude oils to different extents, seem to express that the coatings adsorb different components of the oils, possibly due to difference in hydrophobicity between the coatings. The dissipation measured simultaneously with the mass adsorption showed that most of the oils adsorbed as a compact and rigid layer.

With regards to weathering some trends are observed. For the silica coating, the adsorption of the Norne, Oseberg and Grane oil tends to increase with increased weathering. On the aluminosilicate coating, the adsorption of the Grane oil also increases, whilst the Norne and Oseberg values decrease. For the crystals with the calcium carbonate coating, the Norne adsorption value increases, whilst the Oseberg and Grane values decrease. For all crystal coatings, the Gullfaks A oil adsorption tends to differ less than the other oils when introduced to weathering. For the wettability of the oil types, this seemed to follow adsorption; high mass adsorption gave a low wettability of seawater on the oil covered crystals, especially for the silica and calcium carbonate coated crystals.

When Corexit 9500 were added, some trends were observed. The mass adsorption of the paraffinic oil tended to decrease, whilst the asphaltic oil value tended to increase. This fits well with the literature which states that the dispersant effectiveness correlates positively with high saturate concentration and negatively with high concentration of asphaltic compounds. The other oil types did not have as clear trends.

The oil-in-seawater experiments did not give as clear tendencies as the oil-in-toluene experiments. The aluminosilicate coated crystals seemed to adsorb more than the other two crystal coatings, these two coatings tended to adsorb much less than in the oil-in-toluene experiments.

References

1. Beens, J.; Brinkman, U. A. T. *The role of gas chromatography in compositional analyses in the petroleum industry*, Trends Anal. Chem. 2000, 19(4), pp. 260–275.
2. Aske, N. *Characterisation of Crude Oil Components, Asphaltene Aggregation and Emulsion Stability by means of Near Infrared Spectroscopy and Multivariate Analysis*, NTNU, 2002, pp. 3-4.
3. Øye, G. *Surface and Colloid Chemistry in Produced Water Management*, Presentation in TKP4520, 2012, pp. 5-6.
4. Moldestad M.Ø.; Leirvik, F.; Johansen, Ø.; Daling, P.S.; Alun, L. *Environmental Emulsions: A Practical Approach*, Emulsions and Emulsion Stability, 2005, pp. 355-361.
5. Singasaas, I.; Strøm-Kristiansen, T.; Daling, P.S. *Forvitringsegenskaper på sjøen og kjemisk dispergerbarhet for Njord råolje*, SINTEF, 2002, p. 19.
6. *Q-sense D300 User Manual*, Q-sense AB, 2000, pp. 6-1-6-4, 7-1-7-3 and 8-2.
7. *Q-sense sensors*, <http://www.q-sense.com/q-sense-sensors>, June 2013.
8. Vogt, B.D. et al. *Effect of Film Thickness on the Validity of the Sauerbrey Equation for Hydrated Polyelectrolyte Films*, The Journal of Physical Chemistry, 2004, 108(34), p. 12686.
9. Kallio, T.; Kekkonen, J.; Stenius, P. *The Formation of Deposits on Polymer Surfaces in Paper Machine Wet End*, The Journal of Adhesion, 2010, 80(10-11), p. 937.
10. *CAM 200 Optical Contact Angle Meter Instruction Manual*, KSV, 2001, pp. 3, 41.
11. ramé-hart, *Information on Contact Angle*, 2013, <http://www.ramehart.com/contactangle.htm>, June 2013.
12. Bico, J.; Marzolin, C.; Quéré, D. *Pearl drops*, Europhysics Letters, 1999, 47(2), p. 220.
13. Mørk, P.C. *Overflate og Kolloidkjemi*, NTNU, 8. Ed, 2004, p. 9, 82 and 272.
14. IKA, 2013, http://www.ika.com/owa/ika/catalog.product_image?iProduct=4447300&iNo=1, June 2013.
15. Burns, K.; Harbut, M.R. *Gulf Oil Spill Health Hazards*, 2010, <http://www.sciencecorps.org/crudeoilhazards.htm>, June 2013.
16. IMLAB, *IKA Disperser: T25 Digital ULTRA TURRAX*, 2008, http://www.imlab.be/Imlab_EN/Ika/Crushing/Promotion_Ultra_Turrax_T25_IKA.html, June 2013.
17. Olanya, G.; Iruthayaraj, J.; Poptoshev, E.; Makuska, R.; Vareikis, A.; Claesson, P.M. *Adsorption Characteristics of Bottle-Brush Polymers on Silica: Effect of Side Chain and Charge Density*, Langmuir, 2008, 24(10), p. 5343.
18. Enarsson, L.E.; Wågberg, L. *Polyelectrolyte Adsorption on Thin Cellulose Films Studied with Reflectometry and Quartz Crystal Microgravimetry with Dissipation*, Biomacromolecules, 2009, 10(1), p. 136.

19. Farooq, U.; Sjöblom, J.; Øye, G. *Desorption of Asphaltenes from Silica-Coated Quartz Crystal Surfaces in Low Saline Aqueous Solutions*, 2011, 32(10), pp. 1388-1395.
20. Ekholm, P.; Blomberg, E.; Claesson, P.; Auflem, I.H.; Sjöblom, J.; Kornfeldt, A. *A Quartz Crystal Microbalance Study of the Adsorption of Asphaltenes and Resins onto a Hydrophilic Surface*, *Journal of Colloid and Interface Science*, 2002, 247, p. 345.
21. Auflem, I.H. *Influence of Asphaltene Aggregation and Pressure on Crude Oil Emulsion Stability*, NTNU, 2002, p. 6.
22. Iler, R.K. *The Effect of Surface Aluminosilicate Ions on the Properties of Colloidal Silica*, *Journal of Colloid and Interface Science*, 1976, 55(1), p. 26.
23. Kelesoglu, S.; Volden, S.; Kes, M.; Sjöblom, J. *Adsorption of Naphthenic Acids onto Mineral Surfaces Studied by Quartz Crystal Microbalance with Dissipation Monitoring (QCM-D)*, *Energy Fuels* 2012, 26, pp. 5060–5068.
24. Neff, J.M.; Ostazeski, S.A.; Stejskal, I. *The Weathering Properties of Four Unique Crude Oils From Australia*, *Spill Science & Technology Bulletin*, 1996, 3(4), p. 205.
25. Blondina, G.J.; Singer, M.M.; Lee, I.; Ouano, M.T.; Hodgins, M.; Tjeerdema, R.S.; Sowby, M.L. *Influence of Salinity on Petroleum Accommodation by Dispersants*, *Spill Science & Technology Bulletin*, 1999, 5(2), pp. 132-133.
26. Fingas, M. *A Review of Literature Related to Oil Spill Dispersants 1997-2008*, PWSRCAC, 2008, p. 5.

Appendix A: Risk assessment

NTNU	Hazardous activity identification process			Responsible	Number	Date
HMS				ng	HMS-ord.	HMSRV/2501
			Godkjent av	Sigve	Erstner	

Unit:

ITP-Ljeland lab

Date:

12.01.2013

Line manager:

Professor Gisle Øye

Participants in the identification process (including their function):

Professor Gisle Øye (supervisor), Jostein Kjemperud (student)

Short description of the main activity/main process:

Master thesis in oil spill response, Jostein Kjemperud

ID no.	Activity/process	Responsible person	Laws, regulations etc.	Existing documentation	Existing safety measures	Comment
1	Preparation of samples (diluting the different oil types with toluene to 10 wt% oil)	Jostein Kjemperud	Arbeidsmiljøloven (the working environment act), kjemikalieforskriftene (regulations of chemicals)	Safety data sheet toluene, general laboratory procedures	Safety goggles, gloves, lab coat, fume hood	Oils are treated under fume hoods using gloves and goggles.
2	Use of CAM200	Jostein Kjemperud	Arbeidsmiljøloven (the working environment act), kjemikalieforskriftene (regulations of chemicals)	Instruction manual CAM 200 and procedure, general laboratory procedure, apparatus card	Safety goggles and gloves, lab coat, use of fume hood	
3	Use of Q-sense (QCM)	Jostein Kjemperud	Arbeidsmiljøloven (the working environment act), kjemikalieforskriftene (regulations of chemicals)	User manual Q-Sense D300 and procedure, general laboratory procedure, apparatus card	Safety goggles, gloves, lab coat, fume hood	
4	Cleaning	Jostein Kjemperud	Arbeidsmiljøloven (the working environment act), kjemikalieforskriftene (regulations of chemicals)	Safety data sheet toluene, safety data sheet ethanol, general laboratory procedures	Safety goggles, lab coat, gloves, fume hood	Chemicals used for cleaning are toluene, ethanol and water along with compressed air

NTNU	Risk assessment				Utsjøløst stv	Number	Dato
					HMS-avd.	HMSRV/2503	24/2011
HMS MS					Godkjent av	Stor	Erstatler

Unit:

HCP-Utsjøløst lab

Date:

12.01.2013

Line manager:

Participants in the identification process (including their function):

Professor Gisle Øye (supervisor), Jostein Kjemperud (student)

ID no.	Activity from the identification process form	Potential undesirable incident/strain	Likelihood od (1-5)	Consequence:				Risk value	Comments/status Suggested measures
				Human (A-E)	Environment (A-E)	Economy/ material (A-E)	Reputation (A-E)		
1	Preparation of samples (diluting the different oil types with toluene to 10 wt% oil)	Significant spill of toluene/crude oils on skin, inhalation of large amounts of toluene/other volatile components over time. Although everything is facilitated for safety regarding these chemicals, human error could lead to a spill, e.g. during cleaning or transportation of these chemicals.	2	D				D2	Slow movements in the lab, toluene/oils are always treated under fume hood.
2	Use of CAMD00	Pricking of skin with needle	1	A				A1	The needle is not sharp, so pricking the skin with it is unlikely
3	Use of Q-sense (QCM)	Inhalation of toluene/ volatile crude oil components	3	C				C3	toluene/oil components when these exit the apparatus into beakers (although everything is under
4	Cleaning	Significant spill of solvent when cleaning, and inhalation. Although everything is facilitated for safety regarding these chemicals, human error could lead to a spill, e.g. during cleaning or transportation of these chemicals.	2	C				C2	

Appendix B: Sample calculation of mass adsorption

The Sauerbrey equation, equation 1.1 is used:

$$\Delta m = \frac{-C\Delta f}{n}$$

$C=0.177 \text{ mg}/(\text{Hz cm}^2)$ was found from literature^{17, 18}.

$n=3$ was the chosen overtone number for the QCM-D measurements.

B.1 Oil-in-toluene experiment calculation

Using the fresh Oseberg oil fraction on the silica coated crystal, which had a drop in frequency of -19.0 Hz, the mass adsorption can be calculated as in equation B.1 below:

$$\Delta m = \frac{-0.177 \text{ mg}/(\text{Hz m}^2) \times (-29.0 \text{ Hz})}{3} = 1.711 \text{ mg}/\text{m}^2 \quad (\text{B.1})$$

B.2 Oil-in-seawater experiment calculation

In the oil-in-seawater experiments, Milli-Q water was used to rinse the crystals after oil was added. This was done since rinsing with seawater might cause some of the components in the seawater to bond with the oil components adsorbed on the crystal surface, causing a too high mass adsorption. Rinsing with Milli-Q water and the adding the difference in frequency between the Milli-Q and seawater, gives a precise mass adsorption of the oil-in-seawater experiments.

Using the fresh Oseberg oil fraction, which in the emulsion experiment had an increase in frequency of 55.2 Hz, and the increase in frequency from the seawater baseline when Milli-Q water is added on a silica coated crystal, 60.2 Hz (close to the aluminosilicate coated crystal at 58.1 Hz and the calcium carbonate coated crystal at 60.4 Hz), the mass adsorption can be calculated as in equation B.2 below:

$$\Delta m = \frac{-0.177 \text{ mg}/(\text{Hz m}^2) \times (55.2 - 60.2 \text{ Hz})}{3} = 0.295 \text{ mg}/\text{m}^2 \quad (\text{B.2})$$

Appendix C: Quartz Crystal Microbalance with Dissipation (QCM-D) results

C.1: Oil-in-toluene experiments without dispersants

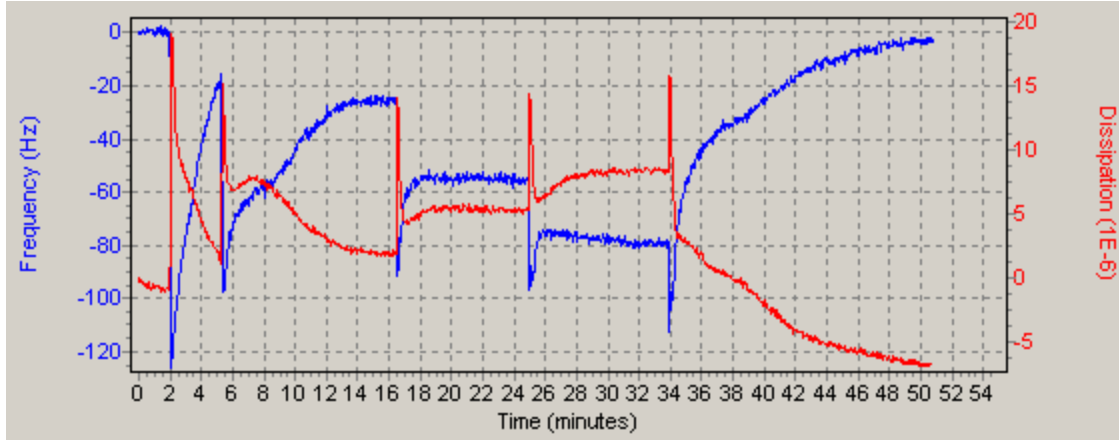


Figure C.1.1: Fresh Norne sample on silica coated crystal.

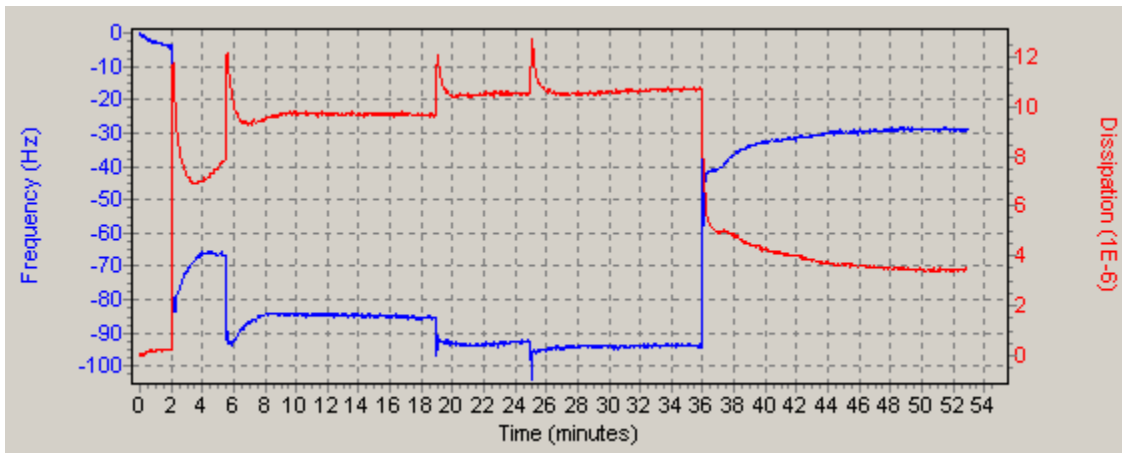


Figure C.1.2: Fresh Oseberg sample on silica coated crystal.

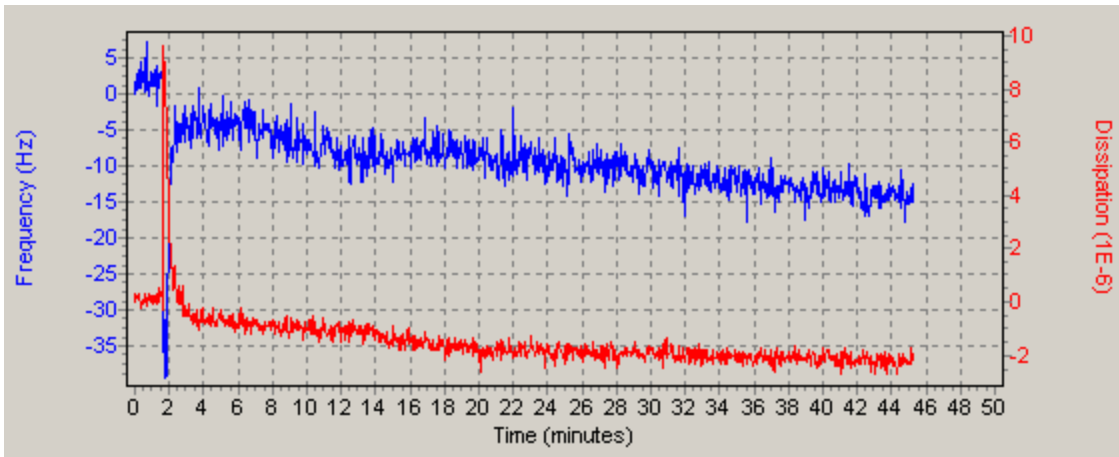


Figure C.1.3: Fresh Gullfaks sample on silica coated crystal.

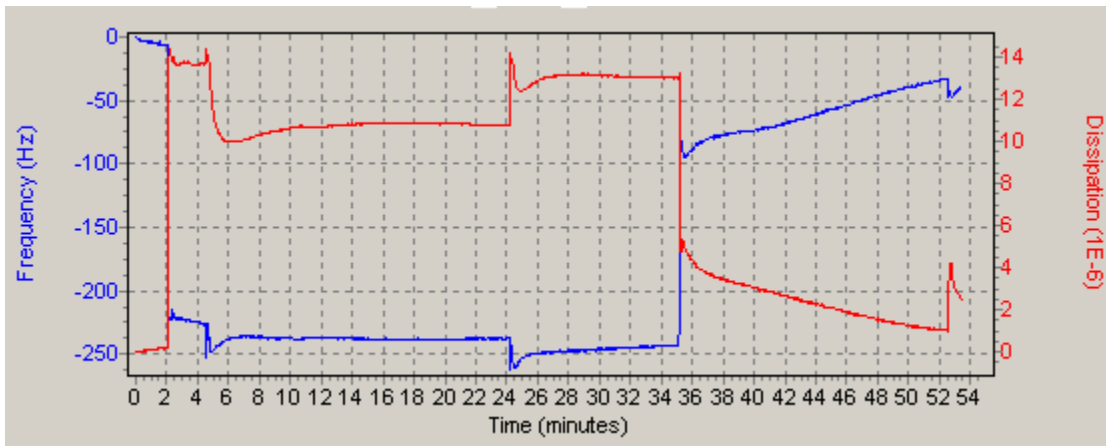


Figure C.1.4: Fresh Grane sample on silica coated crystal.

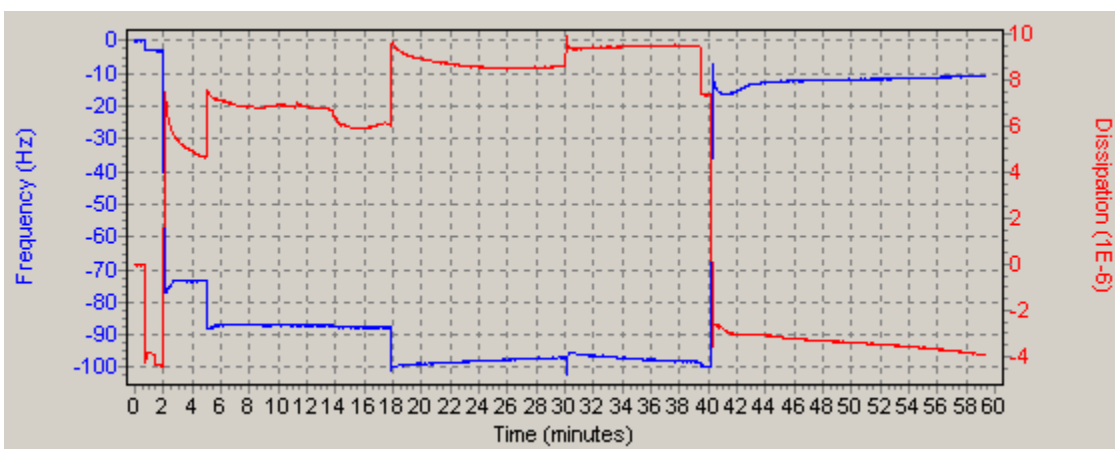


Figure C.1.5: Weathered Norne sample on silica coated crystal.

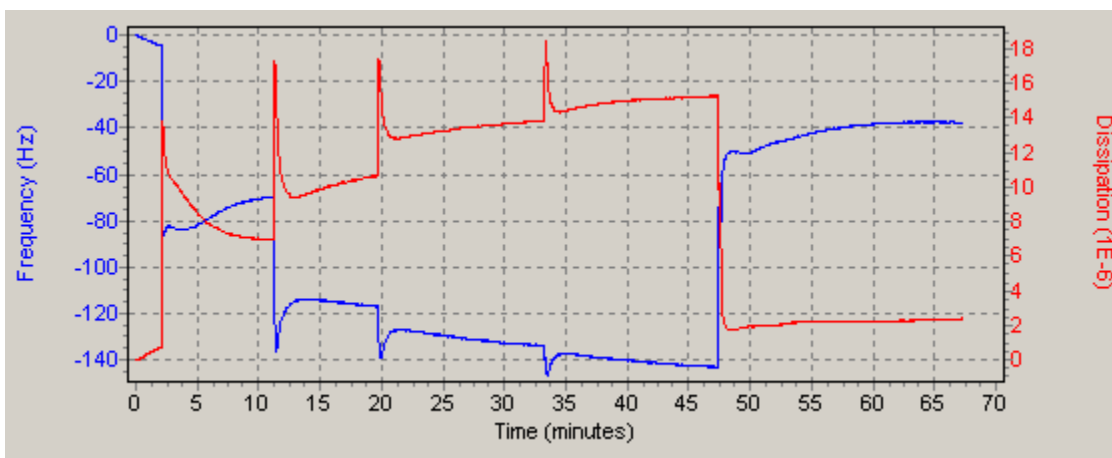
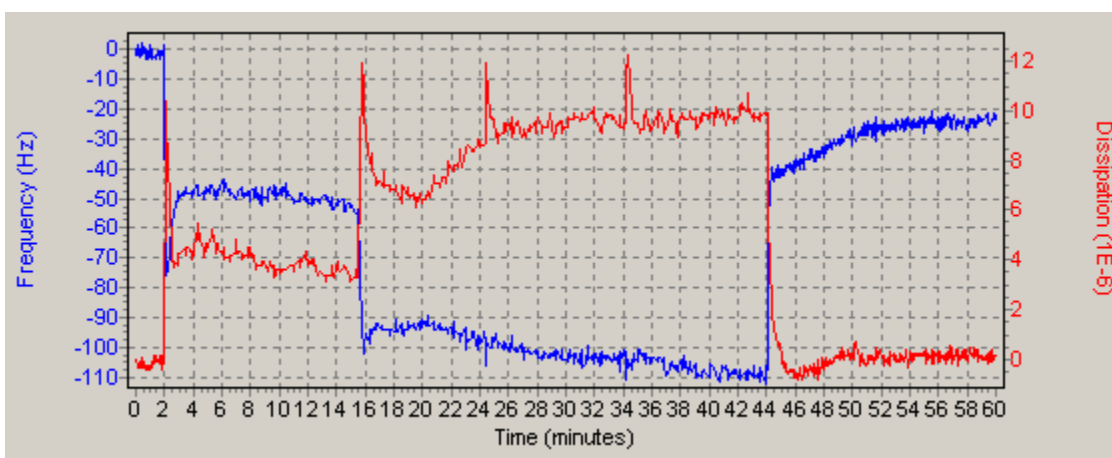
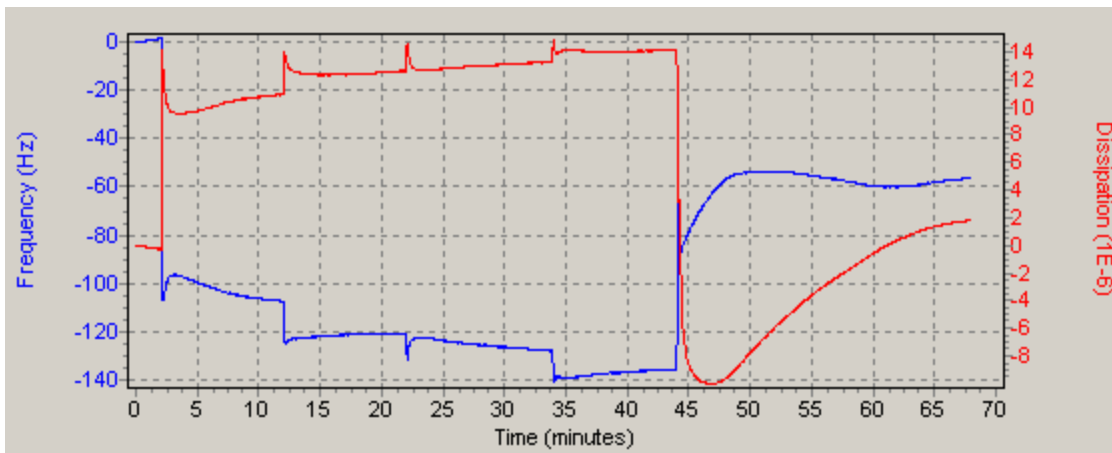


Figure C.1.6 a-c: Weathered Oseberg sample on silica coated crystal.

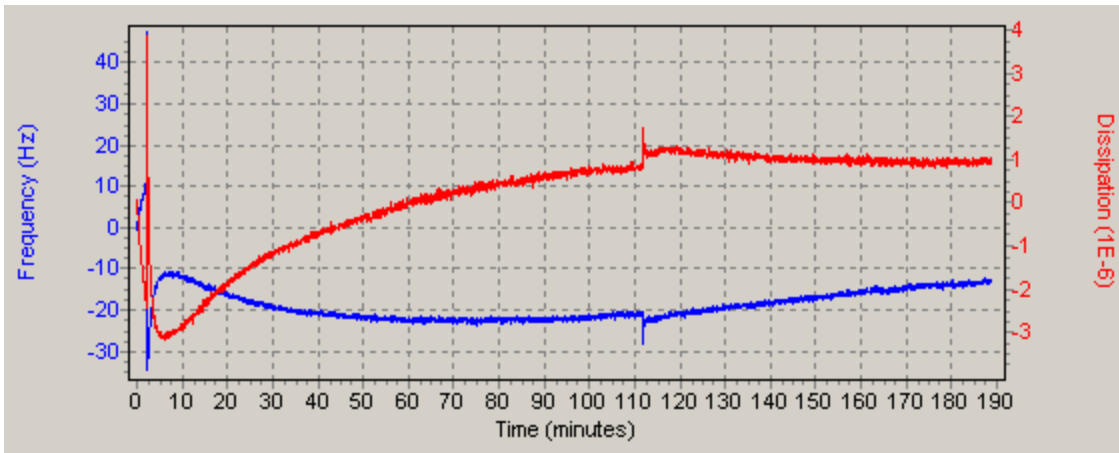


Figure C.1.7: Weathered Gullfaks sample on silica coated crystal.

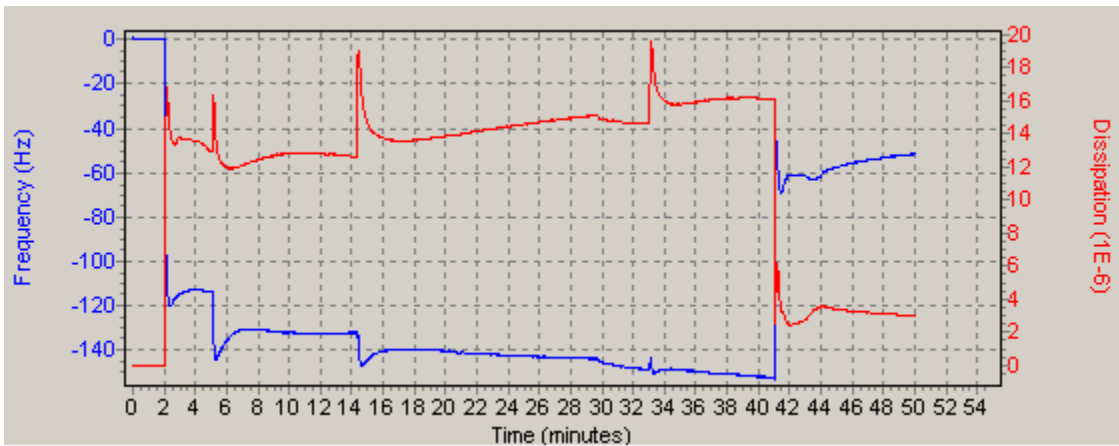


Figure C.1.8: Weathered Grane sample on silica coated crystal.

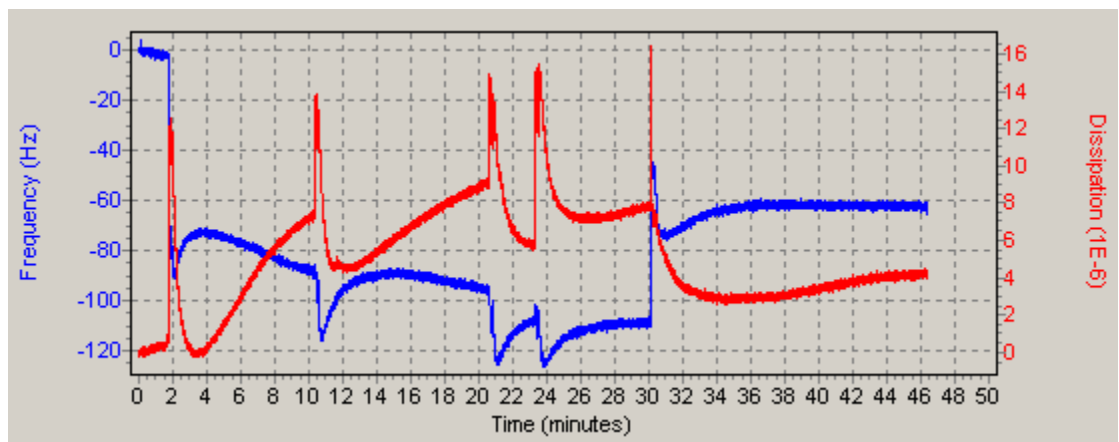


Figure C.1.9: Fresh Norne sample on aluminosilicate coated crystal.

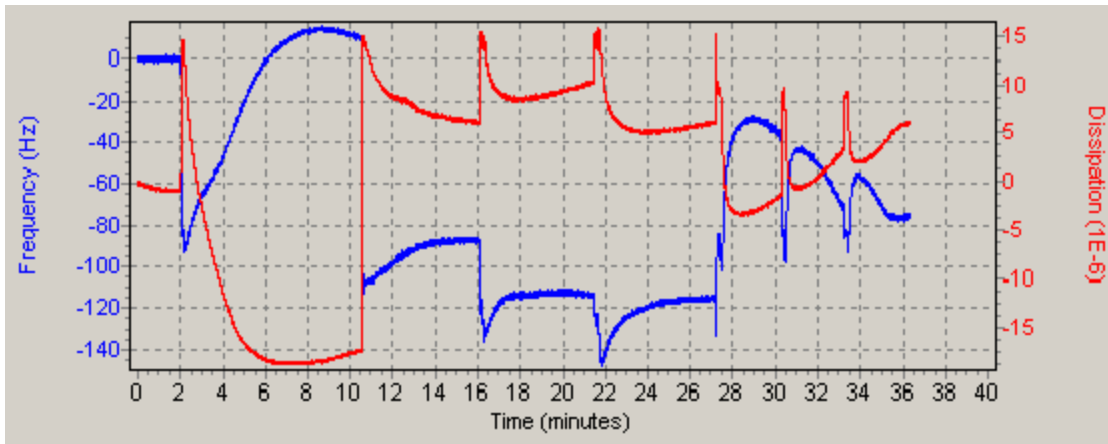


Figure C.1.10: Fresh Oseberg sample on aluminosilicate coated crystal.

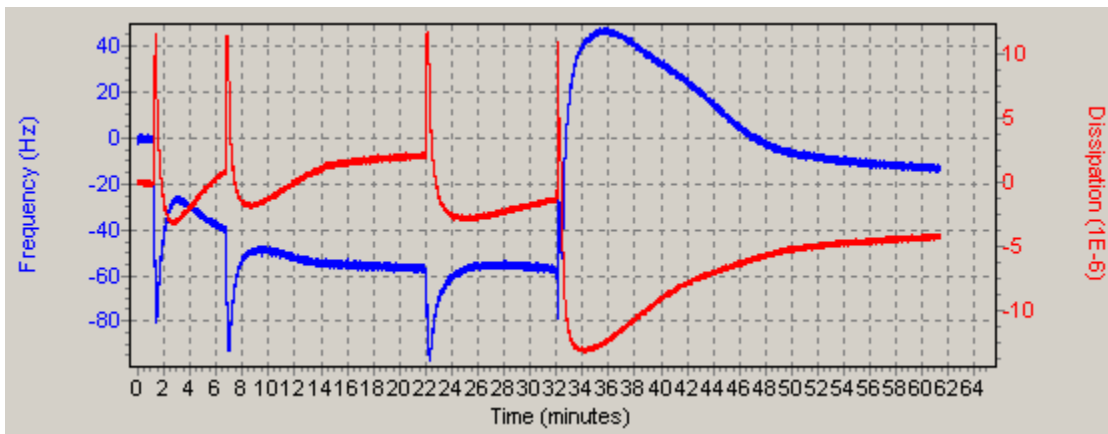


Figure C.1.11: Fresh Gullfaks sample on aluminosilicate coated crystal.

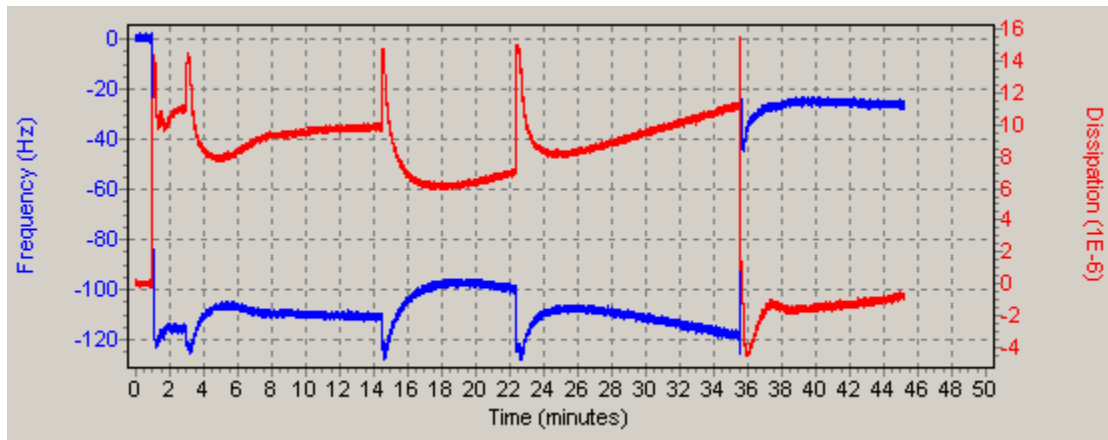


Figure C.1.12: Fresh Grane sample on aluminosilicate coated crystal.

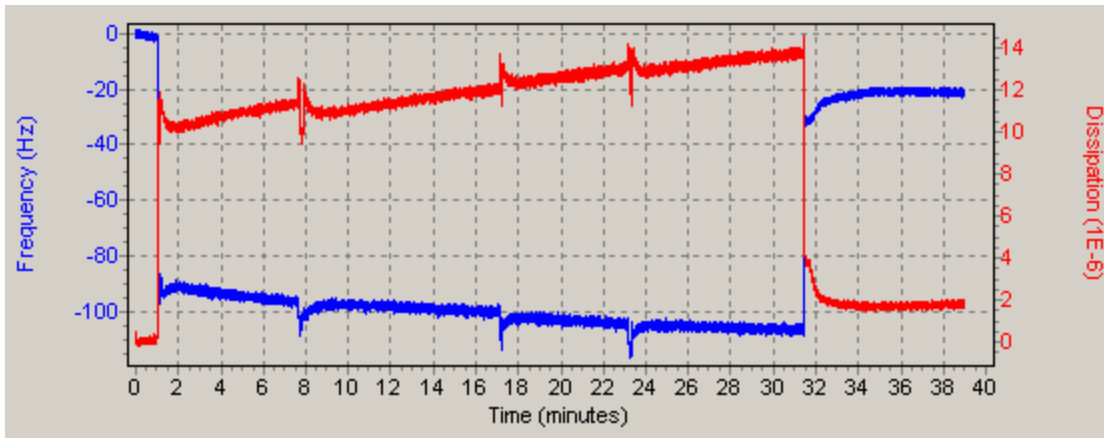


Figure C.1.13: Weathered Norne sample on aluminosilicate coated crystal.

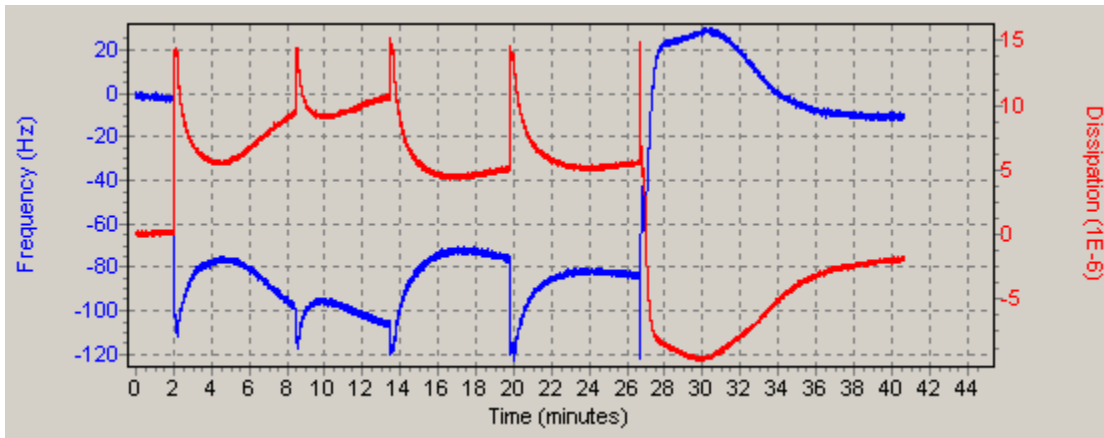


Figure C.1.14: Weathered Oseberg sample on aluminosilicate coated crystal.

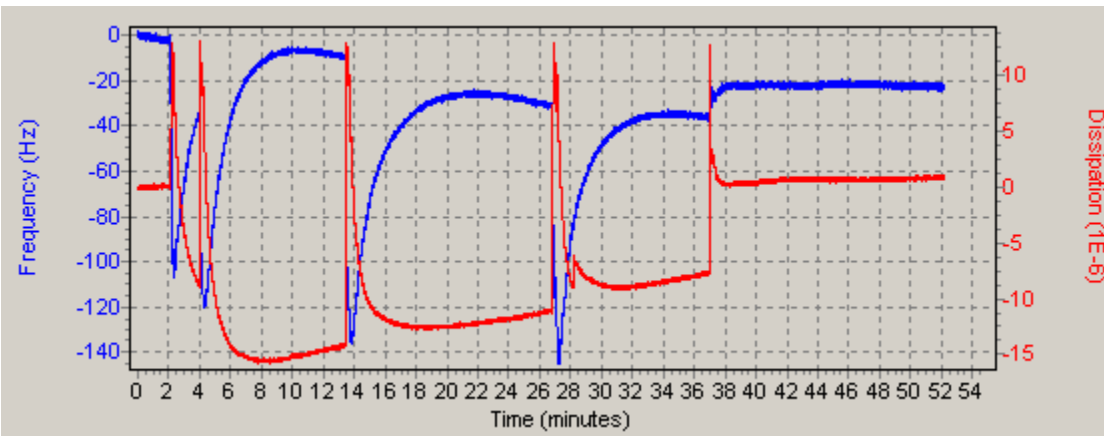


Figure C.1.15: Weathered Gullfaks sample on aluminosilicate coated crystal.

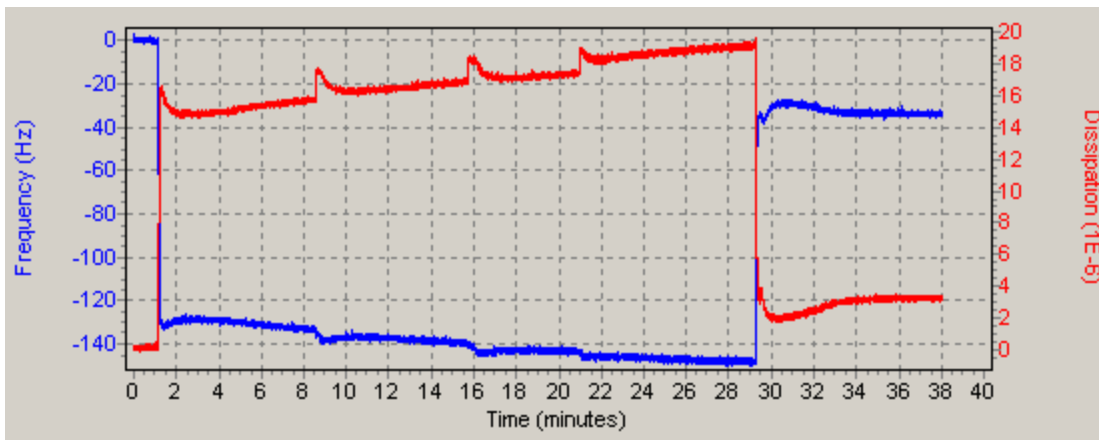


Figure C.1.16: Weathered Grane sample on aluminosilicate coated crystal.

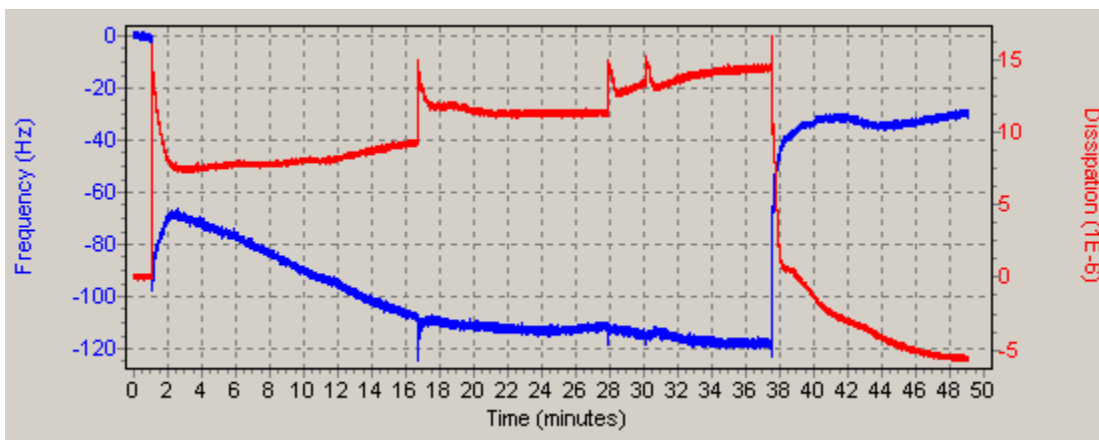


Figure C.1.17: Fresh Norne sample on calcium carbonate coated crystal.

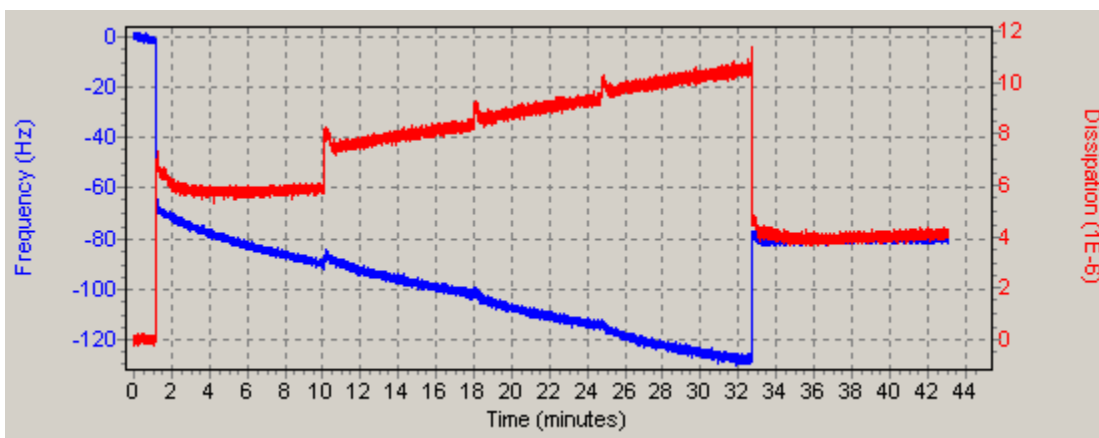


Figure C.1.18: Fresh Oseberg sample on calcium carbonate coated crystal.

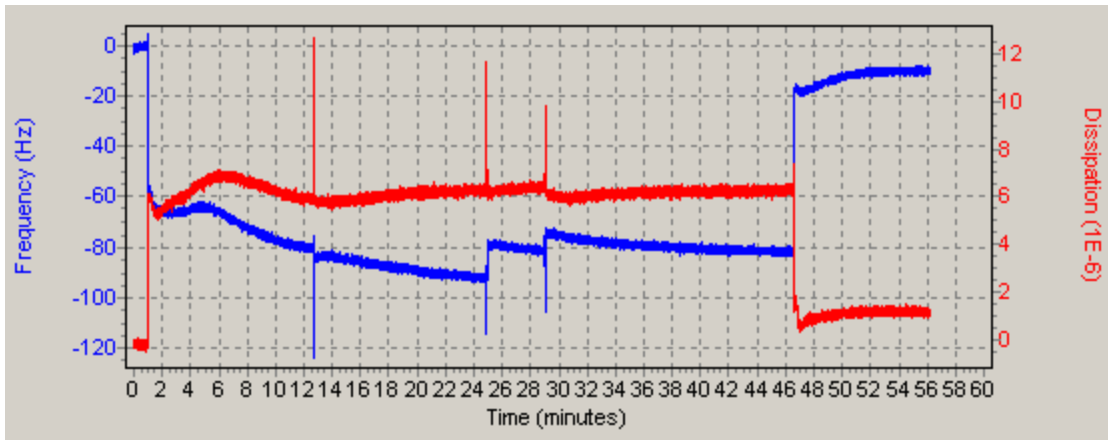


Figure C.1.19: Fresh Gullfaks sample on calcium carbonate coated crystal.

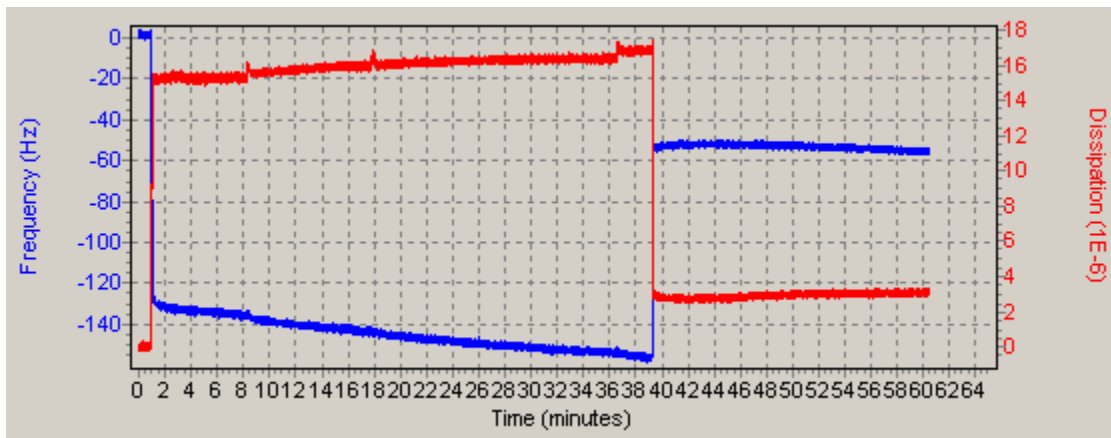


Figure C.1.20: Fresh Grane sample on calcium carbonate coated crystal.

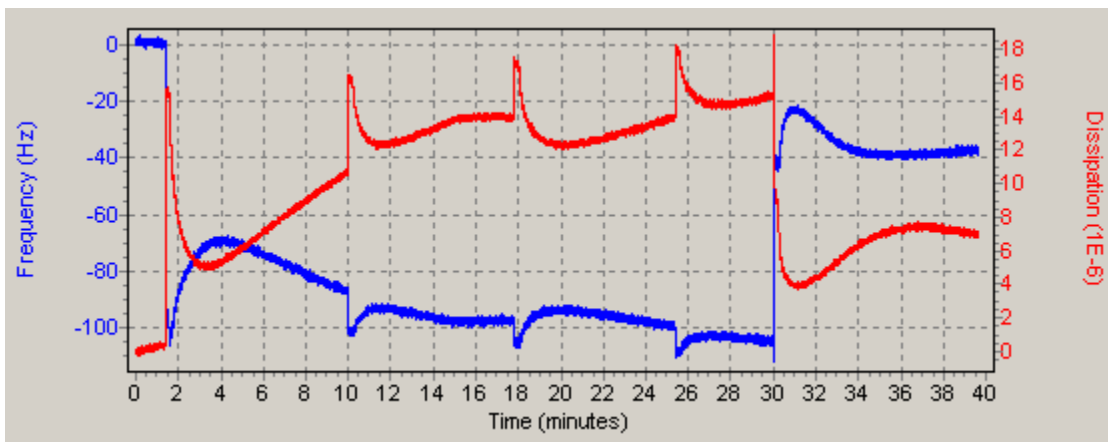


Figure C.1.21: Weathered Norne sample on calcium carbonate coated crystal.

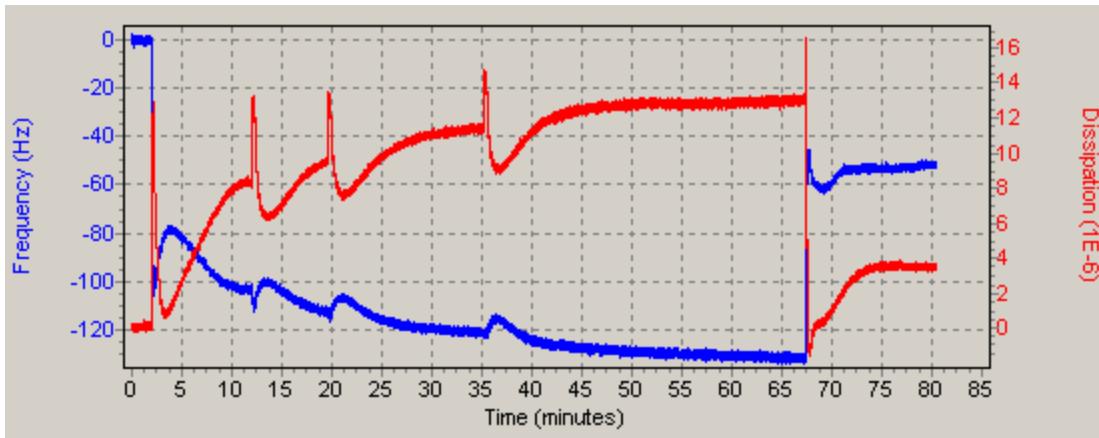


Figure C.1.22: Weathered Oseberg sample on calcium carbonate coated crystal.

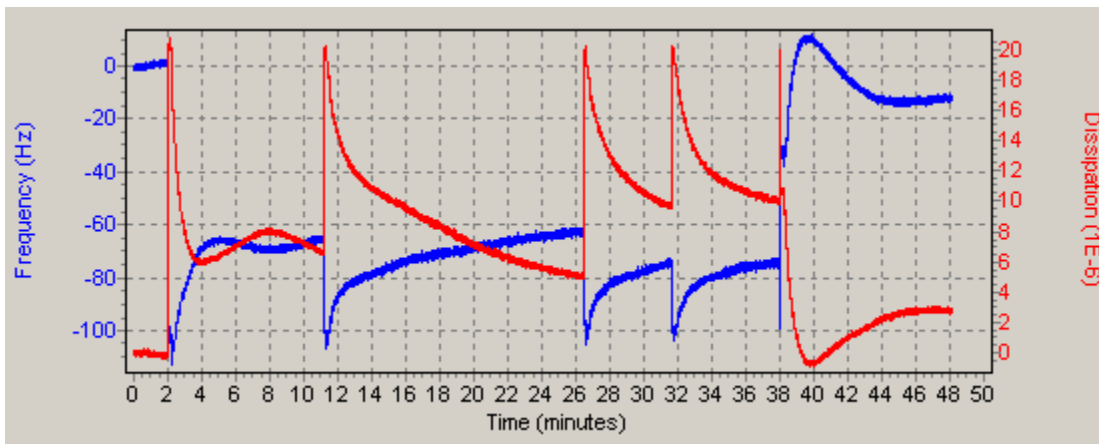


Figure C.1.23: Weathered Gullfaks sample on calcium carbonate coated crystal.

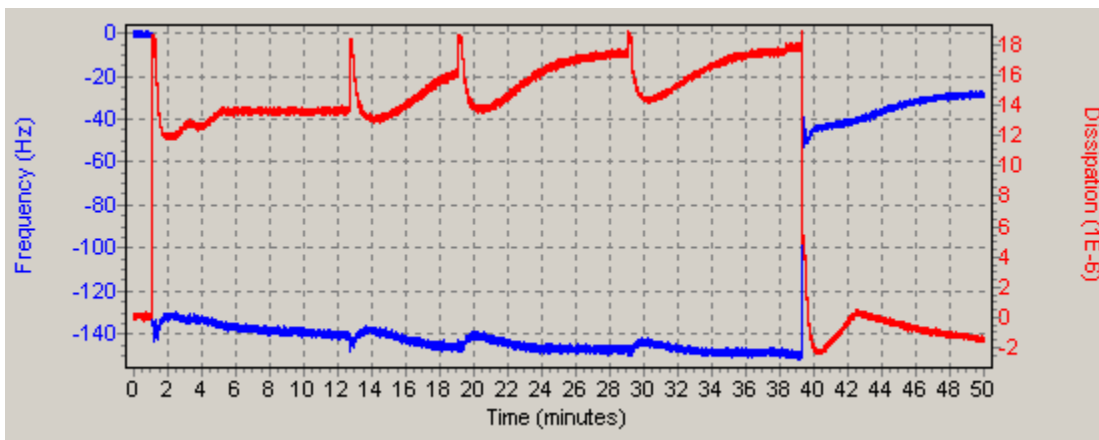


Figure C.1.24: Weathered Grane sample on calcium carbonate coated crystal.

C.2: Oil-in-toluene experiments with dispersants

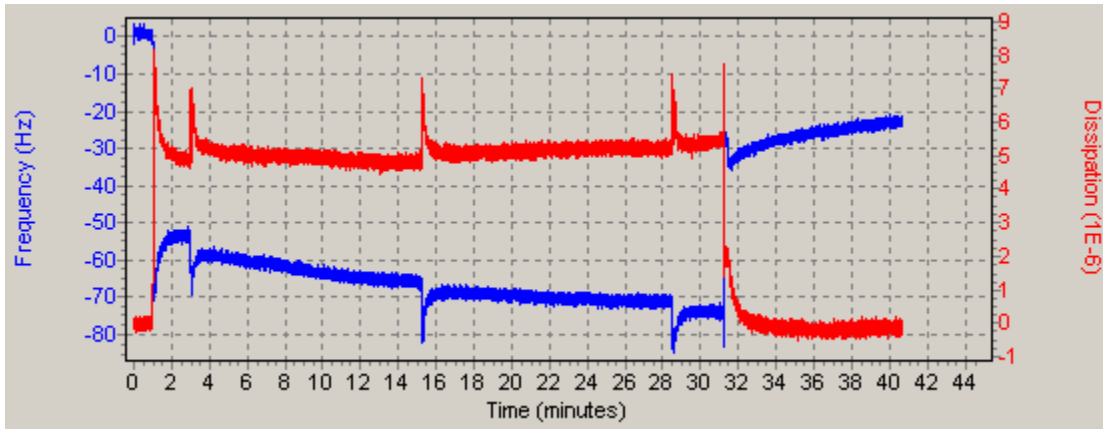


Figure C.2.1: Fresh Norne sample on silica coated crystal.

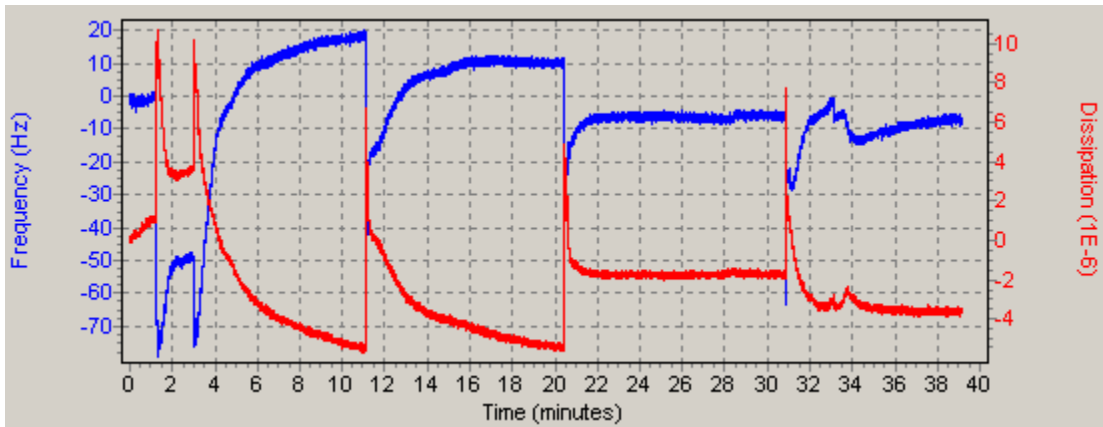


Figure C.2.2: Fresh Sture sample on silica coated crystal.

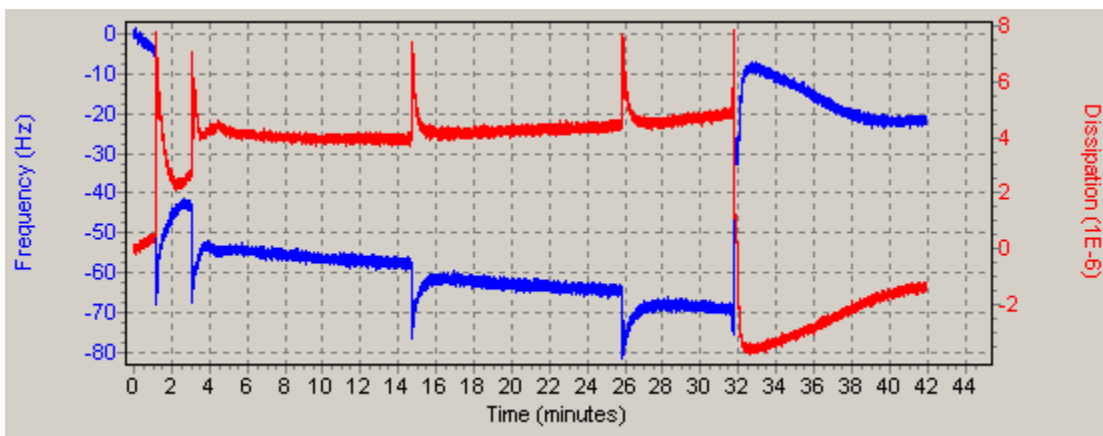


Figure C.2.3: Fresh Gullfaks sample on silica coated crystal.

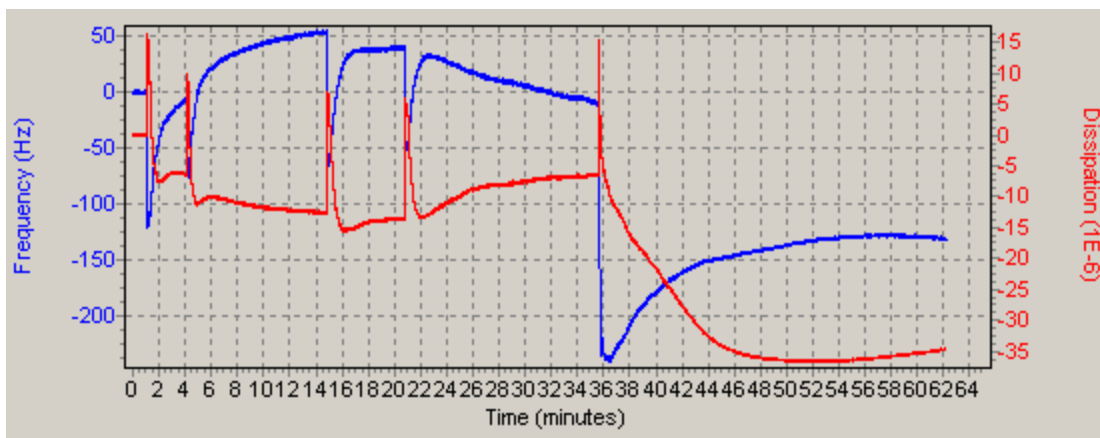


Figure C.2.4: Fresh Grane sample on silica coated crystal.

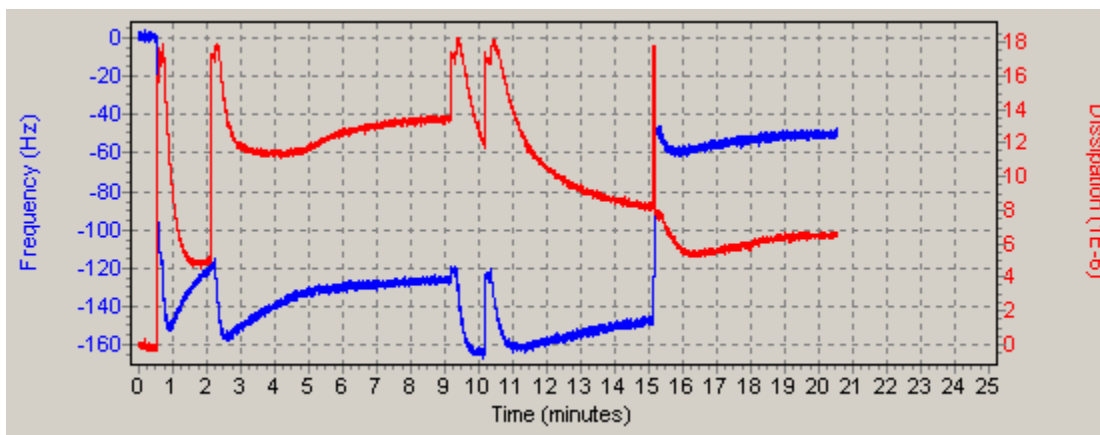


Figure C.2.5: Weathered Norne sample on silica coated crystal.

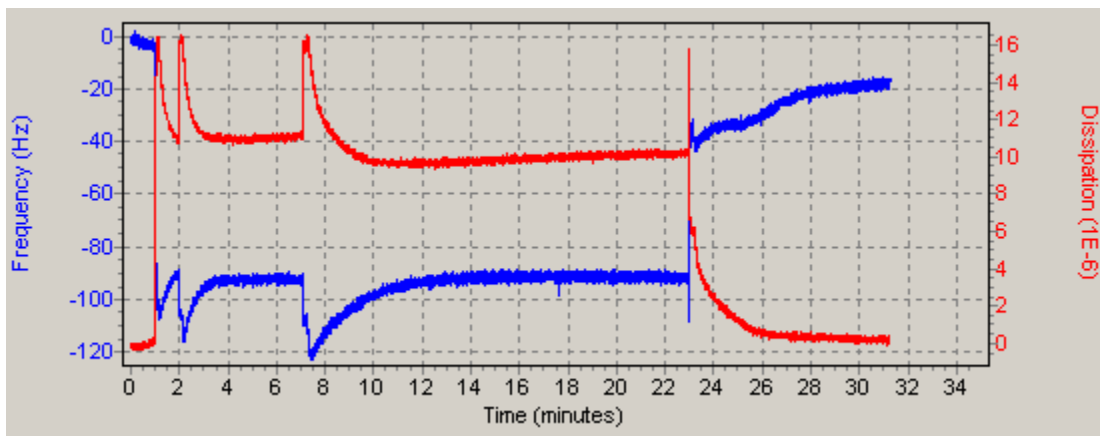


Figure C.2.6: Weathered Sture sample on silica coated crystal.

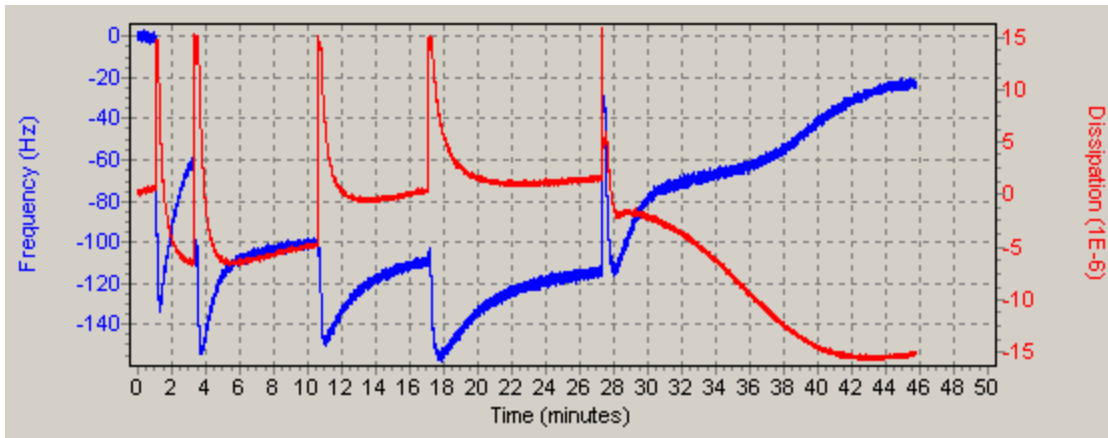


Figure C.2.7: Weathered Gullfaks sample on silica coated crystal.

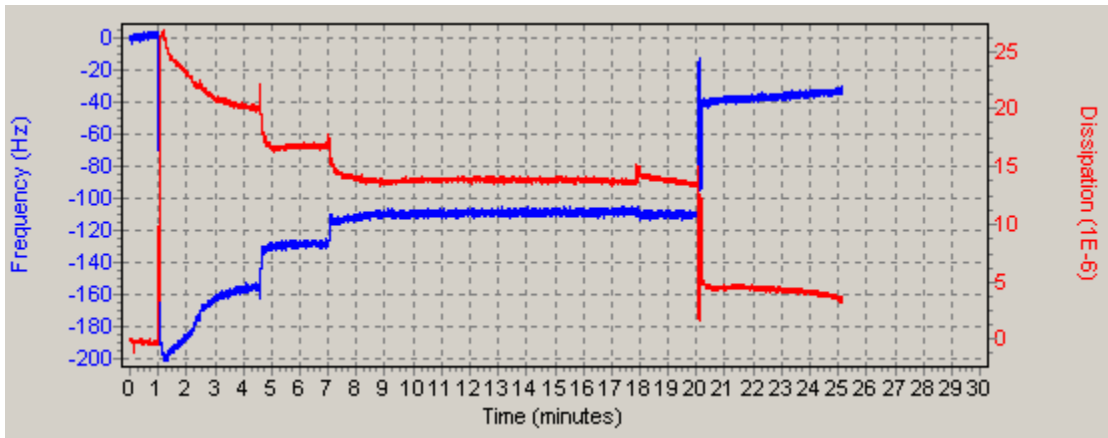


Figure C.2.8: Weathered Grane sample on silica coated crystal.

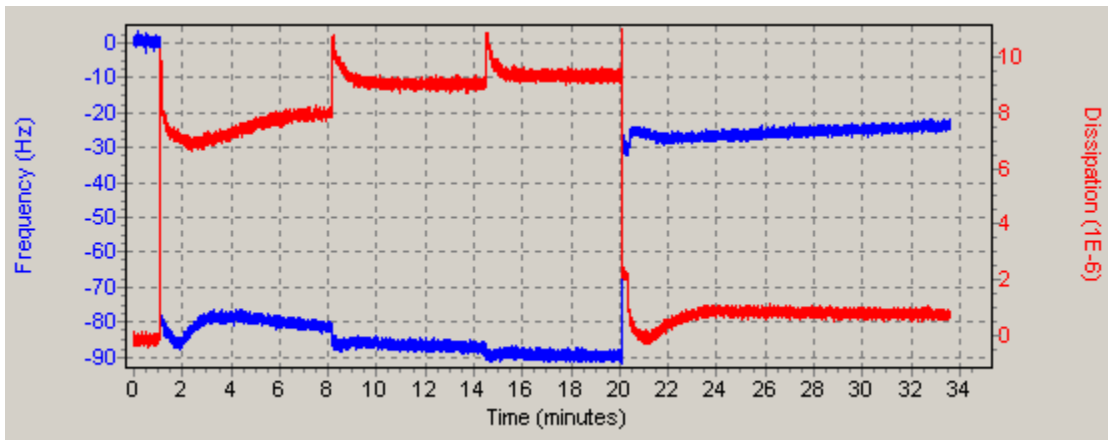


Figure C.2.9: Fresh Norne sample on aluminosilicate coated crystal.

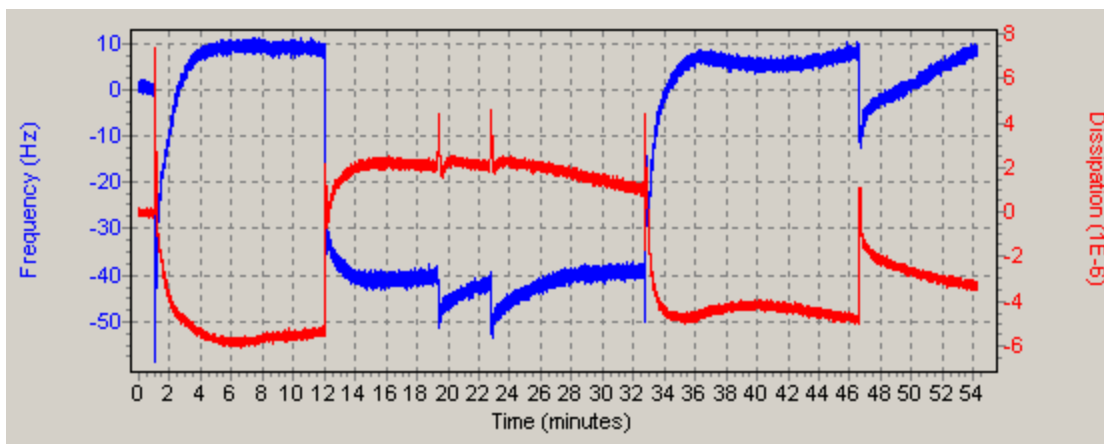


Figure C.2.10: Fresh Sture sample on aluminosilicate coated crystal.

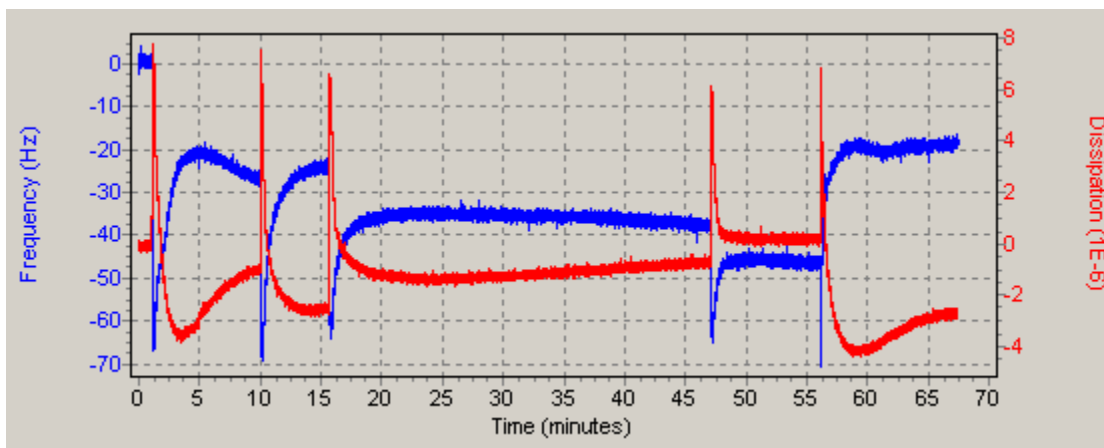


Figure C.2.11: Fresh Gullfaks sample on aluminosilicate coated crystal.

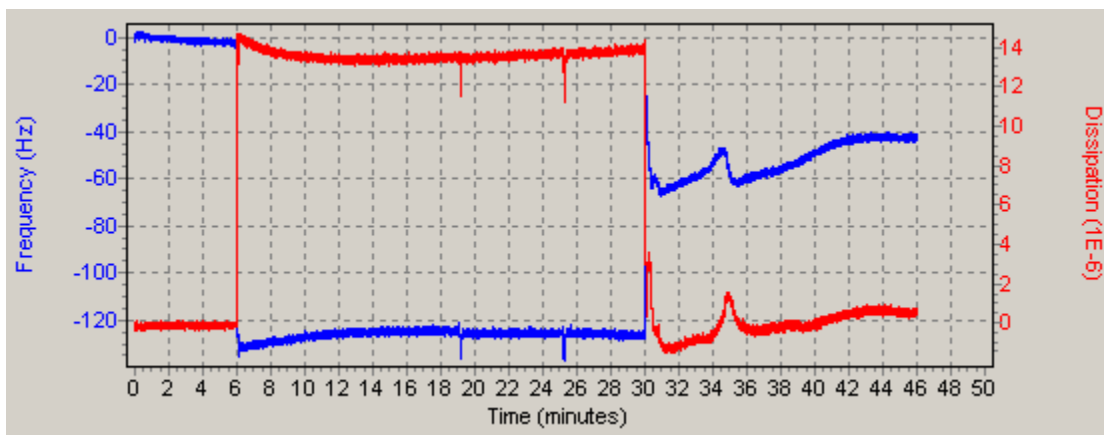


Figure C.2.12: Fresh Grane sample on aluminosilicate coated crystal.

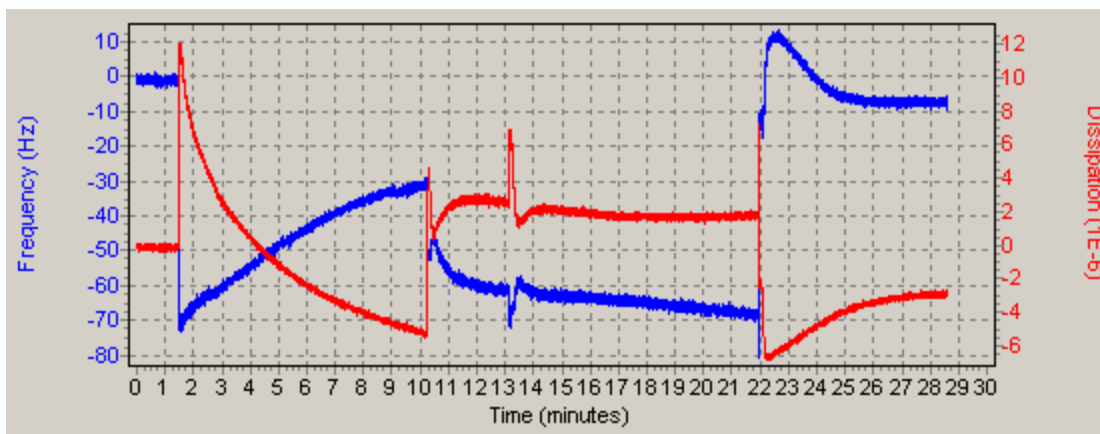


Figure C.2.13: Weathered Norne sample on aluminosilicate coated crystal.

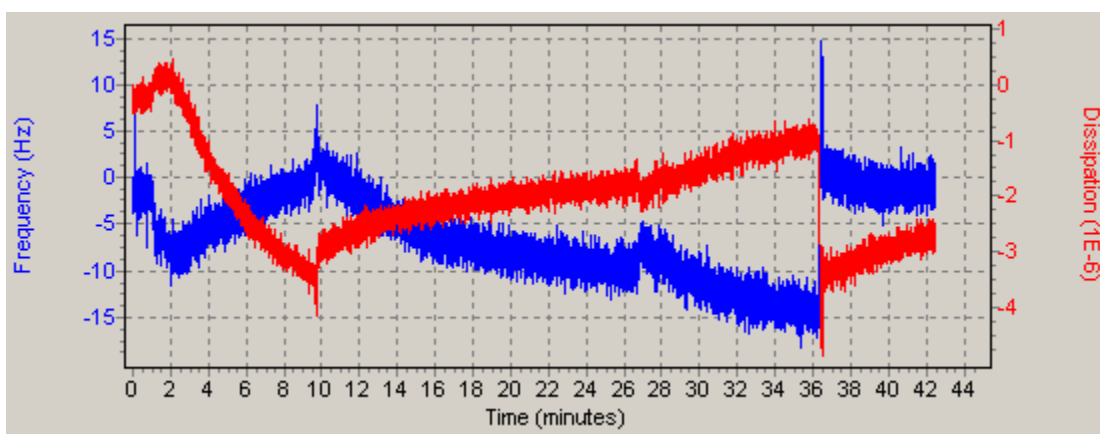


Figure C.2.14: Weathered Sture sample on aluminosilicate coated crystal.

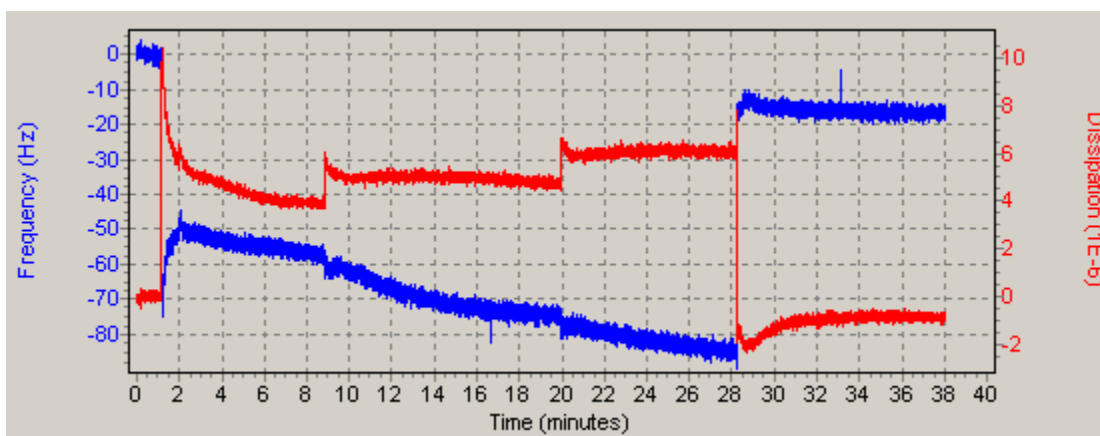


Figure C.2.15: Weathered Gullfaks sample on aluminosilicate coated crystal.

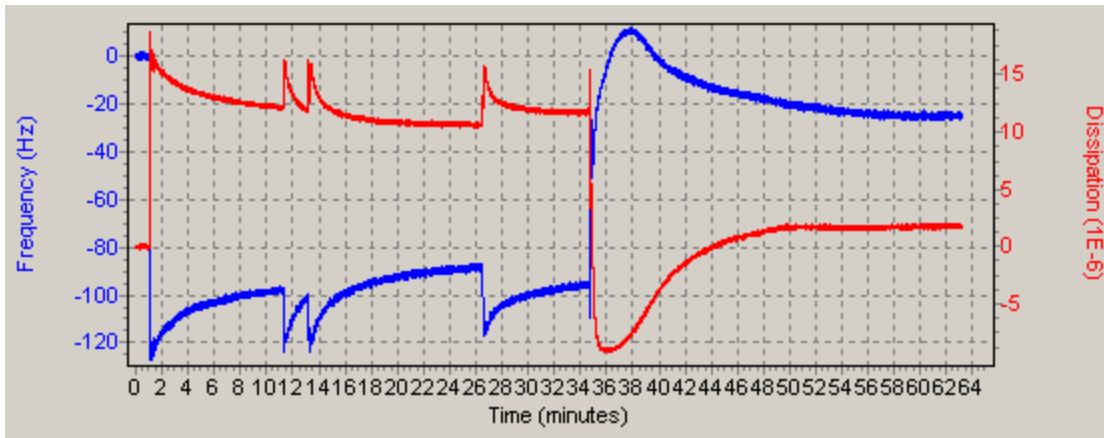


Figure C.2.16: Weathered Grane sample on aluminosilicate coated crystal.

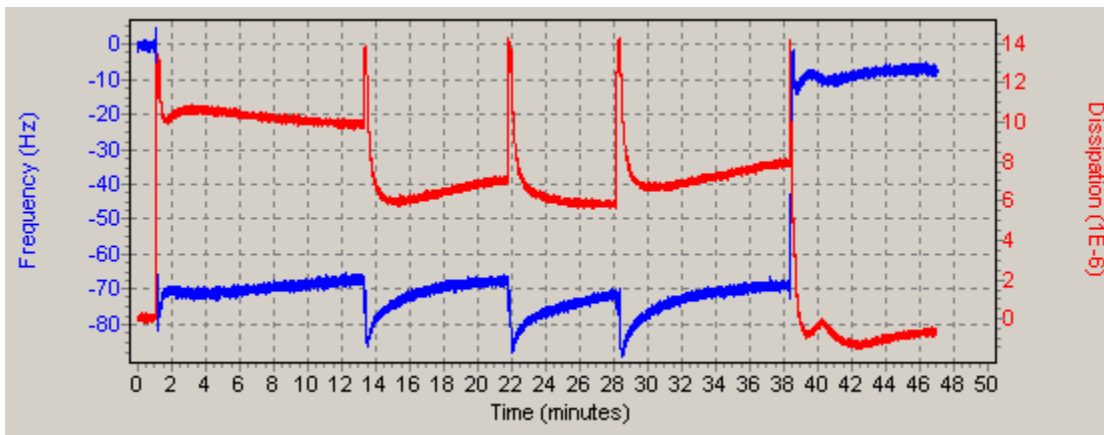


Figure C.2.17: Fresh Norne sample on calcium carbonate coated crystal.

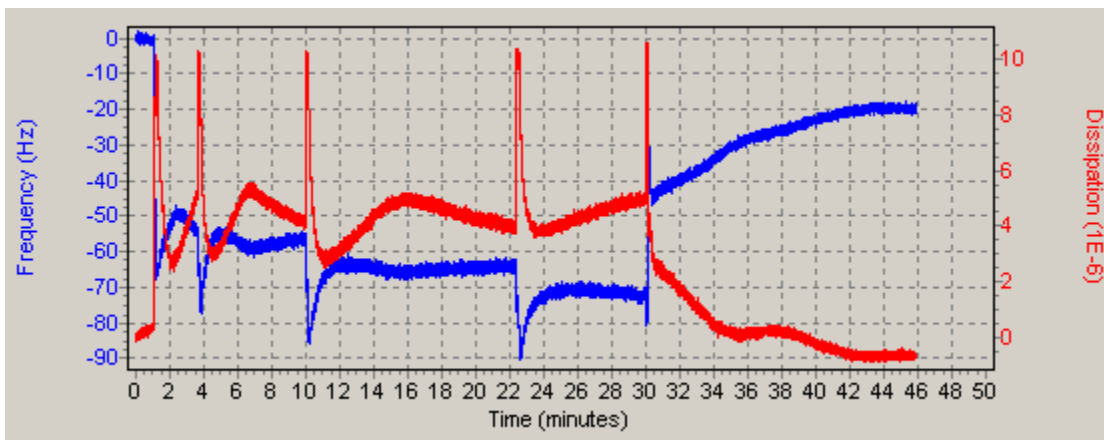


Figure C.2.18: Fresh Sture sample on calcium carbonate coated crystal.

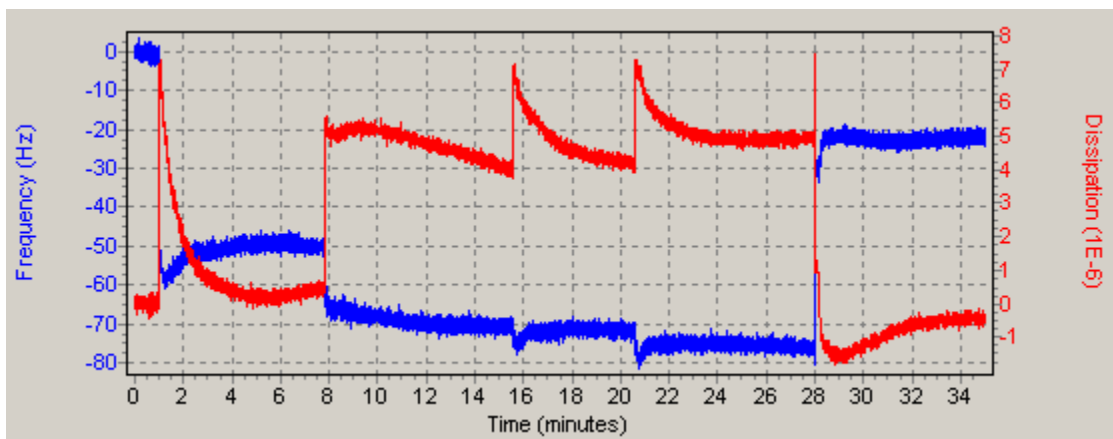
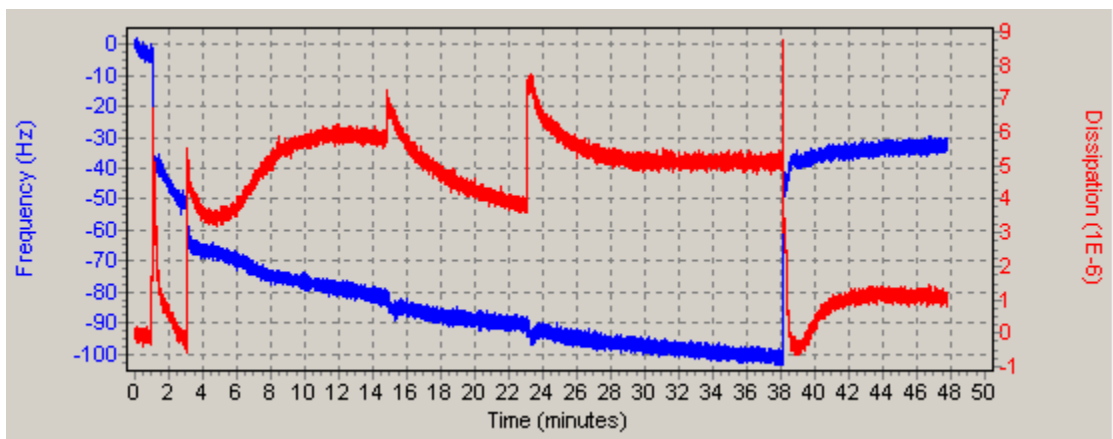
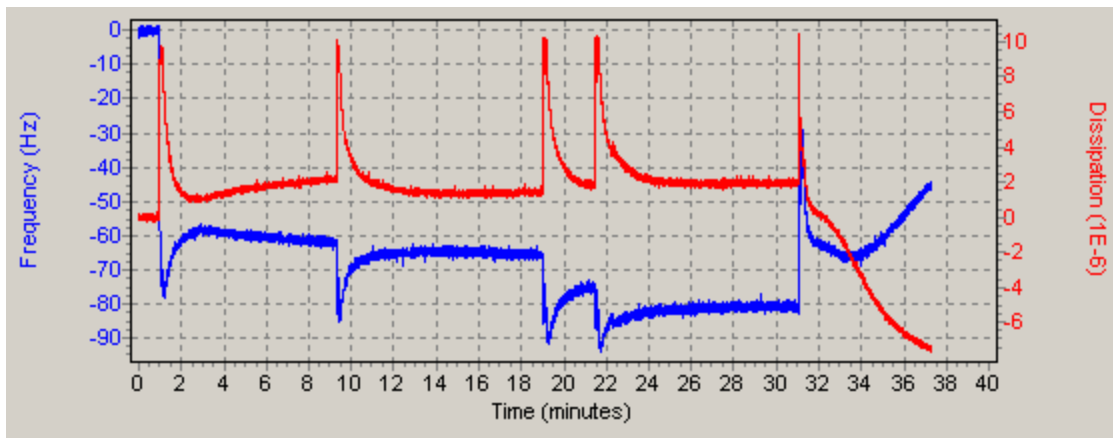


Figure C.2.19 a-c: Fresh Gullfaks samples on calcium carbonate coated crystal.

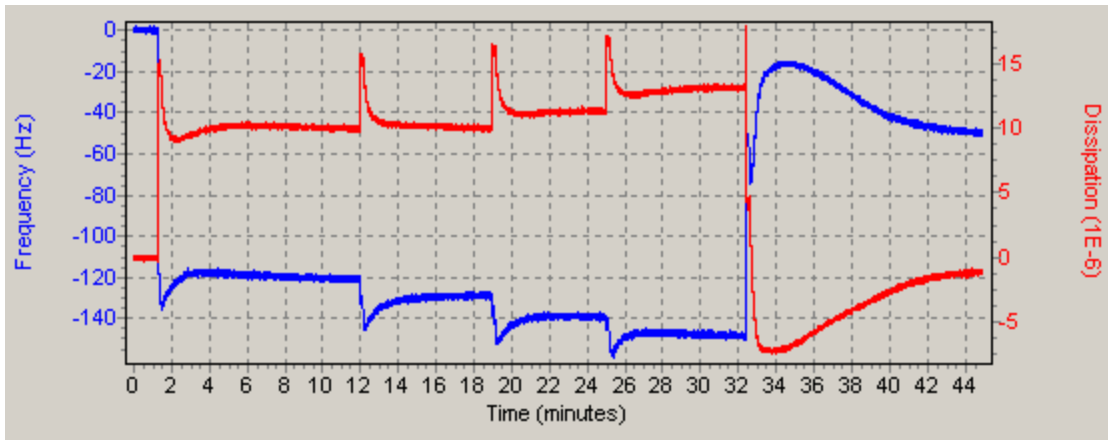


Figure C.2.20: Fresh Grane sample on calcium carbonate coated crystal.

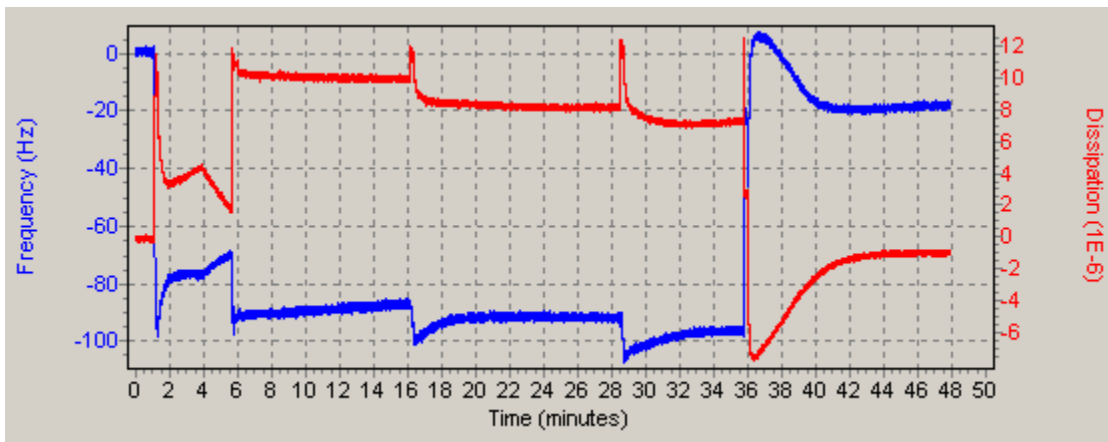


Figure C.2.21: Weathered Norne sample on calcium carbonate coated crystal.

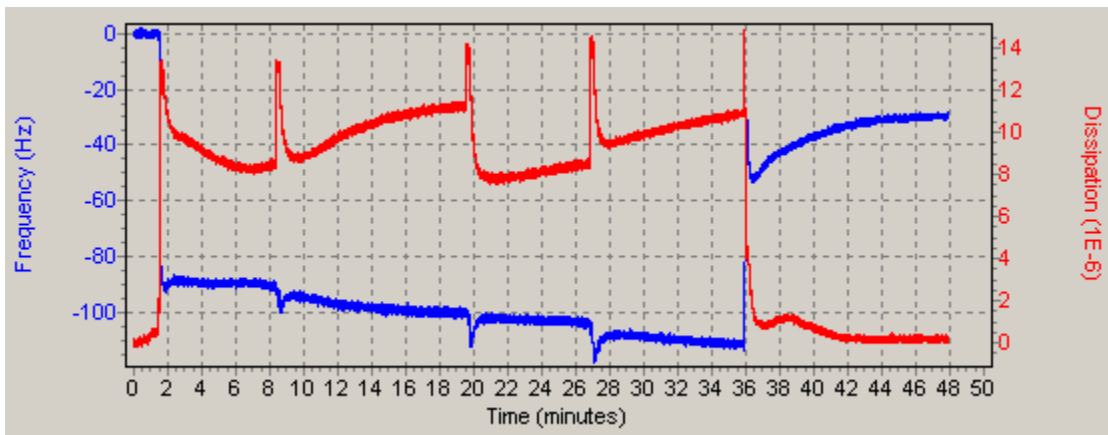


Figure C.2.22: Weathered Sture sample on calcium carbonate coated crystal.

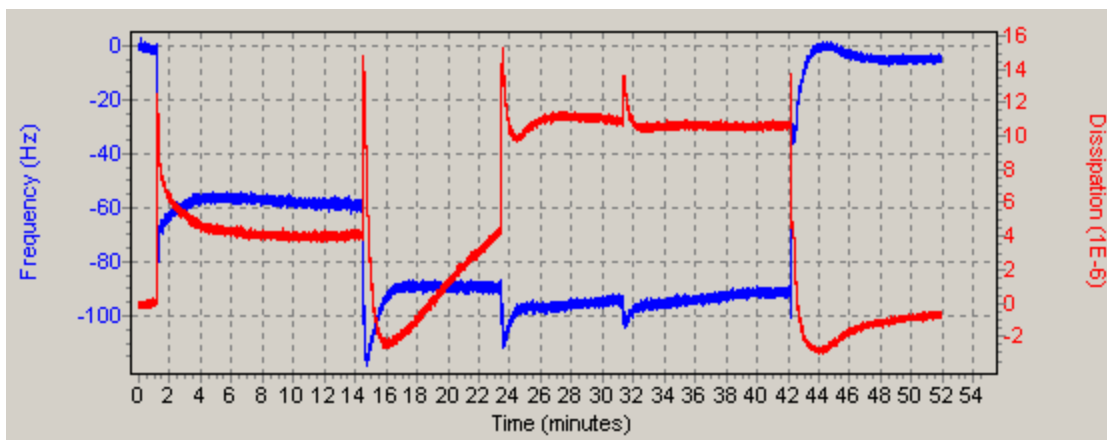


Figure C.2.23: Weathered Gullfaks sample on calcium carbonate coated crystal.

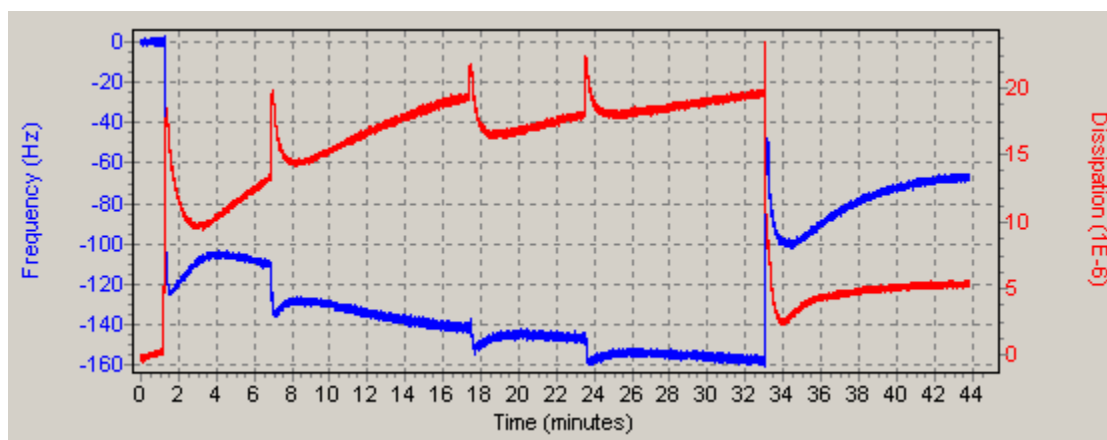


Figure C.2.24: Weathered Grane sample on calcium carbonate coated crystal.

C.3: Oil-in-seawater experiments

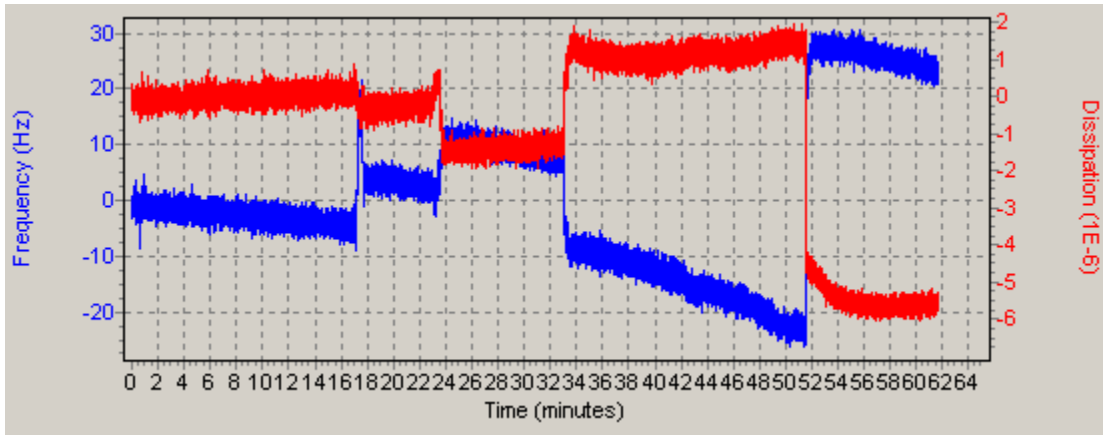


Figure C.3.1: Fresh Norne sample on silica coated crystal.

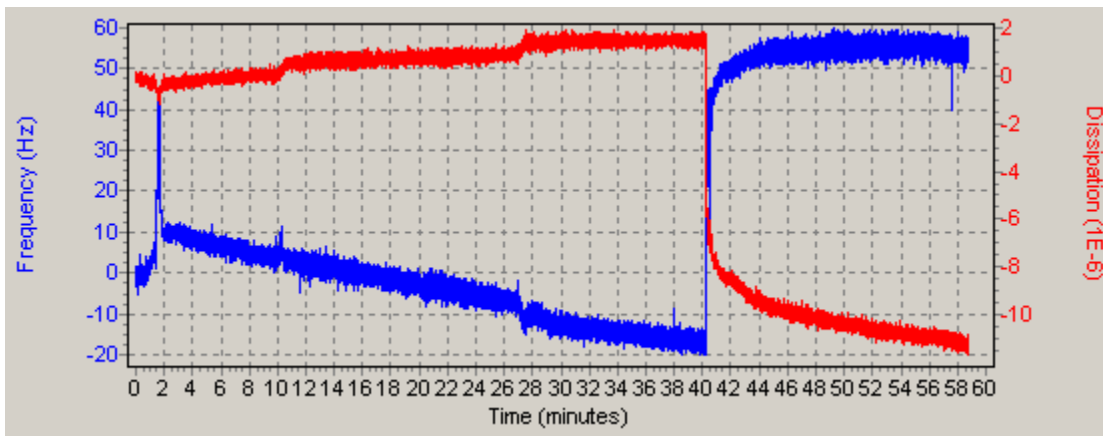


Figure C.3.2: Fresh Oseberg sample on silica coated crystal.

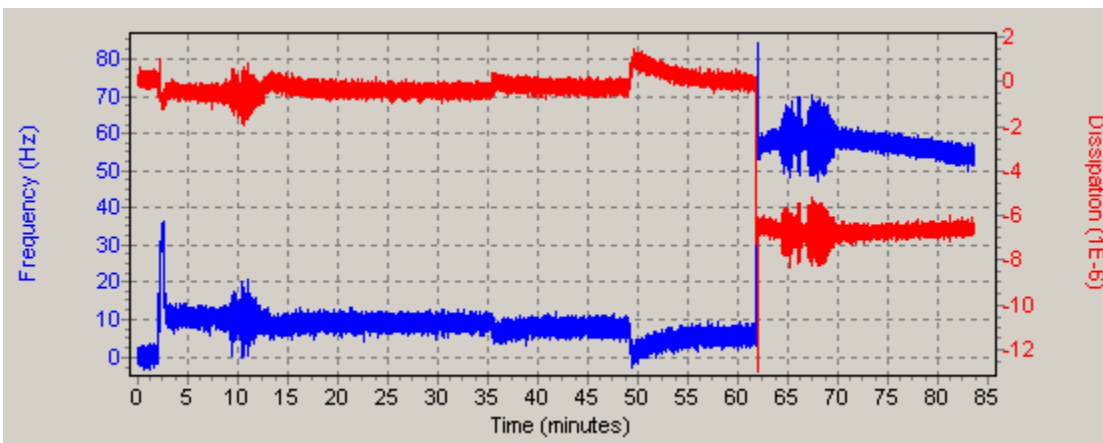


Figure C.3.3: Fresh Gullfaks sample on silica coated crystal.

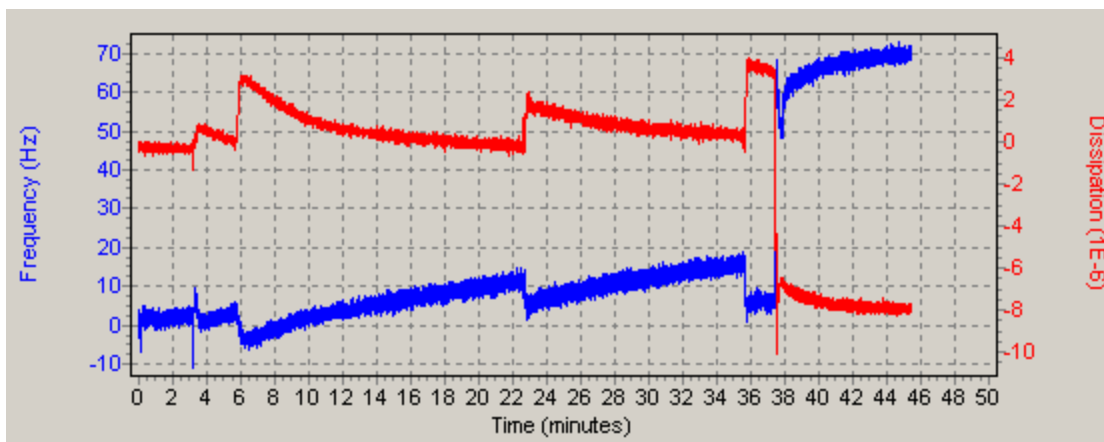


Figure C.3.4: Fresh Grane sample on silica coated crystal.

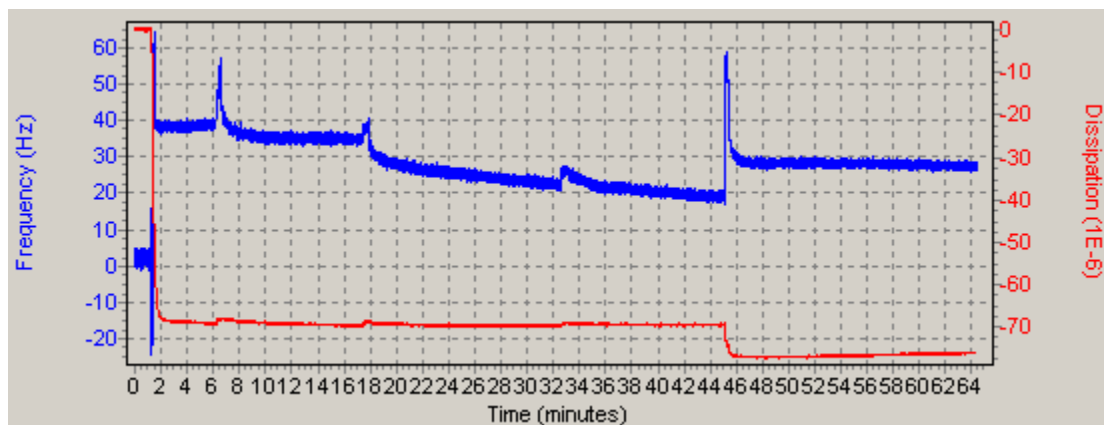


Figure C.3.5: Weathered Norne sample on silica coated crystal.

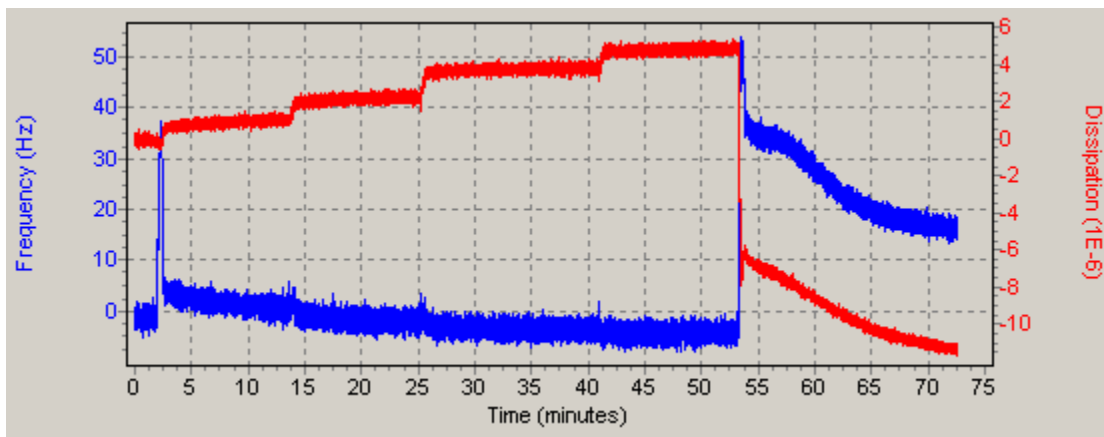


Figure C.3.6: Weathered Oseberg sample on silica coated crystal.

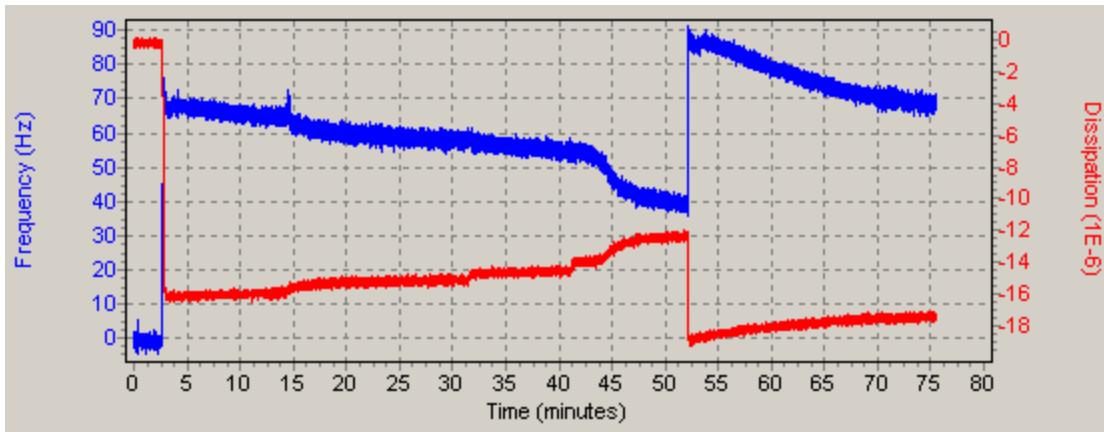


Figure C.3.7: Weathered Gullfaks sample on silica coated crystal.

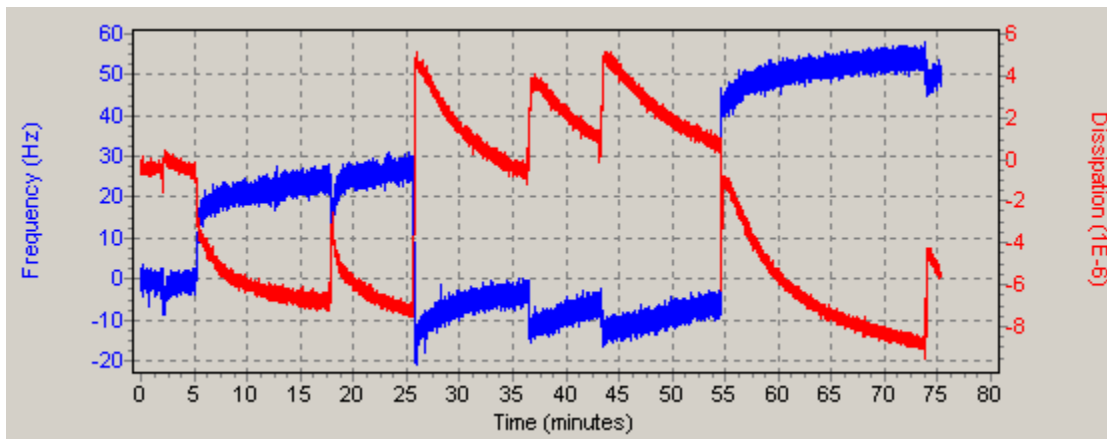


Figure C.3.8: Weathered Grane sample on silica coated crystal.

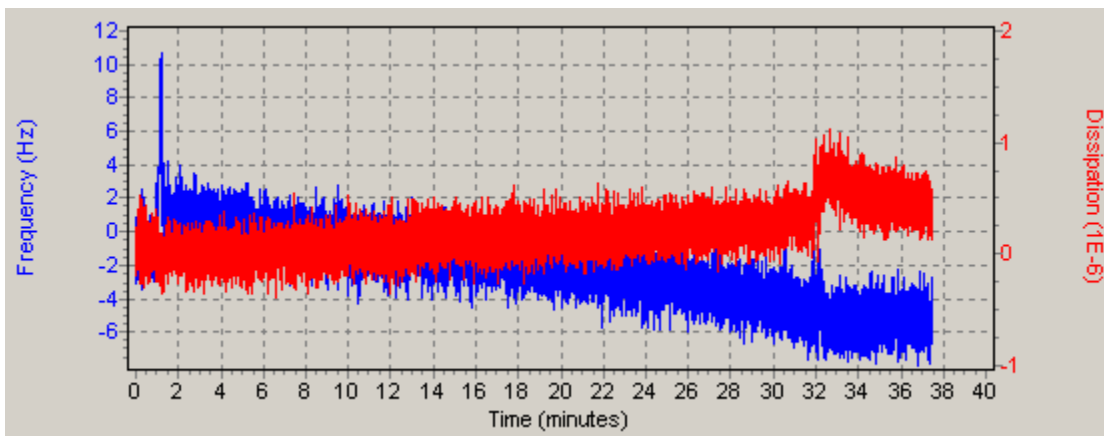


Figure C.3.9: Fresh Norne sample on aluminosilicate coated crystal.

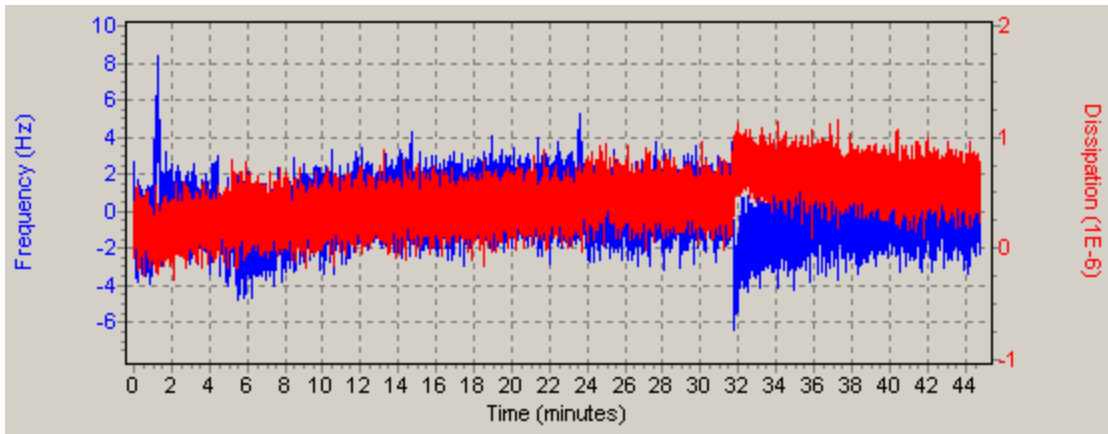


Figure C.3.10: Fresh Oseberg sample on aluminosilicate coated crystal.

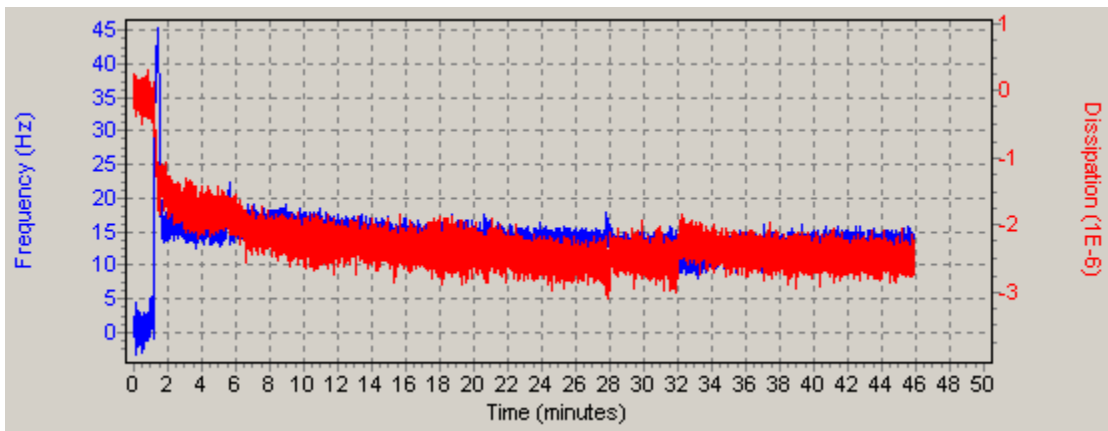


Figure C.3.11: Fresh Gullfaks sample on aluminosilicate coated crystal.

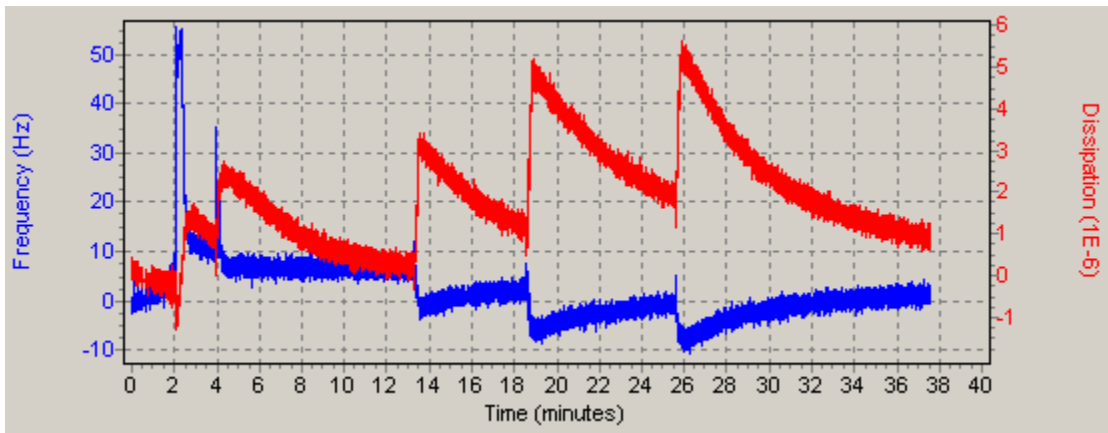


Figure C.3.12: Fresh Grane sample on aluminosilicate coated crystal.

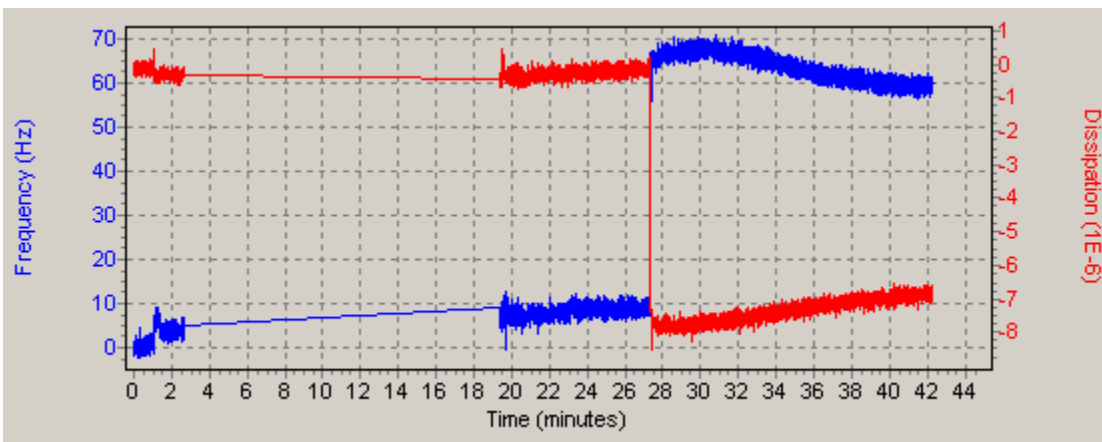
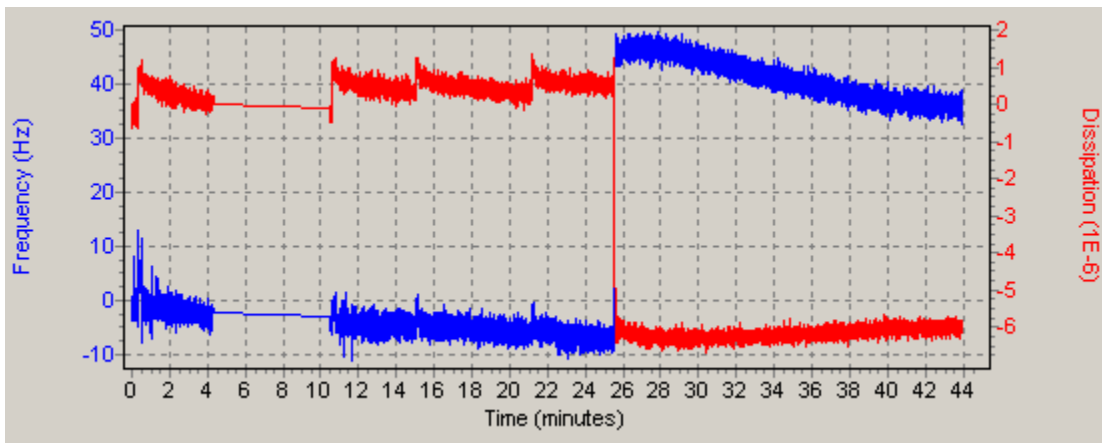
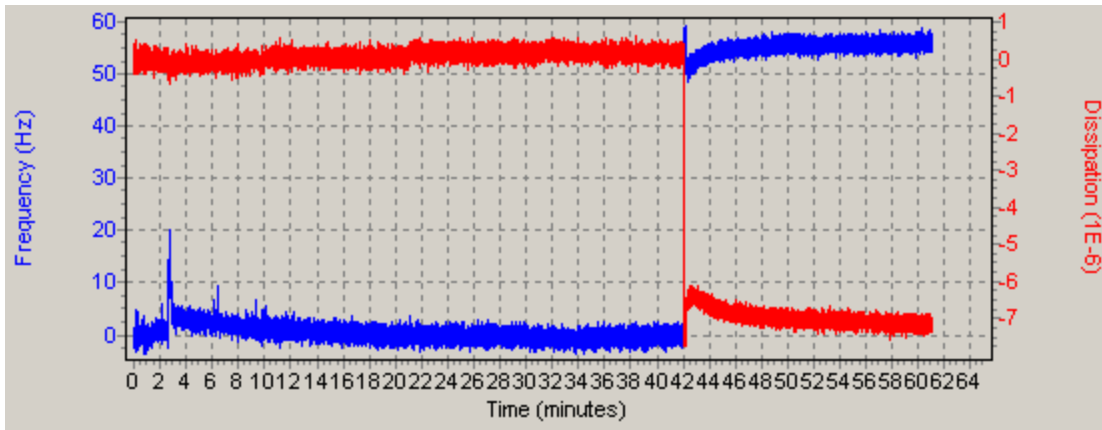


Figure C.3.13 a-c: Weathered Norne sample on aluminosilicate coated crystal.

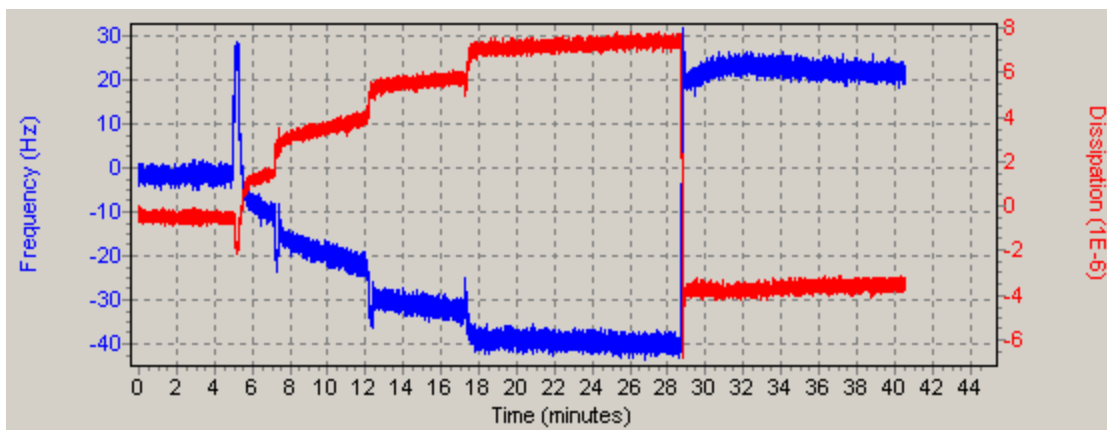


Figure C.3.14: Weathered Oseberg sample on aluminosilicate coated crystal.

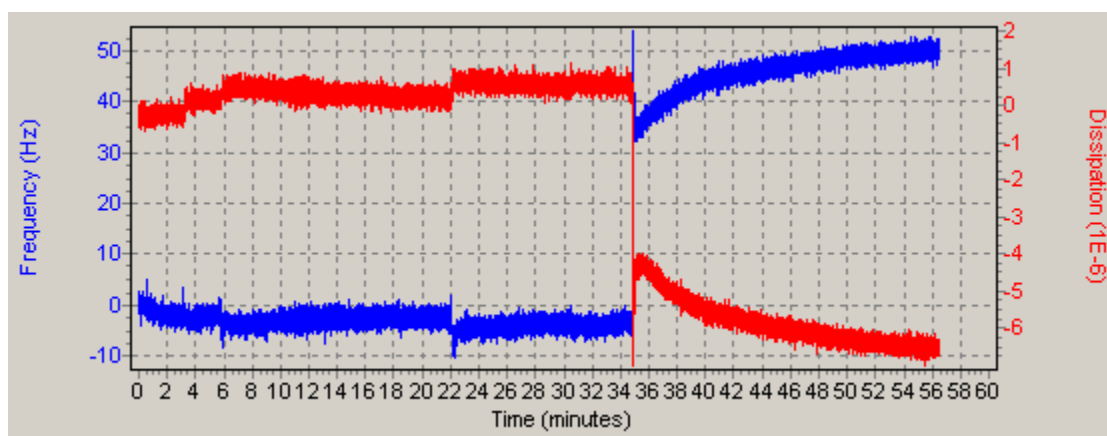


Figure C.3.15: Weathered Gullfaks sample on aluminosilicate coated crystal.

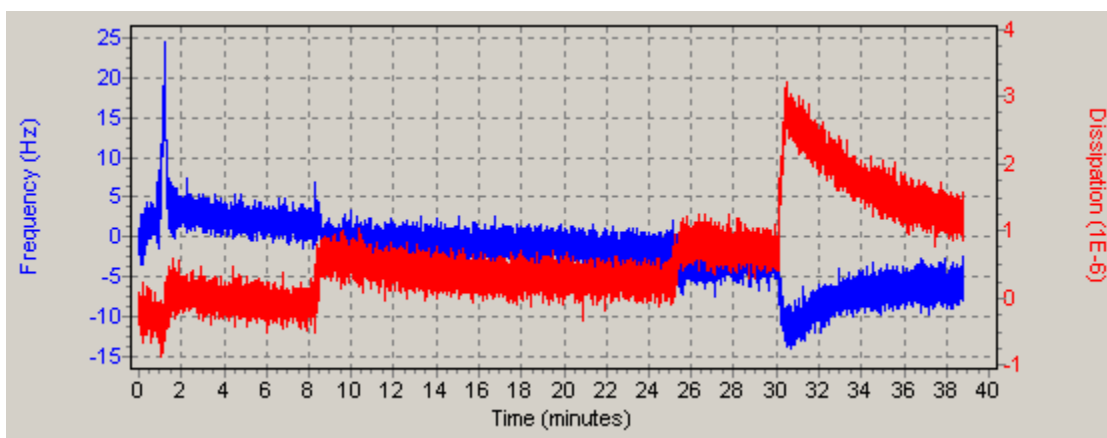


Figure C.3.16: Weathered Grane sample on aluminosilicate coated crystal.

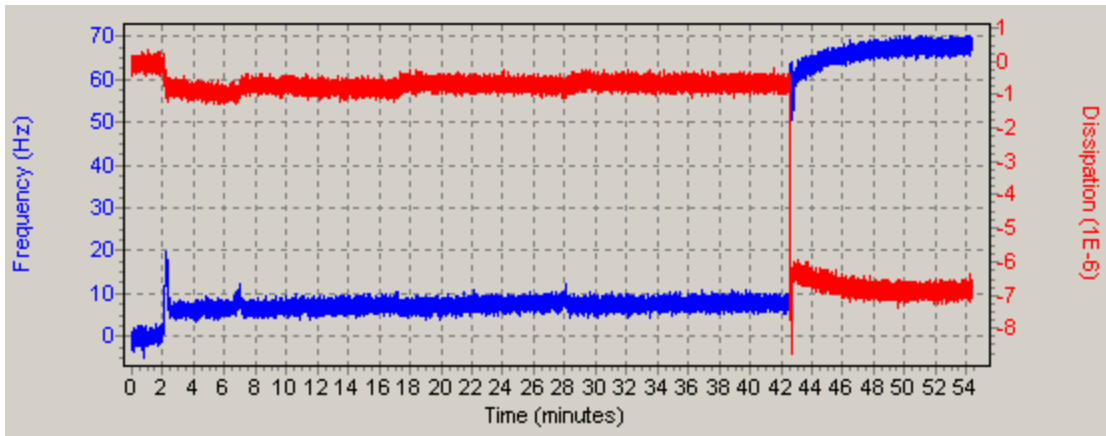


Figure C.3.17: Fresh Norne sample on calcium carbonate coated crystal.

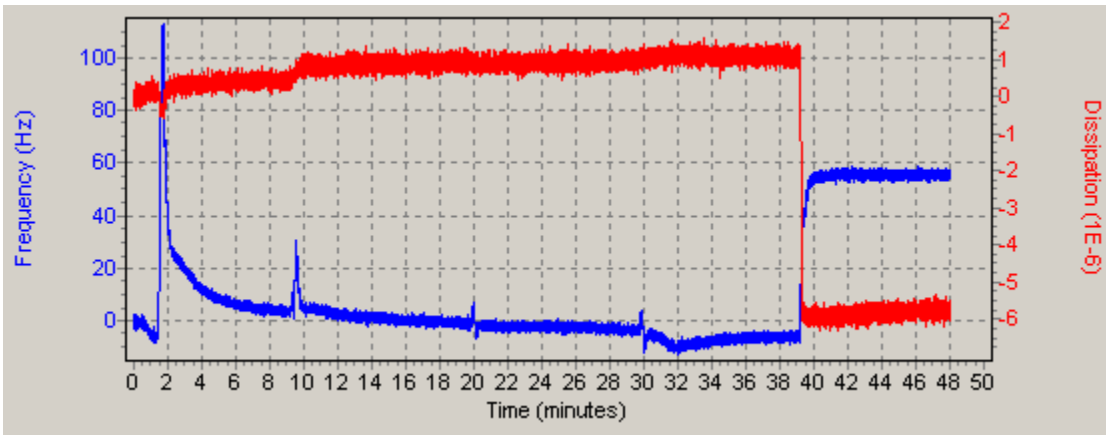


Figure C.3.18: Fresh Oseberg sample on calcium carbonate coated crystal.

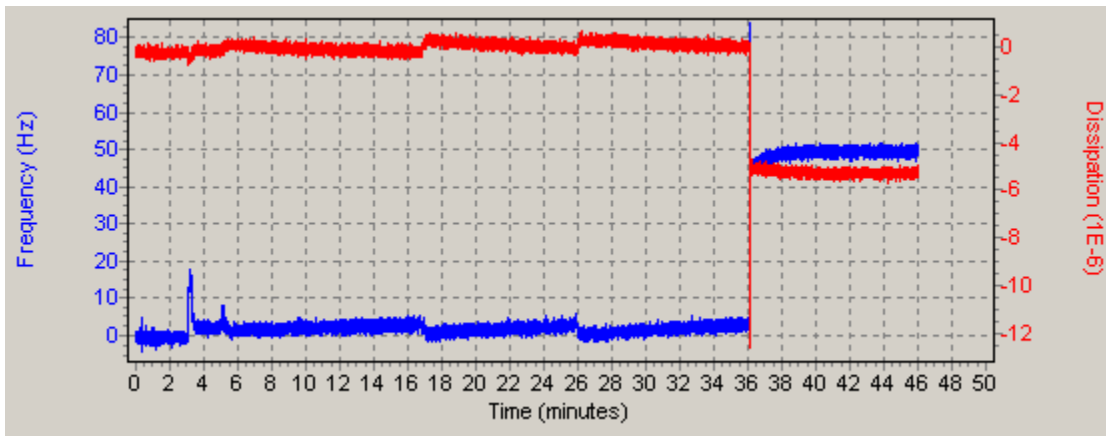


Figure C.3.19: Fresh Gullfaks sample on calcium carbonate coated crystal.

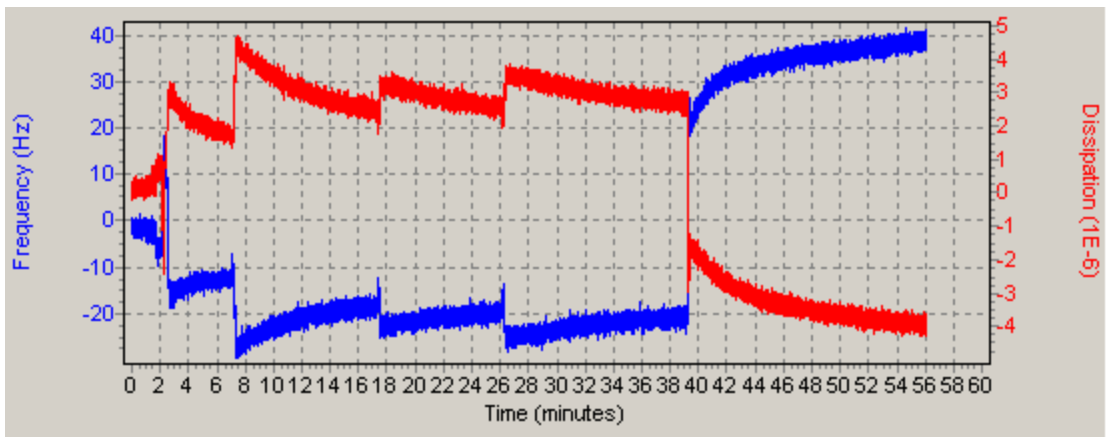


Figure C.3.20: Fresh Grane sample on calcium carbonate coated crystal.

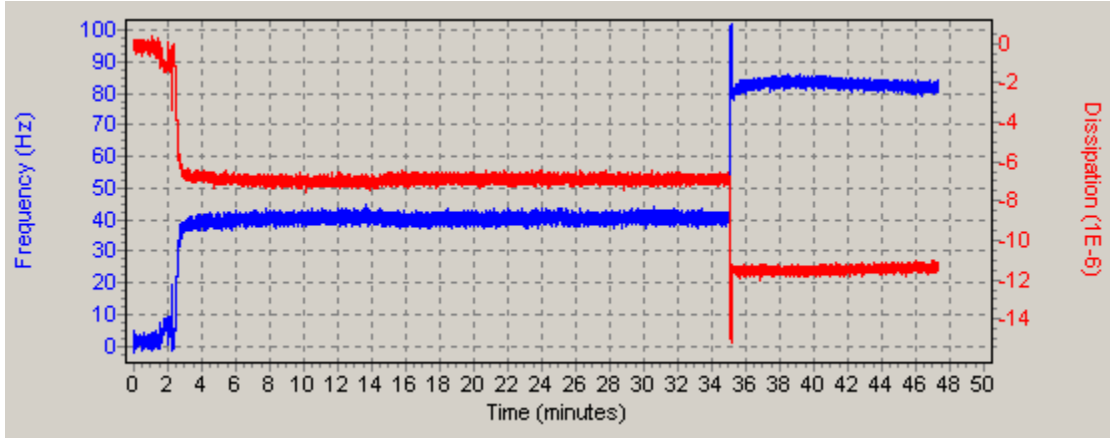


Figure C.3.21: Weathered Norne sample on calcium carbonate coated crystal.

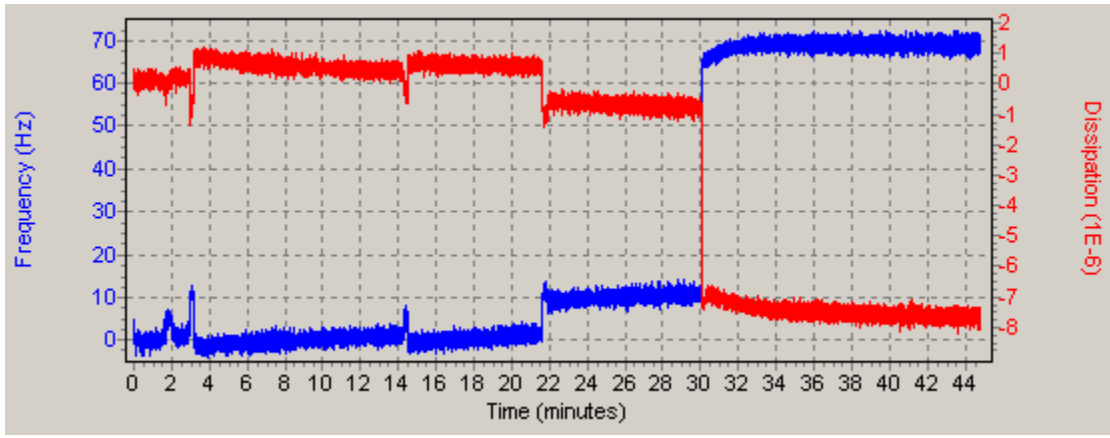


Figure C.3.22: Weathered Oseberg sample on calcium carbonate coated crystal.

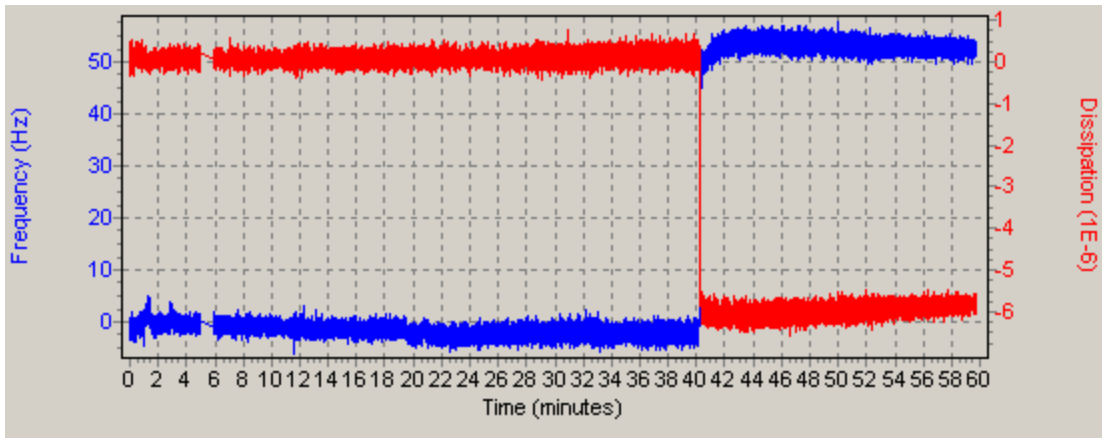


Figure C.3.23: Weathered Gullfaks sample on calcium carbonate coated crystal.

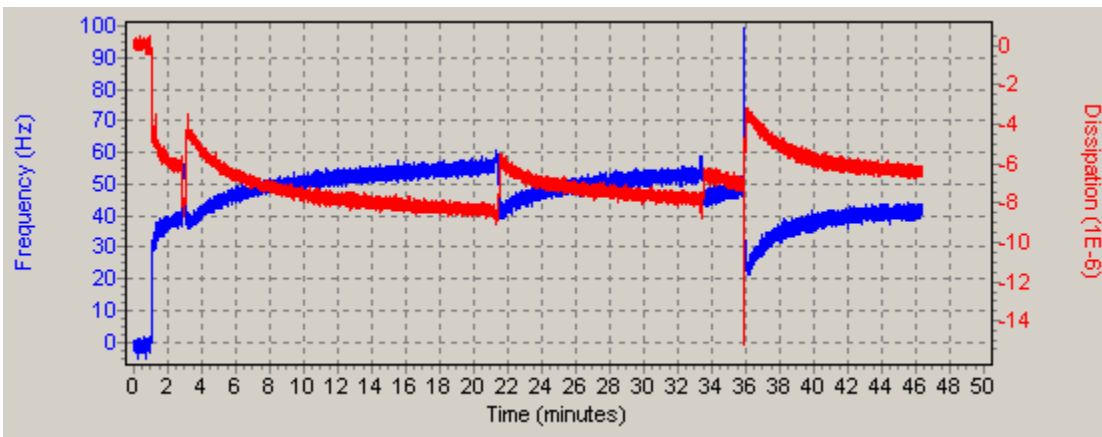


Figure C.3.24: Weathered Grane sample on calcium carbonate coated crystal.